8-13-2015 12:00 AM

Novel Carbon-supported Transition Metal Phosphide Catalysts for Hydrodeoxygenation of Fast Pyrolysis Oil

Cheng Guo, *The University of Western Ontario*

Supervisor: Chunbao (Charles) Xu, *The University of Western Ontario*
Joint Supervisor: Sohrab Rohani, *The University of Western Ontario*
A thesis submitted in partial fulfillment of the requirements for the Master of Engineering Science degree in Chemical and Biochemical Engineering

NOVEL CARBON-SUPPORTED TRANSITION METAL PHOSPHIDE CATALYSTS FOR HYDRODEOXYGENATION OF FAST PYROLYSIS OIL

(Thesis format: Integrated Article)

by

Cheng Guo

Graduate Program in Chemical and Biochemical Engineering

A thesis submitted in partial fulfillment
of the requirements for the degree of
Master of Engineering Science

The School of Graduate and Postdoctoral Studies
The University of Western Ontario
London, Ontario, Canada

Abstract

Catalytic hydrodeoxygenation (HDO) is considered to be the most promising route to upgrade pyrolysis oil to liquid transportation fuels. The objective of this research was to explore inexpensive supported metal oxides/metal phosphide catalysts for the upgrading of pyrolysis oil into advanced drop-in hydrocarbon liquid fuels by HDO.

The first stage of this thesis project investigates a series of molybdenum oxides/phosphide catalysts on different supports that were prepared in-house, such as Al_2O_3, activated carbon (AC), $MgAl_2O_4$ and $Mg_6Al_2(CO_3)(OH)_{16}$. The HDO activity of these catalysts were investigated using a 100 mL bench-scale reactor operating at 300 °C with an initial hydrogen pressure of 50 bar for 3 h. The catalytic efficiency were compared with a commercially available Ru/C catalyst, and the most active catalyst was selected, i.e., MoP/AC. Two other transition metal phosphides Nickel and Cobalt were also prepared in the same manner using AC support, and their catalytic activities for HDO of pyrolysis oil were compared. The activities of the three catalysts were found to be in the order of NiP/AC > CoP/AC > MoP/AC.

The second stage of the project aimed to optimize the addition of phosphorous. A series of supported nickel and cobalt phosphide catalysts with different metal/ phosphorous (M/P) ratios (mol/mol) were prepared and their catalytic activities studied for HDO of pyrolysis oil. Addition of phosphorous to the both Nikel and Cobalt at certain M/P ratios greatly influenced H_2 consumption, oil yield, the degree of deoxygenation and HHV values of the upgraded bio-oils. The fresh/spent catalysts were characterized by BET, XPS, TEM and XRD, and the upgraded bio-oils were characterized using Karl Fischer titration, GPC, elemental analysis and GC/MS.

Keywords

Fast pyrolysis oil, Hydrodeoxygenation, Upgrading, Transition metals, Nickel, Cobalt, Molybdenum, Phosphides, Support effects, Carbon support

Co-Authorship Statement

Chapters 3 and 4 are manuscripts to be submitted to peer-reviewed journals for consideration of publication. The contribution of each author is state below.

Chapter 3:

Development Inexpensive Transition Metal Catalysts for Hydrodeoxygenation of Pyrolysis Oil

Authors: *Cheng Guo, Kasanneni Tirumala Venkateswara Rao, Zhongshun Yuan, Sophia (Quan) He, Sohrab Rohani, Chunbao (Charles) Xu**

Status: To be submitted to Applied Catalysts A: General

Experimental work and data analysis were performed by Cheng Guo. Drs. Charles (Chunbao) Xu, Zhongshun Yuan, Tirumala Kasanneni and Sohrab Rohani provided supervision and consultation regarding the experimental work and interpretation of the results. The manuscript was drafted by Cheng Guo, and reviewed and revised by all co-authors.

Chapter 4:

Hydrodeoxygenation of fast pyrolysis oil on novel carbon-supported transition metal phosphide catalysts

Authors: *Cheng Guo, Kasanneni TirumalaVenkateswara Rao, Zhongshun Yuan, Ehsan Reyhanitash, Sophia (Quan) He, Sohrab Rohani, Chunbao (Charles) Xu**

Experimental work and data analysis were performed by Cheng Guo. Drs. Charles (Chunbao) Xu, Zhongshun Yuan, Tirumala Kasanneni and Sohrab Rohani provided supervision and consultation regarding the experimental work and interpretation of the results. The manuscript was drafted by Cheng Guo, and reviewed and revised by all co-authors.

Acknowledgments

My first thought of thanks goes to my supervisor Dr. Charles Xu, for his tireless support and guidance on my thesis work and for his enduring commitment and contribution to the field of green fuel development. Two years ago, I graduated with a bachelor degree in Food Science and Technology in China, without his deep trust and persistent help, I couldn't have the chance for entering into the field of Green Fuels and Energy.

I would also like to express my great gratitude to my co-supervisors, Prof. Sohrab Rohani, and Prof. Sophia (Quan) He, as well as Dr. Sean (Zhongshun) Yuan and Dr. Hossein Kazemian. Thanks for the patience and encouragement they offered to me during the learning process. These all convey me a spirit of adventure in regard to research.

I also acknowledge the hard work and support of the administrative staff, technologists, colleagues, and friends at the Institute for Chemicals and Fuels from Alternative Resources (ICFAR), Western University. I offer many thanks to Flora (Fang) Cao, Chantal Gloor, Christine Ramsden, Dr. Shanghuan Feng and Dr. Tirumala Kasanneni, Shima Ahmadi for all their expertise and support on my project. I also thank Dr. Jamshid Behin and Salman Bukhari in Dr. Sohrab Rohani's group, and many others for their friendship and support.

My gratitude extends also to the BioFuelNet Canada, NSERC Strategic Research Network (Lignoworks) for Biomaterials and Chemicals partnered with FPInnovations, and the NSERC Discovery Grant, NSERC/FPInnovations Industrial Research Chair program and the ORF-RE grant in Forest Biorefine, for the funding support for my stipend and research project.

I extend further thanks to my parents, Xiumei Gao and Gaobao Guo, for their unconditional love and support for all that I have chosen to in life. Finally, I want to thank my boyfriend Larry (Wencheng) Li, for his incredible love, support, sacrifices and patience during my time as a master student. The many dreary days and laborious lab work would have been much more difficult without his love and support.

Table of Contents

List of Tables

List of Figures

To my beloved mother,

Thank you for your endless love.

Chapter 1

1 Introduction

1.1 Introduction

Due to the economic, environmental and political concerns associated with petroleum-derived fuels and chemicals, there is a growing need to produce renewable fuels and chemicals from bioresources (Huber et al., 2006). Lignocellulosic biomass is considered a compelling resource, as it is the abundant, inexpensive and renewable resource for the production of bio-fuels, biochemicals and materials (Perlack et al., 2011). The main components of lignocellulosic biomass are cellulose, hemicellulose and lignin. Cellulose and hemicellulose contains C6 and C5 sugar monomer units (White et al., 2011). Lignin is branched and amorphous polymers consisting of phenylpropane units, the precursors of which are three monolignols, known as p-coumaryl alcohol, coniferyl alcohol, and sinapyl alcohol (Bu et al., 2012; Buranov & Mazza, 2008; Kuroda, 2000; Yaman, 2004).

Production of biofuels from lignocellulosic biomass can be realized thermochemically by three different technical approaches: (1) syngas (production by gasification) to liquids via Fischer-Tropsch (F-T) or methanol synthesis, (2) bio-oils production by direct liquefaction or (catalytic) pyrolysis, and (3) aqueous phase processing or hydrolysis (Huber et al., 2006). A summary of these pathways for lignocellulosic biomass conversion is presented **Fig 1-1.**

Among the abovementioned thermochemical pathways, fast pyrolysis is probably the only industrially realized process for the conversion of biomass into liquid fuels (Mohan et al., 2006; Ensun Inc). Fast pyrolysis is a thermal chemical conversion process in which the biomass feedstock is rapidly heated at high temperature (500-800 °C) for a short period of time (<2 s) in the absence of air, typically using a inert gas such as nitrogen, followed by rapid quenching of the produced vapors (Bridgwater, 2012a). The vapors formed during pyrolysis condense into liquid products commonly referred to as bio-oil. The yield of produced liquid phased can be as high as 75 wt.% of the original dry biomass, and typically contains between 60 and 75 % of the initial biomass energy

(Bridgwater, 2003; Huber et al., 2006; Mohan et al., 2006). Other products obtained by this process are char (10-20 wt.% of biomass) and non-condensable gases (10-25 wt.% of biomass).

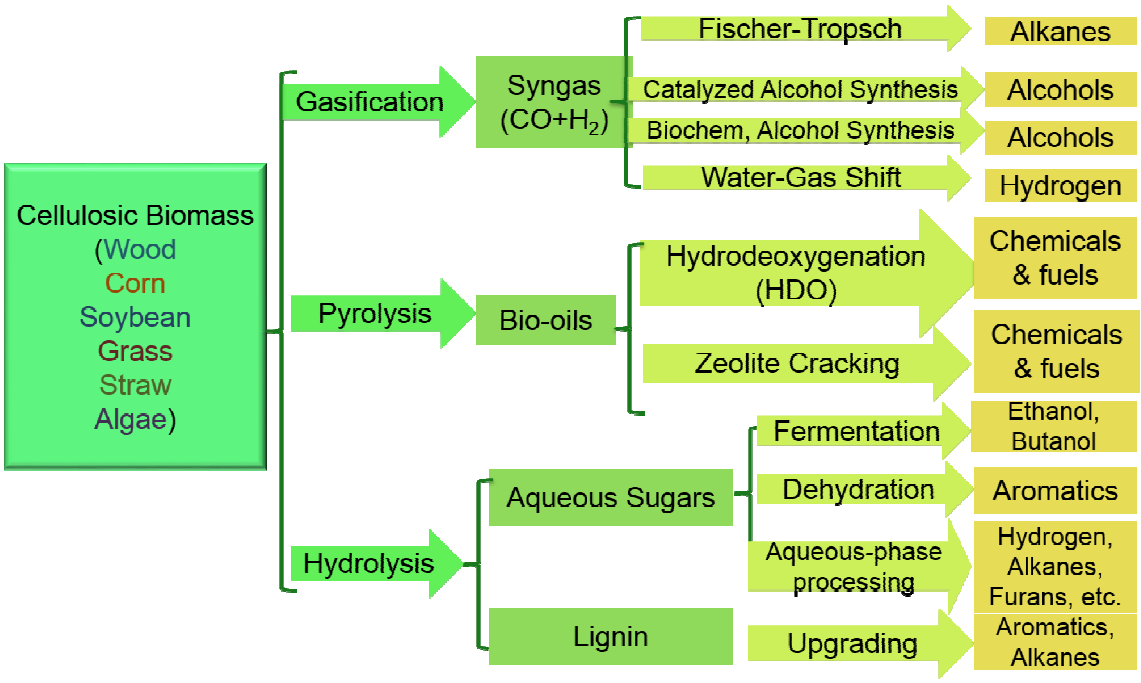

Figure 1-1 Summary of pathways for lignocellulosic biomass conversion to liquid fuels (Huber et al., 2006)

Although bio-oil can be obtained in high yields using the fast pyrolysis process, the inherent characteristics of pyrolysis oils render it distinctly dissimilar to petroleum-derived oils, thus making it less useful as a liquid fuel: high oxygen content, high water content, high viscosity, low heating value, poor ignition properties, chemical and thermal instability, and high acidity and corrosiveness (Huber et al., 2006; Zhang et al., 2013a). The characteristics of bio-oil and fuel oil are compared in **Table 1-1**. The unfavorable properties of bio-oil (e.g., acidity and corrosiveness), negatively impac equipment and processing stability (Bridgwater, 2012b; Diebold, 2000). For example, excess water content, solids, char and alkali metals may increase oil viscosity, clog the handling equipment, cause corrosion and deposition, and possibly deactivate the catalysts used in the downstream upgrading processes (Zacher et al., 2014).

Table 1-1 Comparison of key properties of pyrolysis oil and fuel oil (Bridgwater, 2012a; Oasmaa et al., 2012)

Properties	Pyrolysis oil	Fuel oil
C, dry (wt.%)	56	85
H, dry (wt.%)	6	11.1
O, dry (wt.%)	38	1
Water (wt.%)	20-30	0.025
Solids (wt.%)	0.01-0.1	0
Ash (wt.%)	0.01-0.2	0.01
Nitrogen (wt.%)	0-0.4	0
Sulfur (wt.%)	0-0.05	0.2
Stability	Unstable	Stable
Viscosity @40 °C	15-35	3-7.5
Density @15 °C	1.1-1.3	0.9
Flash point (°C)	40-110	60
Pour point (°C)	-9 to -36	-15
LHV (MJ kg^{-1})	13-18	40.3
PH	2-3	Neutral
Boiling range (°C)	Decomposes	160-140

In order to overcome the harmful properties of pyrolysis oil, upgrading is needed. Bio-oil upgrading involves complex cracking or hydro-processing reactions due to the high diversity of compounds within the feed material (Mortensen et al., 2011). The presence of oxygen containing functional groups in bio-oil is partly responsible for the challenges faced in the direct integration of bio-oil into a petroleum refinery. Thus, removal of oxygen content from bio-oil is considered a logical solution to address this problem.

Currently, two major routes are considered for bio-oil upgrading: (1) cracking over zeolite catalysts and (2) hydrodeoxygenation (HDO) over hydro-processing catalyst (Furimsky, 2000). During either upgrading process, cracking, decarbonylation, decarboxylation, hydrocracking, hydrodeoxygenation, hydrogenation, and re-polymerization reactions are reported to take place (Adjaye & Bakhshi, 1995a; Adjaye & Bakhshi, 1995b; Wildschut et al., 2009).

Bio-oil catalytic cracking is similar to the catalytic cracking process used by the petroleum industry. It is carried out in the absence of H_2 and uses acidic zeolite-based catalyst at a reaction temperature between 500 and 550 °C. Main reactions taking place

are C–C bond cleavage, hydrogen transfer, isomerization, dehydration, decarboxylation and decarbonylation, etc. (Zacher et al., 2014). Although these zeolite-based catalysts consume no hydrogen, heavy coking of the catalyst and high coke formation is reported as the major challenge faced by zeolite cracking. This results in much lower oil yields and higher gaseous products when compared to upgrading of bio-oil by HDO (Mortensen et al., 2011; Zacher et al., 2014).

The process of bio-oil HDO is similar to petroleum hydrotreating, i.e. the catalytic heteroatom removal process under high pressure H_2 at elevated temperatures (usually ≥ 350 °C) in order to produce hydrocarbon fuels (Meier & Faix, 1999). However, the main goal of petroleum hydrotreating is to remove sulphur (hydrodesulphurization), nitrogen (hydrodenitrogenation) and metals (hydrodemetallation) from the petroleum stream, while bio-oil HDO is primarily setup to remove oxygen. Oxygen can be removed as H_2O, CO_2 and CO through a combination of decarbonylation, decarboxylation, HDO, and dehydration reactions. Because oxygen removal through carbon dioxide and/or carbon monoxide occurs at the expense of a lowered carbon yield, removing oxygen in the form of water is a preferred route because the carbon yields are not lowered.

Three classes of catalysts were initially considered for HDO: (1) Sulfides of molybdenum, nickel, and cobalt, (2) zeolites and (3) noble metal catalysts. However, each of these classes of catalysts has limitations. Sulfide catalysts are unstable in water and require a continuous supply of sulfur to prevent re-oxidation, which is not attractive to produce low sulfur fuel meeting the fuel standards. Zeolite catalysts produce polycyclic aromatic hydrocarbons with moderate yields of carbon dioxide as a result of cracking (Bridgwater & Cottam, 1992; Williams & Horne, 1994; Williams & Nugranad, 2000). Noble metal catalysts are not selective towards the hydrogenation of C=O bonds. Moreover, the high cost of these metals limit their use in large-scale operations. Thus, the design of inexpensive supported metallic catalysts (such as Al_2O_3 or carbon supported Mo or NiMo or CoMo catalysts) for HDO of bio-oil has received growing interest in the last 20-30 years (Chen et al., 2014; Elliott et al., 2009; Leiva et al., 2013; Xu et al., 2010; Yang et al., 2009; Zhang et al., 2013b). Metal phosphides were recently found active bio-oil hydro-processing (Leiva et al., 2013; Yang et al., 2009; Zhao et al., 2011). Furthermore,

it has been widely reported that catalyst support plays a pivotal role in determining the activity and performance of a heterogeneous catalyst in a catalytic process (Mortensen et al., 2011). Hence, selection of suitable catalyst support for metal or metal phosphides was of interest in this study.

1.2 Thesis objectives

The main objectives of this research are summarized as follows:

- Investigating the effects of four different catalyst supports (Al_2O_3, activated carbon (AC), $MgAl_2O_4$ and $Mg_6Al_2(CO_3)(OH)_{16}$) for Mo phosphides on their performance in HDO of fast pyrolysis oil.
- Comparing the catalytic activity of MoP, NiP and CoP catalysts supported on AC for HDO of pyrolysis oil.
- Investigating the effects of P addition amount to Ni/Co catalysts on HDO of pyrolysis oil.
- Investigating the effects of small amounts of Ru additive on the activities of Ni/Co catalysts with/without P for HDO of pyrolysis oil.

1.3 Overview of the present work

Chapter 1 provides a brief introduction into the development of bio-oil as potential substitute for petroleum for the production of fuels or chemicals. The composition of biomass, biomass conversion pathways to liquid fuels, and bio-oil upgrading processes were briefly discussed.

Chapter 2 provides a detailed state-of-the-art literature review related to bio-oil HDO process and HDO catalysts. In this chapter, the pyrolysis process and typical composition of pyrolysis oil were described. The mechanism of HDO was discussed and finally the performance of different classes of HDO catalysts were compared.

Chapters 3 and 4 portray the results and discussion related to the synthesis, characterization and catalytic evaluation of supported metal phosphide catalysts for HDO of fast pyrolysis oil using a batch setup. Chapter 3 provides detailed results of the

screening of different metal phosphide catalysts and catalyst supports. Effects of P addition in the catalysts for HDO activity are also discussed in detail. Chapter 4 focused on synthesis, characterization and HDO activity of activated carbon (AC) supported Ni and Co phosphide catalysts. Effects of P addition amount (with different metal-to-phosphorous ratios, i.e., M/P ratio, were discussed and the fresh/spent catalysts were characterized.

Chapter 5 presents the overall conclusions of the thesis work and recommendations for future studies.

References

Adjaye, J.D., Bakhshi, N.N. 1995a. Catalytic conversion of a biomass-derived oil to fuels and chemicals I: model compound studies and reaction pathways. *Biomass and Bioenergy*, **8**(3), 131-149.

Adjaye, J.D., Bakhshi, N.N. 1995b. Production of hydrocarbons by catalytic upgrading of a fast pyrolysis bio-oil. Part I: Conversion over various catalysts. *Fuel Processing Technology*, **45**(3), 161-183.

Bridgwater, A.V. 2003. Renewable fuels and chemicals by thermal processing of biomass. *Chemical Engineering Journal*, **91**(2), 87-102.

Bridgwater, A.V. 2012a. Review of fast pyrolysis of biomass and product upgrading. *Biomass and bioenergy*, **38**, 68-94.

Bridgwater, A.V. 2012b. Upgrading biomass fast pyrolysis liquids. *Environmental Progress & Sustainable Energy*, **31**(2), 261-268.

Bridgwater, A.V., Cottam, M.L. 1992. Opportunities for biomass pyrolysis liquids production and upgrading. *Energy & Fuels*, **6**(2), 113-120.

Bridgwater, A.V., Meier, D., Radlein, D. 1999. An overview of fast pyrolysis of biomass. *Organic Geochemistry*, **30**(12), 1479-1493.

Bu, Q., Lei, H., Zacher, A.H., Wang, L., Ren, S., Liang, J., Wei, Y., Liu, Y., Tang, J., Zhang, Q. 2012. A review of catalytic hydrodeoxygenation of lignin-derived phenols from biomass pyrolysis. *Bioresource Technology*, **124**, 470-477.

Buranov, A.U., Mazza, G. 2008. Lignin in straw of herbaceous crops. *Industrial Crops and Products*, **28**(3), 237-259.

Chen, J., Shi, H., Li, L., Li, K. 2014. Deoxygenation of methyl laurate as a model compound to hydrocarbons on transition metal phosphide catalysts. *Applied Catalysis B: Environmental*, **144**, 870-884.

Diebold, J.P. 2002. A review of the chemical and physical mechanisms of the storage stability of fast pyrolysis bio-oils. In Fast Pyrolysis of Biomass: A Handbook; Bridgwater, A. V., Ed.; CPL Press: Newbury, U.K.; Vol. 2, p 424.

Elliott, D.C., Hart, T.R., Neuenschwander, G.G., Rotness, L.J., Zacher, A.H. 2009. Catalytic hydroprocessing of biomass fast pyrolysis bio‐oil to produce hydrocarbon products. *Environmental Progress & Sustainable Energy*, **28**(3), 441-449.

Furimsky, E. 2000. Catalytic hydrodeoxygenation. *Applied Catalysis A: General*, **199**(2), 147-190.

Huber, G.W., Iborra, S., Corma, A. 2006. Synthesis of transportation fuels from biomass: chemistry, catalysts, and engineering. *Chemical Reviews*, **106**(9), 4044-4098.

Kuroda, K.-i. 2000. Analytical pyrolysis products derived from cinnamyl alcohol-end groups in lignins. *Journal of Analytical and Applied Pyrolysis*, **53**(2), 123-134.

Leiva, K., Sepúlveda, C., García, R., Fierro, J.L.G., Águila, G., Baeza, P., Villarroel, M., Escalona, N. 2013. Effect of P content in the conversion of guaiacol over Mo/γ-Al_2O_3 catalysts. *Applied Catalysis A: General*, **467**, 568-574.

Meier, D., Faix, O. 1999. State of the art of applied fast pyrolysis of lignocellulosic materials—a review. *Bioresource Technology*, **68**(1), 71-77.

Mohan, D., Pittman, C.U., Steele, P.H. 2006. Pyrolysis of wood/biomass for bio-oil: a critical review. *Energy & Fuels*, **20**(3), 848-889.

Mortensen, P.M., Grunwaldt, J.D., Jensen, P.A., Knudsen, K.G., Jensen, A.D. 2011. A review of catalytic upgrading of bio-oil to engine fuels. *Applied Catalysis A: General*, **407**(1), 1-19.

Oasmaa, A., Kuoppala, E., Elliott, D.C. 2012. Development of the basis for an analytical protocol for feeds and products of bio-oil hydrotreatment. *Energy & Fuels*, **26**(4), 2454-2460.

Perlack, R.D., Eaton, L.M., Turhollow Jr, A.F., Langholtz, M.H., Brandt, C.C., Downing, M.E., Graham, R.L., Wright, L.L., Kavkewitz, J.M., Shamey, A.M. 2011. Department of Energy, U.S. 2011. Billion-Ton Update: Biomass Supply for a Bioenergy and Bioproducts Industry (Oak Ridge National Laboratory Report ORNL/TM-2011/224, Oak Ridge, TN).

White, J.E., Catallo, W.J., Legendre, B.L. 2011. Biomass pyrolysis kinetics: a comparative critical review with relevant agricultural residue case studies. *Journal of Analytical and Applied Pyrolysis*, **91**(1), 1-33.

Wildschut, J., Mahfud, F.H., Venderbosch, R.H., Heeres, H.J. 2009. Hydrotreatment of fast pyrolysis oil using heterogeneous noble-metal catalysts. *Industrial & Engineering Chemistry Research*, **48**(23), 10324-10334.

Williams, P.T., Horne, P.A. 1994. Characterisation of oils from the fluidised bed pyrolysis of biomass with zeolite catalyst upgrading. *Biomass and Bioenergy*, **7**(1), 223-236.

Williams, P.T., Nugranad, N. 2000. Comparison of products from the pyrolysis and catalytic pyrolysis of rice husks. *Energy*, **25**(6), 493-513.

Xu, Y., Wang, T., Ma, L., Zhang, Q., Liang, W. 2010. Upgrading of the liquid fuel from fast pyrolysis of biomass over MoNi/γ-Al_2O_3 catalysts. *Applied Energy*, **87**(9), 2886-2891.

Yaman, S. 2004. Pyrolysis of biomass to produce fuels and chemical feedstocks. *Energy Conversion and Management*, **45**(5), 651-671.

Yang, Y., Gilbert, A., Xu, C.C. 2009. Hydrodeoxygenation of bio-crude in supercritical hexane with sulfided CoMo and CoMoP catalysts supported on MgO: a model compound study using phenol. *Applied Catalysis A: General*, **360**(2), 242-249.

Zacher, A.H., Olarte, M.V., Santosa, D.M., Elliott, D.C., Jones, S.B. 2014. A review and perspective of recent bio-oil hydrotreating research. *Green Chemistry*, **16**(2), 491-515.

Zhang, L., Liu, R., Yin, R., Mei, Y. 2013a. Upgrading of bio-oil from biomass fast pyrolysis in China: A review. *Renewable and Sustainable Energy Reviews*, **24**, 66-72.

Zhang, X., Wang, T., Ma, L., Zhang, Q., Jiang, T. 2013b. Hydrotreatment of bio-oil over Ni-based catalyst. *Bioresource Technology*, **127**, 306-311.

Zhao, H.Y., Li, D., Bui, P., Oyama, S.T. 2011. Hydrodeoxygenation of guaiacol as model compound for pyrolysis oil on transition metal phosphide hydroprocessing catalysts. *Applied Catalysis A: General*, **391**(1), 305-310.

Chapter 2

2 Literature Review

2.1 Fast pyrolysis

2.1.1 Fast pyrolysis process

Fast pyrolysis is a thermal degradation process in which the feedstock is rapidly heated in the absence of air, where the volatile matters vaporize and condense to a dark brown liquid, i.e., pyrolysis oil, which has a heating value of around 20 MJ/kg, approx. half of that of a conventional fuel oil. Comparing to traditional slow pyrolysis process used for making charcoal, fast pyrolysis is a more advanced process that can be carefully controlled to obtain high yields of oil products. Yields of pyrolysis oil up to 80 wt.% on dry feedstock can be obtained with other by-products, i.e., char and gases (Bridgwater & Peacocke, 2000). Woody biomass, owing to its high lignin content, has been the most common type of biomass for bio-oil production via pyrolysis due to its high oil yield and reliability of the pyrolysis process (Mohan et al., 2006).

There are several crucial features of a fast pyrolysis process. First, it requires a finely ground biomass feed to acquire very fast and homogenous heat transfer rates. Then, the temperature should be controlled at 450-600 °C. Finally, rapid cooling of pyrolysis vapors is required to obtain the oil product (Bridgwater & Peacocke, 2000). According to many experimental studies, a high heating rate can lead to a high oil yield with low char formation. However, more gas will be produced if raising the temperature to higher than 500 °C (Bridgwater, 2012; Yaman, 2004).

Different types of reactor such as bubbling fluid beds, cyclonic reactor and transport reactor have been used in the pyrolysis process (Oasmaa & Czernik, 1999). A conceptual fluidized bed fast pyrolysis system is shown in **Fig 2-1.** Biomass is first dried and ground into particles before it enters to the pyrolysis reactor. The produced vapor passes through cyclones to remove the char and ash before entering a condenser, in which the vapor is quenched by re-circulated oil. Char is burned with air to provide heat required for the pyrolysis process or for other use. Pyrolysis oil is the main product in the process, and

non-condensable pyrolysis gases are combusted and can be used e.g. to generate additional steam. Excess heat can be used for drying the feedstock.

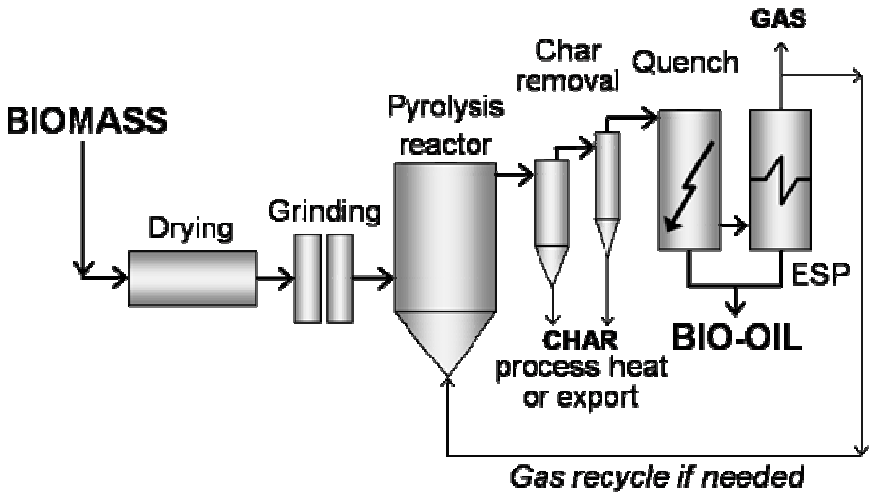

Figure 2-1 Conceptual fluidized bed fast pyrolysis system (Aston.ac.uk)

2.1.2 Fast pyrolysis oil (Bio-oil)

Cellulose, hemicellulose and lignin are the main components of lignocellulose biomass (Wu et al., 2013). Cellulose is the basic structural framework of wood cell walls which comprises approximately between 40-50 wt.% of dry wood (Pettersen & Rowell, 1984). Chemically cellulose is a high-molecular-weight linear polymer of β-(1, 4)-D-glucopyranose units in the $^{4}C_{1}$ conformation. It is believed that cellulose chains contain 5000-10000 glucose units (Mohan et al., 2006). The basic repeating unit of the cellulose polymer consists of two glucose anhydride units.

Hemicellulose is one of the other main wood components. It constitutes about 25-35 % by mass of dry wood (Pettersen & Rowell, 1984). Hemicellulose is a heteropolysaccharide made up of monosaccharides, e.g., galactose, glucose, mannose, xylose and arabinose, as well as 4-O-methyl glucuronic acid and galacturonic acid residues. Compare to cellulose, which has a crystalline structure, hemicellulose has an amorphous structure due to its branched structure. Hemicellulose can be hydrolyzed and broken down to its monomer more easily than cellulose.

Lignin is the third major wood component, comprising of 23-33 wt.% of softwood and 16-25 wt.% of hardwood (Bridgwater & Peacocke, 2000). Structurally, lignin is a three-dimensional, highly branched, polyphenolic substance that consists of an irregular array of variously bonded “hydroxy-” and “methoxy-”substituted phenylpropane units (Glasser et al., 2000). Lignin is an amorphous cross-link resin with no exact structure, functionally serving as a binder in lignicellulosic biomass for the agglomeration of fibrous cellulosic components and also acts as a shield against rapid microbial or fungal destruction of the cellulosic fibers.

Fast pyrolysis oil (referred as bio-oil hereafter) is a complex mixture of large amounts of different molecular weight compounds because of the fragmentation reactions of cellulose, hemicelluloses and lignin polymers (Mohan et al., 2006). Bio-oil typically is a dark brown, homogenous, free-flowing liquid. However, bio-oil cannot be directly utilized as fuel or co-processed with petroleum in a refinery due to its undesirable properties (Bridgwater, 2003), such as low heating values, thermal instability, high viscosity, less miscibility, high acidity and low volatility mainly caused by its high oxygen content (Zacher et al., 2014), which will be further discussed in this chapter.

Bio-oils are very different from petroleum fuels in chemically composition as it is composed of a very complex mixture of oxygenated hydrocarbons (containing oxygen in the range of 45-50 wt.% depending on the feedstock) with an appreciable proportion of water (ranging from 15-35 wt.%). Bio-oil has polar nature due to its high water and oxygen content, and is therefore immiscible with petroleum. The high water content and high oxygen content can further result in a low heating value, only about half of that of crude oil (Czernik & Bridgwater, 2004; Lu et al., 2009; Venderbosch & Prins, 2010; Zhang et al., 2007).

A variety of reactions such as hydrolysis, dehydrogenation, aromatization, condensation and coking take place during the pyrolysis process. Over 300 organic compounds have been detected by GC-MS in the volatile fraction of pyrolysis oil, which include acids, alcohols, ketones, aldehydes, phenols, ethers, esters, sugars, furans, nitrogen compounds and multifunctional compounds (Christensen et al., 2011; Diebold & Czernik, 1997).

Figure 2-2 shows different pathways for the conversion of lingocellulosic biomass into value-added chemicals during pyrolysis process (Zhang et al., 2013c). Comparing to cellulose, which has a crystalline structure, hemicellulose has an amorphous structure due to its branched nature, and it can be easily hydrolyzed and broken down to its monomer at a temperature of 200-260 °C, lower than that is needed for cellulose. Because of the aromatic nature of lignin, phenols and guaiacols (**Fig. 2-2**) are commonly the main depolymerization products detectable during fast pyrolysis process. Light oxygenated compounds, e.g., acetic acid and acetol are also observed in fast pyrolysis process, which are the derived products by ring scission reaction of carbohydrates (Patwardhan et al., 2011a; Patwardhan et al., 2011b) and by depolymerization of lignin (de Wild et al., 2011; Patwardhan et al., 2011b).

Levoglucosan (1,6-anhydro-b-D-glucopyranose), an anhydrosugar derived from the glucosidic bond cleavage, has been recognized as a crucial intermediate in the thermal decomposition of cellulose (Zhang et al., 2013c). Thermal decomposition of cellulose involves either the initial decomposition to levoglucosan followed by the subsequent dehydration, retro aldol condensation, and fragmentation reactions of levoglucosan (Lin et al., 2009) or depolymerization of cellulose or other intermediates, which competes with the formation of levoglucosan (Ohnishi et al., 1975; Ranzi et al., 2008). Furan derivatives (such as cyclopentenones) and other aliphatic oxygenates could be obtained through decomposition of cellulose and dehydration of levoglucosan (Zhang et al., 2013c).

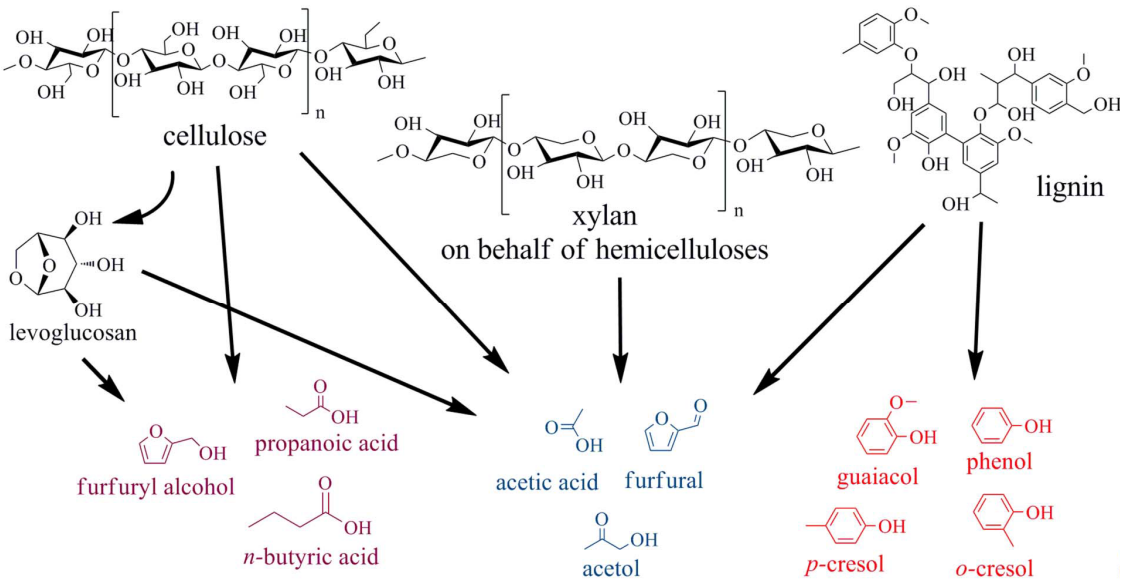

Figure 2-2 Possible pathway of depolymerization of cellulose, hemicellulose and lignin during fast pyrolysis process (Zhang et al., 2013c)

The highly reactive organic compounds, etc. aldehydes and phenols are the main reason for bio-oil chemically unstable as they can react to form resins over time. These compounds can react with each other to produce high molecular weight resin products, especially in an acidic environment. On the other hand, the organic acids present in bio-oil such as formic and acetic acid lead to a low pH in the range of 2-3. The high acidity of bio-oil leads to corrosion of equipment (Zhang et al., 2013a). Fast pyrolysis oil is also immiscible with conventional petroleum derived oil due to the considerable amount of polar and hydrophilic compounds (Mortensen et al., 2011). The average molecular weight of bio-oil was reported in the range of 370-1000 g/mol (Oasmaa & Czernik, 1999), and it could increase with time (also called "aging"). The main reactions which occur during aging include polymerization, etherification, esterification, and condensation (Diebold & Czernik, 1997; Zhang et al., 2013a).

2.2 Catalytic hydrodeoxygenation (HDO)

Bio-oilhydrodeoxygenation (HDO) process involves hydrogenation, cracking, decarbonylation, decarboxylation, hydrocracking, HDO and polymerization reactions (Zacher et al., 2014) as shown in **Fig. 2-3.** The main objective of HDO of bio-oil is to

produce oil products with reduced water and oxygen contents, decreased acidity and viscosity, and increased heating value (Gandarias et al., 2013). Due to the complexity of the reactions and the high variety of oxygenated compounds, detailed evaluation of bio-oil HDO is difficult in practice. In many cases, model compounds such as phenol, guaicol, 2-ethylphenol, methyl heptanoate or benzofuran were applied to test the activity of different catalysts and to understand the characteristics and mechanisms of the HDO process. During HDO process, H_2 plays a critical role in cracking of the oxygenated compounds (hydro-cracking) and saturating the unsaturated bonds (hydrogenation). Major reactions associated with catalytic bio-oil upgrading are illustrated in **Figure 2-3** (Zacher et al., 2014).

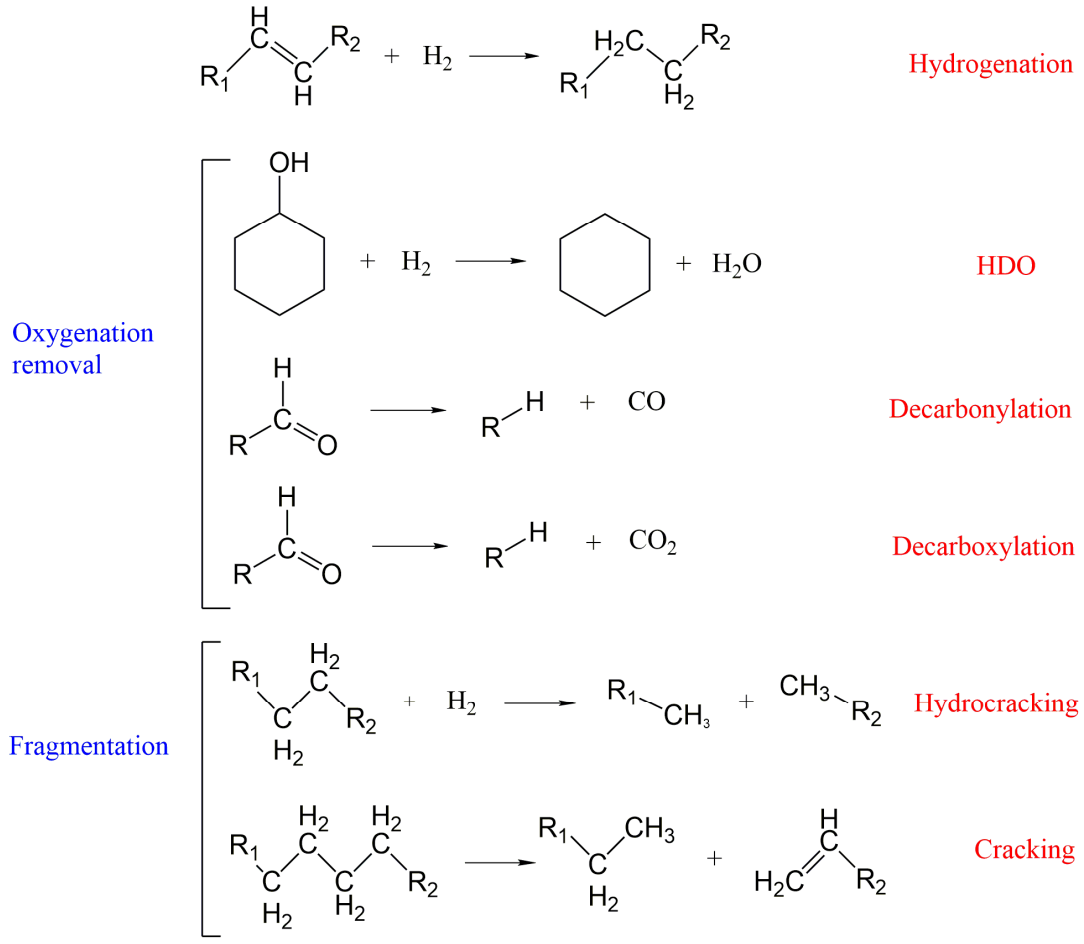

Figure 2-3 Major reactions associated with catalytic bio-oil upgrading (Zacher et al., 2014)

2.2.1 Bio-oil HDO mechanism over conventional metal sulphide catalysts

The process of bio-oil HDO is similar to hydrodesulphurization (HDS) for petroleum refining (Elliott, 2007; Furimsky, 2000; Kwon et al., 2011), where hydrogen is applied to expel heteroatom in the form of H_2O and H_2S, respectively. This is the reason why in many early HDO research works, conventional HDS catalysts, Co-MoS_2 and Ni-MoS_2 had been widely used. In terms of catalytic mechanism for these sulfide catalysts in bio-oil HDO, Co or Ni serves as promoters, donating electrons to the molybdenum atoms, which weakens the bond between molybdenum and sulphur and therefore creates a sulphur vacancy site. The sulphur vacancy site is widely believed the active site for both HDO and HDS reactions. On the other hand, heterolytic dissociation of H_2 over the catalyst surface leads to the formation of one S-H and one Mo-H groups (Blanchin et al., 2001; Kasztelan & Guillaume, 1994; Paul & Payen, 2003; Thomas et al., 1998). Then oxygen atoms of the bio-oil molecules could then adsorb on vacancies of the MoS_2 matrix. The addition of a proton to the absorbed oxygenated molecule leads to formation of an adsorbed carbocation, which can directly undergo C-O bond cleavage and the aromatic ring is regenerated leading to ethylbenzene. Finally, the vacancy is regenerated by elimination of water (Gandarias et al., 2013). Detailed reaction pathway for HDO over metal sulfide catalysts can be depicted in **Fig. 2-4**.

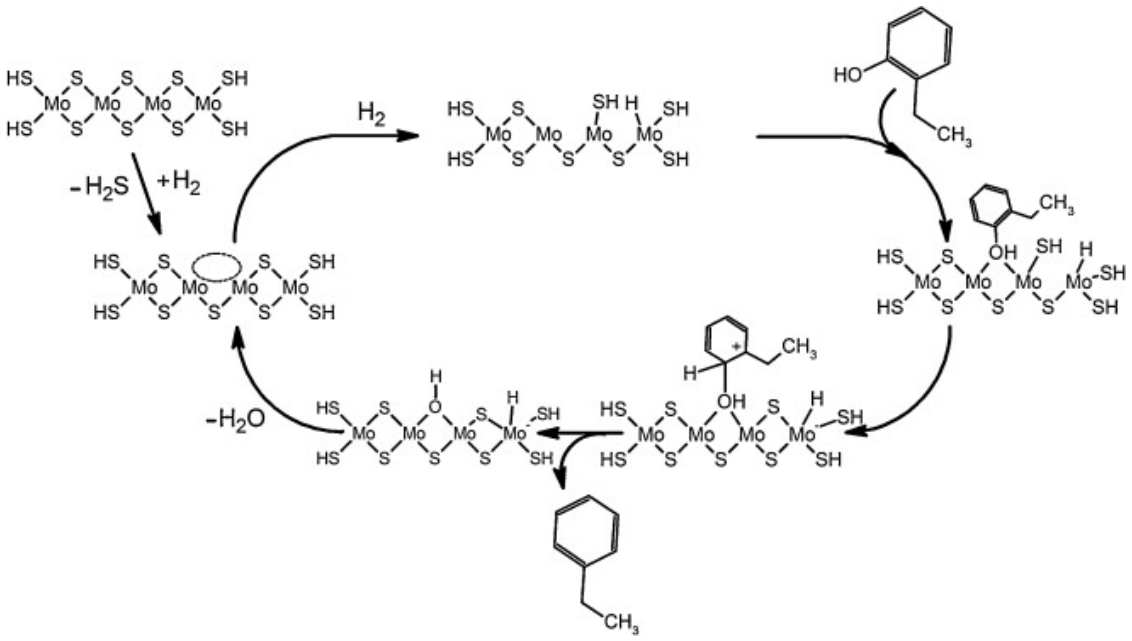

Figure 2-4 HDO mechanism over Co-MoS_2 catalysts. The cycle showed on Mo atoms indicates the catalytically active vacancy site. Refs (Mortensen et al., 2011)

However, compared with petroleum derived oil, the sulfur content of bio-oil is significantly low (mostly less than 0.1 wt %) (Ba et al., 2004). Deactivation of catalysts would occur when sulphur (in the catalysts) stripping and oxidation on the surface of catalysts during prolonged operation without sulphur in the reaction system (Gandarias et al., 2013). The alternative is co-feeding of H_2S to the system to regenerate the sulphide sites. However, using these types of catalysts for bio-oil HDO is challenging, because bio-oil could be contaminated by sulphur.

2.2.2 Bio-oil HDO mechanism over transition metal catalysts

A great deal of research was carried out using transition metal catalysts for HDO of bio-oil. The mechanism of HDO over a metallic catalyst is still not confirmed. It is generally believed that the catalysts play bifunctional roles in the process (Mortensen et al., 2011). On one hand, activation of oxy-compounds is enabled while interacting of the compound with catalyst support as shown in **Figure 2-5**. On the other hand, OH hydrogenation takes place on the metal surface to form H_2O (Mendes et al., 2001).

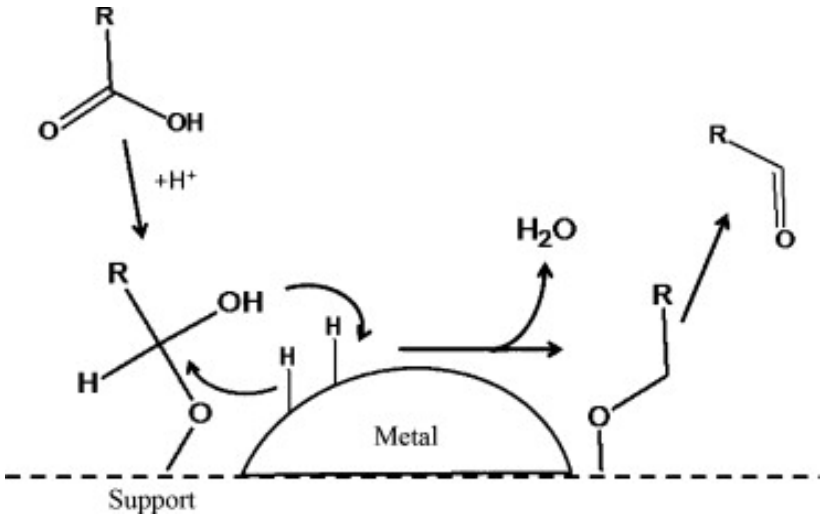

Figure 2-5 HDO mechanism over transition metal catalysts. Refs (Mortensen et al., 2011; Wildschut et al., 2009)

2.3 HDO catalysts

Various HDO catalysts have been investigated under different reaction conditions. A summary of reaction operation parameters, oil yield and degree of deoxygenation (DOD) for some of the bio-oil HDO work are shown in **Table 2-1**. From the table, we can get a brief overview of the effect of metal, catalyst support and reaction condition on HDO process.

Table 2-1 Overview of catalysts investigated for bio-oil hydrodeoxygenation (HDO)

	Oil yield (wt.%)[a]	DOD (wt.%)[a]	Catalyst	Temperature (℃)	Pressure (bar)	Time (h)	Reactor type
(Wildschut et al., 2009)	30	36	$NiMoS/Al_2O_3$	250	100	4	Batch
	43	56	Pd/C	250	100	4	Batch
	27	41	$CoMoS/Al_2O_3$	250	100	4	Batch
	35	45	Ru/C	250	100	4	Batch
	27	74	$NiMoS/Al_2O_3$	350	200	4	Batch
	65	85	Pd/C	350	200	4	Batch
	25	82	$CoMoS/Al_2O_3$	350	200	4	Batch
	53	86	Ru/C	350	200	4	Batch
(Elliott et al., 2009)	62	71	Pd/C	340	135	4	Continuous
	45	75	Pd/C	343	135	4	Continuous
	61	98.8	Proprietary cat.	405	102	5	Continuous
	81	98.7	Proprietary cat.	405	102	5	Continuous
	50	98.4	Pd/C & Proprietary cat.	250/410	135	6.67	Continuous

	54	99	Pd/C & Proprietary cat.	250/410	135	6.67	Continuous
	37	99.3	Pd/C & Proprietary cat.	250/410	135	6.67	Continuous
(Venderbosch et al., 2010)	63	26.9	Ru/C	300	250	-	Continuous
	95	16.9	Ru/C	175	200	0.1	Continuous
	50	35.4	Ru/C	225	200	0.1	Continuous
	54	44.7	Ru/C	175/225/375/400	241	0.1	Continuous
	52	64.1	Ru/C	350/225/375/400	230	0.18	Continuous
(Elliott et al., 2012)	45	99	RuS/C-NiMoS/C	170/390	135	5.26/5.26	Continuous
	37	94	RuS/C-CoMoS/C	170/390	135	5.26/5.26	Continuous
	43	95	RuS/C-CoMoS/C	170/390	135	5.26/5.26	Continuous
(de Miguel Mercader et al., 2011)	53	31.0	Ru/C	220	190	4	Batch
	58	40.8	Ru/C	270	190	4	Batch
	56	59.7	Ru/C	310	190	4	Batch
	15	43.4	Ru/C	220	190	4	Batch
	30	43.4	Ru/C	270	190	4	Batch

	31	51.7	Ru/C	310	190	4	Batch
	83	38.0	Ru/C	220	190	4	Batch
	74	41.9	Ru/C	270	190	4	Batch
	70	64.9	Ru/C	310	190	4	Batch
(Ardiyanti et al., 2012)	45.5	62.3	NiCu/TiO_2	150/350	200	1/3	Batch
	35.9	86.5	NiCu/Sibunite	150/350	200	1/3	Batch
	42.2	57.4	NiCu/δ-Al_2O_3	150/350	200	1/3	Batch

[a] dry feed basis

2.3.1 Influence of operating condition

For petroleum hydroprocessing, it has been observed that NiMoS and CoMoS catalysts were very active when the reaction temperature was greater than 350 °C. However, for bio-oil hydroprocessing reaction temperature should not be too high to prevent massive reactor coking (Baker & Elliott, 1988). Elliot et al. developed a two-stage hydrotreatment process, where in the first stage the temperature was maintained between 250 °C to 280 °C in which the reactive components in the oil were "stabilized". Subsequently in the second stage, the stabilized oil can be further processed at 370 °C to 400 °C. Since then, two-stage (even multi-stage) systems (Elliott, 2007; Elliott et al., 2012; Elliott et al., 2009; Traynor & Brandvold, 2010; Traynor et al., 2011; Venderbosch et al., 2010) have been incorporated in the catalytic HDO of bio-oil.

In 2009, Elliott et al. employed combined carbon supported noble metal catalyst Pd/C and a proprietary sulphide catalyst in a down-flow reactor. With this two-staged configurations, they successfully achieved 98 ~ 99 % deoxygenation of bio-oils (Elliott et al., 2009).

Later, they conducted a series of experiments using two-stage non-isothermal reactor configuration for HDO of pyrolysis oil. In the low-temperature stage (150 °C to 200 °C) RuS/C was used as catalyst and in the high temperature (350 °C to 405 °C) stage, $CoMoS_2$/C was used as catalyst under H_2 pressure of 140 bar. The obtained oil yields were in the range of 35-45 % depending on different feedstocks, and the degree of deoxygenation was as high as 99 % even after 89 h time-on-stream analysis (Venderbosch et al., 2010).

de Miguel Mercader et al. also investigated the HDO of sawdust-derived pyrolysis oil over commercial Ru/C (5 wt.%) in a batch reactor (de Miguel Mercader et al., 2010). Typical runs were conducted for 4 h at a temperature ranging from 230 to 340 °C, using 290 bar H_2 pressure. Three distinct phases were obtained when temperature was above 300 °C, i.e., a heavy bottom oil/catalyst layer, a light oil product in the middle and an aqueous layer on the top. The amount of top-oil micro-carbon residue decreased from 4.7

wt.% to 2.2 wt.% accompanied with an decrease in oxygen content by 6 wt.% while increasing the temperature from 230 to 340 °C, but the total dry oil yields were insensitive to temperature and remained relatively constant at 50 %. Similar effects of reaction temperature (in the range of 220-310 °C) on the removal of oxygen in a pyrolysis oil during HDO over Ru/C catalyst was also reported in another study by the same authors (de Miguel Mercader et al., 2011).

Low temperature stabilization before HDO of bio-oil was found to be an effective measure to increase lifetime of the HDO catalyst (Teella et al., 2011). Ru/C was able to remain its activity for a longer operation time in a non-isothermal reactor (Zacher et al., 2014), However, the lifetime of HDO catalysts is an important knowledge gap that has tremendous impact on the current catalytic upgrading process (Arbogast et al., 2013; Jones et al., 2009), although Elliott et al. reported Pd/C catalysts lifetime could be as high as 100 h for HDO of bio-oil in a continuous flow setup at 340 °C, and about 200 h lifetime was reported in another study on HDO of bio-oils with Co-MoS_2/Al_2O_3 (Zacher et al., 2014).

2.3.2 Transition metals/metal oxides

Various catalyst formulations have been examined for the HDO process, mainly including the transition metals or metal oxides (such as Co, Ni, Mo, W, Fe) as well as noble metals (such as Ru, Pt, Pd, Rh).

Wildschut et al. investigated the effects of the noble-metal catalysts Ru, Pt, Pd supported on carbon for HDO of bio-oils in a batch reactor under a two stage operating conditions (250 °C at 100 bar for mild HDO and 350 °C at 200 bar for deep HDO). The HDO activity results indicated that both the oil yields and the degree of deoxygenation were higher with the noble-metal catalysts than those with the conventional hydro-treatment catalysts (Co-MoS_2/Al_2O_3 and Ni-MoS_2/Al_2O_3 catalysts). Besides, the carbon/coke deposition on the noble metal catalysts was much less evident compared with the conventional hydro-treatment catalysts (Wildschut et al., 2009).

Gutierrez et al. investigated bio-oil HDO activity of Pd, Rh and Pt supported on ZrO_2, compared with a conventional hydro-treatment catalyst Co–MoS_2/Al_2O_3 in a batch reactor under 8 MPa H_2 pressure at 100 °C reaction temperature. The HDO activity was found to be in the following order: Rh/ZrO_2 > Co–MoS_2/Al_2O_3 > Pd/ZrO_2 > Pt/ZrO_2 (Gutierrez et al., 2009).

Metal oxide and metal sulphide-based catalysts are believed to follow the similar HDO mechanism, where the catalytic activity relies mainly on the amount of acid sites (Mortensen et al., 2011). Gervasini et al (Gervasini & Auroux, 1991) reported that the relative Lewis acid site concentration (strength) on the surface of the following oxides decreases in the following order: Cr_2O_3 > WO_3 > Nb_2O_5 > Ta_2O_5 > V_2O_5 ≈ MoO_3. Referring to the combinations of oil yields, degree of deoxygenation (DOD), hydrogen consumption and coke formation, they proposed that Ru/C can be the most promising catalyst for further study of catalytic HDO comparing with other noble metal catalysts. However, these noble metal catalysts are not attractive from practical point of view due to their high price, unless good strategy for catalyst recycling can be developed.

Efforts on developing less expensive in-house prepared Ru catalysts as substitutes for the commercial Ru/C have been made by Wildschut et al.. They investigated the stability of some in-house synthesized Ru catalysts supported on carbon in HDO process at 350 °C and 20 MPa in a batch reactor. They found that Ru/C prepared using $RuCl_3$ as the precursor (among all three ruthenium precursor: $RuCl_3$, $Ru(NO)(NO_3)_3$ and $Ru(acac)_3$) with loading of 5 wt.% performed best (Wildschut et al., 2010). More research is undergoing to develop inexpensive HDO catalysts.

2.3.3 Metal phosphides

Recently, phosphides of transition metals have attracted a significant attention for bio-oil upgrading due to their improved activities compared with metals or metal oxides. In the past 20-30 years, a great deal of work has shown that MoP, WP (Eijsbouts et al., 1991; Oyama et al., 2002), CoP (Tischer et al., 1987), Fe_2P (Dhandapani et al., 1998), and Ni_2P (Dhandapani et al., 1998) are highly active for hydrodesulfurization (HDS) and hydrodenitrogenation (HDN) of petroleum. Most studies demonstrated that P could

enhance the activity of the catalyst owing to their following characteristics: (1) good hydrogen-transfer properties; (2) stabilization of metal precursor solutions (even with high metal concentrations) in the metal loading process, leading to better dispersion of metal ions in the catalyst support (Oyama et al., 2002); (3) improvement of coke resistance, support strength and stability of the catalyst (Tolman et al., 1988); (4) improvement of dispersion of metal active phases (Lewis & Kydd, 1992; Morales & de Agudelo, 1986; Oyama et al., 2002); (5) optimization of the catalyst's acidity (Gishti et al., 1984; Lewis & Kydd, 1992); (6) formation of new kinds of active sites involving phosphorus (Crajé et al., 1991); and (7) alteration of the reaction mechanism (Eijsbouts et al., 1991; Mangnus et al., 1991).

Chadwick et al. evaluated MoP/Al_2O_3 catalyst for bio-oil HDO, they reported that phosphorus altered the acid–base characteristics of alumina and improved dispersion of molybdenum on the alumina support. It also enhanced the solubility of the precursor metal compounds, which allow synthesis of catalysts with metal high-loadings (Chadwick et al., 1983).

Zhao et al. tested a series of novel transition metal phosphides supported on SiO_2 for hydroprocessing using guaiacol as a model compound for pyrolysis oil at temperatures ranging from 200 to 300 °C. They reported that the activity of these catalysts followed the order of $Ni_2P > Co_2P > Fe_2P \cong WP \cong MoP$. When compared these catalysts with the commercial hydroprocessing catalysts 5 % Pd/Al_2O_3 and $Co\text{-}MoS/Al_2O_3$, they concluded that although Pd/Al_2O_3 was more active than the metal phosphides at a shorter contact time but produced only catechol. The metal phosphides were more active than $Co\text{-}MoS/Al_2O_3$ for bio-oil HDO (Breaking the et al., 2008). Bui et al. also reported the following order of catalysts activity for bio-oil HDO: $Ni_2P > WP > MoP > CoP > FeP > Pd/Al_2O_3$ (Bui et al., 2012).

Chen et al. investigated the performance of a series of silica-supported metals (Ni, Co, Fe, Mo and W) phosphides in HDO of methyl laurate model compound at 573 K under 2 MPa H_2 cold pressure. They reported that the catalyst activity followed the order of $Ni_2P > MoP > CoP\text{-}Co_2P > WP > Fe_2P\text{-}FeP$ and $Ni \approx Ni_2P > Ni_{12}P_5 > Ni_3P$. These studies

demonstrated that the high HDO activity of these catalysts was mainly attributed to the increased metal site density on the surface, electron density of metal and the Brönsted acidity (Chen et al., 2014a).

The phosphorus content also exhibits significant effects on the HDO activities of the metal phosphide. A high phosphorus loading could result in negative effects on catalytic activities. Leiva et al. evaluated the effects of P content on MoS_2/γ-Al_2O_3 catalysts for HDO of a bio-oil model compound, i.e., guaiacol, at 573 K and 5 MPa. The catalysts were prepared by incipient wetness impregnation method by varying the P (0.5, 1.0, 2.0. 3.0 and 5.0 wt.%) content with fixed Mo (15 wt.%) loading. They claimed that the increase in activity with increasing P content was ascribed to the formation of two-dimensional MoS_2, while the subsequent decrease in activity with further increasing P content was due to the formation of three-dimensional MoS_2 resulting in the loss of activity sites (Leiva et al., 2013).

2.3.4 Bimetallic catalysts

Bimetallic catalysts, e.g., $NiMo/Al_2O_3$ sulfided catalyst, were found to be more active than the mono-metallic catalysts, such as, Ni/Al_2O_3 and Mo/Al_2O_3 sulfided catalysts in hydrotreating of rapeseed oil (Kubička & Kaluža, 2010). The selectivity to hydrocarbons over the bimetallic NiMo catalyst was also significantly higher than the monometallic catalysts, suggesting synergy between Ni and Mo during the bio-oil HDO process (Choudhary & Phillips, 2011). Another research conducted by Yakovlev et al. also demonstrated that bimetallic Ni–Cu catalysts were superior to Ni catalysts for biodiesel upgrading by hydro-processing. In their study, deoxygenation over the $Ni–Cu/CeO_2$ catalyst was through decarboxylation, while the major route over Ni/CeO_2 was C–O bond hydrogenolysis (Dundich et al., 2010).

In 2014, Chen et al. investigated SiO_2-supported Ni_2P, MoP and Ni–Mo bimetallic phosphides with different Ni/Mo ratios for the HDO of methyl laurate to C11 and C12 hydrocarbons (at 300–340 °C, 3 MPa cold pressure of H_2). Catalyst characterization results revealed that the metal dispersion and acidity of phosphide catalyst decreased with the increase of Ni/Mo ratio. In addition, X-ray photoelectron spectroscopy indicated that

the electron transfer occurred not only from metal (Ni and Mo) to P but also from Ni to Mo derived from the incorporation of Mo into Ni_2P as well as the formation of $MoNiP_2$ phase. The electronic interaction between Ni and Mo might account for the enhanced performance of the bimetallic catalysts for the HDO reactions (Chen et al., 2014b).

2.3.5 Effects of catalyst support

The choice of catalyst support is a crucial aspect of heterogeneous catalyst formulation (Yakovlev et al., 2009). However, a limited number of studies have been reported on the effects of catalyst support on the performance of catalysts in bio-oil HDO. Generally, two perspectives need to take into account when choosing catalyst support: (1) the catalyst's resistance to carbon deposition, and (2) its ability to activate oxy-compounds to facilitate the HDO reactions (Mortensen et al., 2011).

Al_2O_3 has been commonly utilized as a catalyst support for traditional petroleum oil hydro-processing. However, it has been reported that the support alumina could be transformed to boemite (AlO(OH)) in the presence of large amount of water during HDO of bio-oil. (Elliott, 2007; Laurent & Delmon, 1994; Venderbosch et al., 2010). Besides, coke deposition was found extremely severe on Al_2O_3 supported catalysts which was likely due to the high acidity of Al_2O_3 (Popov et al., 2010). Alternatively, activated carbon (AC) has been recognized as a more promising support (Echeandia et al., 2010; Elliott & Hart, 2008; Maggi & Delmon, 1994; Pawelec & Fierro, 2014; Wildschut et al., 2009). Not only because carbon has a larger surface area than alumina, but also the neutral nature of carbon has some major advantages, which gives better resistance to carbon/coke deposition compared to Al_2O_3 (Echeandia et al., 2010; Elliott et al., 2009). SiO_2 has also been identified as a promising support material, like activated carbon, as it is generally neutral in nature and therefore has relatively low affinity for coke formation (Zhao et al., 2011). ZrO_2 and CeO_2 had also been investigated as potential supports for HDO catalysts due to their ability in activating oxy-compounds on their surface and their weaker acidity compared with Al_2O_3 (Bui et al., 2011).

Newman et al. prepared a series of Ru catalysts supported on different supports including activated carbon, silica, alumina and titania and tested their activities for HDO of

substituted phenols as bio-oil model compounds. The results revealed that the catalyst supports seemed to have little to do with its activity in the HDO tests, but the selectivity of the catalysts was greatly influenced by the type of the support. TiO_2 was found to be highly active and selective. This can be explained by the spillover effect in which Ti^{3+} sites are created and interact strongly with the oxygen atoms in the oxy-compounds, weakening the aromatic C-O bond by hydrogenolysis (Newman et al., 2014).

Zhang et al. synthesized a series of non-sulphided Ni-based catalysts supported on HZSM-5 with different ratio of Si/Al. Phenol was used as a model compound to evaluate the HDO activity of the prepared catalysts. The activity of tested catalysts was found to decrease in the following order: Ni/HZSM-5 (Si/Al = 38) > Ni/HZSM-5(Si/Al = 50) > Ni/γ-Al_2O_3, suggesting that acidity of the support has a negative effect on the catalyst's activity (Zhang et al., 2013b).

Nava et al. investigated the effects of mesoporous silicate supports (SBA-15, HMS, SBA-16, DMS-1) on the hydroprocessing of an olive oil by-product in a fixed bed reactor at 250 °C, 3 MPa H_2 pressure using sulphided CoMo catalysts (Nava et al., 2009). The stability of catalysts with respect to resistance to coking follows the trend of CoMo/HMS > CoMo/SBA-15 ≈ CoMo/DMS-1 > CoMo/SBA-15. Thus, obvious correlation between the stability (resistance to coking) and acidity of the catalyst support was not found, but rather the resistance to coking of the catalysts depends more on the morphological structure of catalyst support materials (Pieck et al., 1989).

2.4 Effects of solvent

The solvents used in HDO process were believed to play a critical role in preventing or decreasing the re-polymerization/condensation reactions of the bio-oil derived intermediates or products via esterification, acetalization or phenol-aldehyde resinification reactions (Wan et al., 2014; Xu et al., 2013; Zhang et al., 2007). Also, some solvents such as tetralin, long chain alkanes and isopropanol, etc., can act as hydrogen donor to restrain coke formation, and hence improve the yield and H/C molar ratio of the upgraded oil products (Elliott, 2007; Zhang et al., 2005).

Zhang et al. studied HDO of fast pyrolysis oil using sulphided Co–Mo–P catalyst in an autoclave using tetralin and tar oil as solvents, where a higher liquid yield was resulted when tetralin was used as solvent, suggesting that tetralin can serve as a hydrogen donor that transfers hydrogen from the gas phase into reaction medium as hydrogen atoms/radicals that stabilize the reaction intermediates, preventing the formation of coke and enhancing the yield of the upgraded oil products (Zhang et al., 2005).

Xu et al. employed four kinds of organic solvents i.e. tetraline, decalin, diesel and a mixture of diesel and isopropanol in their mild HDO process (the first stage HDO process), with commercial Ru/C catalyst at 300 °C, 10 MPa H_2 for 3 h (Xu et al., 2013). The coke formation with a solvent was about 2 % less than that obtained at the same condition but without solvent. Wan et al. reported a systematic study of solvent effects on low-temperature hydrogenation of various model oxygenates in bio-oils (such as 2-butanone, 2-pentanone, and phenol) with the commercial Ru/C catalyst (Wan et al., 2014). Three types of solvents, protic (e.g., water and C_1–C_4 primary alcohols), aprotic polar, and aprotic apolar solvents were investigated. The results showed that for 2-butanone hydrogenation over Ru/C led to the highest hydrogenation activity in water, followed by alcohols. A remarkably lower hydrogenation activity was observed in aprotic apolar solvents (i.e., cyclohexane and n-heptane). However, almost no hydrogenation activity was observed in aprotic polar solvents (i.e., c-butyrolactone, acetonitrile, and tetrahydrofuran).

In another study, He et al. examined the HDO of phenol by employing three different solvents: water, methanol, and hexadecane over mixture of Pd/C and HZSM-5 catalyst at 473 K. Individual phenol hydrogenation rates are much lower in methanol and hexadecane than in water, while rate of cyclohexanol dehydration and cyclohexene hydrogenation were similar in three solvents (He et al., 2014).

2.5 Challenges of bio-oil HDO and concluding remarks

Bio-oil has many advantages such as less toxic, carbon-neutral and stronger biodegradation, but also comes with a number of disadvantages: high contents of water/oxygen/impurity levels, molecular complexity, coking propensity, low pH value

(high corrosiveness), high viscosity, chemical and thermal instability, low heating value, and poor ignition and combustion properties. Bio-oil can be upgraded via HDO into liquid transportation fuels or a feedstock that can be co-processed with petroleum in conventional oil refineries. However, in addition to non-technical challenges for bio-fuel production (such as infrastructure requirement, logistics and economics), the existing HDO processes have several major technical challenges, e.g., low process efficiency, expensive catalysts, instability and low lifetime of the HDO catalysts and poor product quality (Al-Sabawi & Chen, 2012; Choudhary & Phillips, 2011; de Miguel Mercader et al., 2010). All these technical challenges may be addressed by developing inexpensive and active HDO catalysts.

References

Al-Sabawi, M., Chen, J. 2012. Hydroprocessing of biomass-derived oils and their blends with petroleum feedstocks: a review. *Energy & Fuels*, **26**(9), 5373-5399.

Arbogast, S., Bellman, D., Paynter, J.D., Wykowski, J. 2013. Advanced biofuels from pyrolysis oil… Opportunities for cost reduction. *Fuel Processing Technology*, **106**, 518-525.

Ardiyanti, A.R., Khromova, S.A., Venderbosch, R.H., Yakovlev, V.A., Melián-Cabrera, I.V., Heeres, H.J. 2012. Catalytic hydrotreatment of fast pyrolysis oil using bimetallic Ni–Cu catalysts on various supports. *Applied Catalysis A: General*, **449**, 121-130.

Aston.ac.uk,. 'Fast Pyrolysis'. N.p., 2015. Web. 17 Aug. 2015.

Ba, T., Chaala, A., Garcia-Perez, M., Rodrigue, D., Roy, C. 2004. Colloidal properties of bio-oils obtained by vacuum pyrolysis of softwood bark. Characterization of water-soluble and water-insoluble fractions. *Energy & Fuels*, **18**(3), 704-712.

Baker, E.G., Elliott, D.C. 1988. Catalytic upgrading of biomass pyrolysis oils. in: *Research in thermochemical biomass conversion*, Springer, pp. 883-895.

Blanchin, S., Galtier, P., Kasztelan, S., Kressmann, S., Penet, H., Pérot, G. 2001. Kinetic modeling of the effect of H_2S and of NH_3 on toluene hydrogenation in the presence of a $NiMo/Al_2O_3$ hydrotreating catalyst. Discrimination between homolytic and heterolytic models. *The Journal of Physical Chemistry A*, **105**(48), 10860-10866.

Breaking the, C., Engineering Barriers to Lignocellulosic, B., Huber, G.W. 2008. *Breaking the chemical and engineering barriers to lignocellulosic biofuels: next generation hydrocarbon biorefineries*. Washington, DC: National Science Foundation, Chemical, Biogengineering, Environmental and Transport Systems Division.

Bridgwater, A.V. 2003. Renewable fuels and chemicals by thermal processing of biomass. *Chemical Engineering Journal*, **91**(2), 87-102.

Bridgwater, A.V. 2012. Review of fast pyrolysis of biomass and product upgrading. *Biomass and Bioenergy*, **38**, 68-94.

Bridgwater, A.V., Peacocke, G.V.C. 2000. Fast pyrolysis processes for biomass. *Renewable and Sustainable Energy Reviews*, **4**(1), 1-73.

Bui, P., Cecilia, J.A., Oyama, S.T., Takagaki, A., Infantes-Molina, A., Zhao, H., Li, D., Rodríguez-Castellón, E., López, A.J. 2012. Studies of the synthesis of transition metal phosphides and their activity in the hydrodeoxygenation of a biofuel model compound. *Journal of Catalysis*, **294**, 184-198.

Bui, V.N., Laurenti, D., Delichère, P., Geantet, C. 2011. Hydrodeoxygenation of guaiacol: Part II: Support effect for CoMoS catalysts on HDO activity and selectivity. *Applied Catalysis B: Environmental*, **101**(3), 246-255.

Chadwick, D., Aitchison, D.W., Badilla-Ohlbaum, R., Josefsson, L. 1983. Influence of phosphorus on the HDS activity of Ni-Mo/γ-Al_2O_3 catalysts. *Studies in Surface Science and Catalysis*, **16**, 323-332.

Chen, J., Shi, H., Li, L., Li, K. 2014a. Deoxygenation of methyl laurate as a model compound to hydrocarbons on transition metal phosphide catalysts. *Applied Catalysis B: Environmental*, **144**, 870-884.

Chen, J., Yang, Y., Shi, H., Li, M., Chu, Y., Pan, Z., Yu, X. 2014b. Regulating product distribution in deoxygenation of methyl laurate on silica-supported Ni–Mo phosphides: Effect of Ni/Mo ratio. *Fuel*, **129**, 1-10.

Choudhary, T.V., Phillips, C.B. 2011. Renewable fuels via catalytic hydrodeoxygenation. *Applied Catalysis A: General*, **397**(1), 1-12.

Christensen, E.D., Chupka, G.M., Luecke, J., Smurthwaite, T., Alleman, T.L., Iisa, K., Franz, J.A., Elliott, D.C., McCormick, R.L. 2011. Analysis of oxygenated compounds in hydrotreated biomass fast pyrolysis oil distillate fractions. *Energy & Fuels*, **25**(11), 5462-5471.

Crajé, M.W.J., De Beer, V.H.J., Van der Kraan, A.M. 1991. Mössbauer emission study on 57 Co doped carbon-supported Ni and Ni-Mo sulfide hydrotreating catalysts. The influence of phosphorus on the structure. *Catalysis Today*, **10**(3), 337-344.

Czernik, S., Bridgwater, A.V. 2004. Overview of applications of biomass fast pyrolysis oil. *Energy & Fuels*, **18**(2), 590-598.

de Miguel Mercader, F., Groeneveld, M.J., Kersten, S.R.A., Way, N.W.J., Schaverien, C.J., Hogendoorn, J.A. 2010. Production of advanced biofuels: Co-processing of upgraded pyrolysis oil in standard refinery units. *Applied Catalysis B: Environmental*, **96**(1), 57-66.

de Miguel Mercader, F., Koehorst, P.J.J., Heeres, H.J., Kersten, S.R.A., Hogendoorn, J.A. 2011. Competition between hydrotreating and polymerization reactions during pyrolysis oil hydrodeoxygenation. *AIChE Journal*, **57**(11), 3160-3170.

de Wild, P., Reith, H., Heeres, E. 2011. Biomass pyrolysis for chemicals. *Biofuels*, **2**(2), 185-208.

Dhandapani, B., Ramanathan, S., Yu, C.C., Frühberger, B., Chen, J.G., Oyama, S.T. 1998. Synthesis, Characterization, and Reactivity Studies of Supported Mo_2C with Phosphorus Additive. *Journal of catalysis*, **176**(1), 61-67.

Diebold, J.P., Czernik, S. 1997. Additives to lower and stabilize the viscosity of pyrolysis oils during storage. *Energy & Fuels*, **11**(5), 1081-1091.

Dundich, V.O., Khromova, S.A., Ermakov, D.Y., Lebedev, M.Y., Novopashina, V.M., Sister, V.G., Yakimchuk, A.I., Yakovlev, V.A. 2010. Nickel catalysts for the hydrodeoxygenation of biodiesel. *Kinetics and Catalysis*, **51**(5), 704-709.

Echeandia, S., Arias, P.L., Barrio, V.L., Pawelec, B., Fierro, J.L.G. 2010. Synergy effect in the HDO of phenol over Ni–W catalysts supported on active carbon: Effect of tungsten precursors. *Applied Catalysis B: Environmental*, **101**(1), 1-12.

Eijsbouts, S., Van Gestel, J.N.M., Van Veen, J.A.R., De Beer, V.H.J., Prins, R. 1991. The effect of phosphate on the hydrodenitrogenation activity and selectivity of alumina-supported sulfided Mo, Ni, and Ni-Mo catalysts. *Journal of Catalysis*, **131**(2), 412-432.

Elliott, D.C. 2007. Historical developments in hydroprocessing bio-oils. *Energy & Fuels*, **21**(3), 1792-1815.

Elliott, D.C., Hart, T.R. 2008. Catalytic hydroprocessing of chemical models for bio-oil. *Energy & Fuels*, **23**(2), 631-637.

Elliott, D.C., Hart, T.R., Neuenschwander, G.G., Rotness, L.J., Olarte, M.V., Zacher, A.H., Solantausta, Y. 2012. Catalytic hydroprocessing of fast pyrolysis bio-oil from pine sawdust. *Energy & Fuels*, **26**(6), 3891-3896.

Elliott, D.C., Hart, T.R., Neuenschwander, G.G., Rotness, L.J., Zacher, A.H. 2009. Catalytic hydroprocessing of biomass fast pyrolysis bio-oil to produce hydrocarbon products. *Environmental Progress & Sustainable Energy*, **28**(3), 441-449.

Furimsky, E. 2000. Catalytic hydrodeoxygenation. *Applied Catalysis A: General*, **199**(2), 147-190.

Gandarias, I., Arias, P.L., Fang, Z. 2013. *Hydrotreating catalytic processes for oxygen removal in the upgrading of bio-oils and bio-chemicals*. INTECH Open Access Publisher.

Gervasini, A., Auroux, A. 1991. Acidity and basicity of metal oxide surfaces II. Determination by catalytic decomposition of isopropanol. *Journal of Catalysis*, **131**(1), 190-198.

Gishti, K., Iannibello, A., Marengo, S., Morellili, G., Tittarelli, P. 1984. On the role of phosphate anion in the MoO_3/Al_2O_3 based catalysts. *Applied Catalysis*, **12**(4), 381-393.

Glasser, W.G., Northey, R.A., Schultz, T.P. 2000. *Lignin: historical, biological, and materials perspectives*. American Chemical Society Washington, DC.

Gutierrez, A., Kaila, R.K., Honkela, M.L., Slioor, R., Krause, A.O.I. 2009. Hydrodeoxygenation of guaiacol on noble metal catalysts. *Catalysis Today*, **147**(3), 239-246.

He, J., Zhao, C., Lercher, J.A. 2014. Impact of solvent for individual steps of phenol hydrodeoxygenation with Pd/C and HZSM-5 as catalysts. *Journal of Catalysis*, **309**, 362-375.

Jones, S.B., Valkenburg, C., Walton, C.W., Elliott, D.C., Holladay, J.E., Stevens, D.J., Kinchin, C., Czernik, S. 2009. *Production of gasoline and diesel from biomass via fast pyrolysis, hydrotreating and hydrocracking: a design case*. Pacific Northwest National Laboratory Richland, WA.

Kasztelan, S., Guillaume, D. 1994. Inhibiting effect of hydrogen sulfide on toluene hydrogenation over a molybdenum disulfide/alumina catalyst. *Industrial & Engineering Chemistry Research*, **33**(2), 203-210.

Kubička, D., Kaluža, L. 2010. Deoxygenation of vegetable oils over sulfided Ni, Mo and NiMo catalysts. *Applied Catalysis A: General*, **372**(2), 199-208.

Kwon, K.C., Mayfield, H., Marolla, T., Nichols, B., Mashburn, M. 2011. Catalytic deoxygenation of liquid biomass for hydrocarbon fuels. *Renewable Energy*, **36**(3), 907-915.

Laurent, E., Delmon, B. 1994. Influence of water in the deactivation of a sulfided NiMoγ-Al2O3 catalyst during hydrodeoxygenation. *Journal of Catalysis*, **146**(1), 281-291.

Leiva, K., Sepúlveda, C., García, R., Fierro, J.L.G., Águila, G., Baeza, P., Villarroel, M., Escalona, N. 2013. Effect of P content in the conversion of guaiacol over Mo/γ-Al_2O_3 catalysts. *Applied Catalysis A: General*, **467**, 568-574.

Lewis, J.M., Kydd, R.A. 1992. The MoO_3-Al_2O_3 interaction: Influence of phosphorus on MoO_3 impregnation and reactivity in thiophene HDS. *Journal of Catalysis*, **136**(2), 478-486.

Lin, Y.-C., Cho, J., Tompsett, G.A., Westmoreland, P.R., Huber, G.W. 2009. Kinetics and mechanism of cellulose pyrolysis. *The Journal of Physical Chemistry C*, **113**(46), 20097-20107.

Lu, Q., Li, W.-Z., Zhu, X.-F. 2009. Overview of fuel properties of biomass fast pyrolysis oils. *Energy Conversion and Management*, **50**(5), 1376-1383.

Maggi, R., Delmon, B. 1994. Comparison between 'slow' and 'flash' pyrolysis oils from biomass. *Fuel*, **73**(5), 671-677.

Mangnus, P.J., Van Langeveld, A.D., De Beer, V.H.J., Moulijn, J.A. 1991. Influence of phosphate on the structure of sulfided alumina supported cobalt-molybdenum catalysts. *Applied Catalysis*, **68**(1), 161-177.

Mendes, M.J., Santos, O.A.A., Jordão, E., Silva, A.M. 2001. Hydrogenation of oleic acid over ruthenium catalysts. *Applied Catalysis A: General*, **217**(1), 253-262.

Mohan, D., Pittman, C.U., Steele, P.H. 2006. Pyrolysis of wood/biomass for bio-oil: a critical review. *Energy & Fuels*, **20**(3), 848-889.

Morales, A., de Agudelo, M.M.R. 1986. Promoter role of octahedral Co (and Ni) in modified Co(Ni)Mo-Al_2O_3 catalysts for hydrodesulfurization reactions. *Applied Catalysis*, **23**(1), 23-34.

Mortensen, P.M., Grunwaldt, J.D., Jensen, P.A., Knudsen, K.G., Jensen, A.D. 2011. A review of catalytic upgrading of bio-oil to engine fuels. *Applied Catalysis A: General*, **407**(1), 1-19.

Nava, R., Pawelec, B., Castaño, P., Álvarez-Galván, M.C., Loricera, C.V., Fierro, J.L.G. 2009. Upgrading of bio-liquids on different mesoporous silica-supported CoMo catalysts. *Applied Catalysis B: Environmental*, **92**(1), 154-167.

Newman, C., Zhou, X., Goundie, B., Ghampson, I.T., Pollock, R.A., Ross, Z., Wheeler, M.C., Meulenberg, R.W., Austin, R.N., Frederick, B.G. 2014. Effects of support identity and metal dispersion in supported ruthenium hydrodeoxygenation catalysts. *Applied Catalysis A: General*, **477**, 64-74.

Oasmaa, A., Czernik, S. 1999. Fuel oil quality of biomass pyrolysis oils state of the art for the end users. *Energy & Fuels*, **13**(4), 914-921.

Ohnishi, A., Kato, K., Takagi, E. 1975. Curie-point pyrolysis of cellulose. *Polymer Journal*, **7**(4), 431-437.

Oyama, S.T., Wang, X., Lee, Y.K., Bando, K., Requejo, F.G. 2002. Effect of phosphorus content in nickel phosphide catalysts studied by XAFS and other techniques. *Journal of catalysis*, **210**(1), 207-217.

Patwardhan, P.R., Brown, R.C., Shanks, B.H. 2011a. Product distribution from the fast pyrolysis of hemicellulose. *ChemSusChem*, **4**(5), 636-643.

Patwardhan, P.R., Brown, R.C., Shanks, B.H. 2011b. Understanding the fast pyrolysis of lignin. *ChemSusChem*, **4**(11), 1629-1636.

Paul, J.-F., Payen, E. 2003. Vacancy formation on MoS_2 hydrodesulfurization catalyst: DFT study of the mechanism. *The Journal of Physical Chemistry B*, **107**(17), 4057-4064.

Pawelec, B., Fierro, J.L.G. 2014. Hydrodeoxygenation of Biomass-Derived Liquids over Transition-Metal-Sulfide Catalysts. *Catalytic Hydrogenation for Biomass Valorization*(13), 174.

Pettersen, R.C., Rowell, R.M. 1984. The chemistry of solid wood. *Madison (WI): US Departament of Agriculture, Forest service, Forest Products Laboratory*.

Pieck, C.L., Verderone, R.J., Jablonski, E.L., Parera, J.M. 1989. Burning of coke on $PtRe/Al_2O_3$ catalyst: Activation energy and oxygen reaction order. *Applied Catalysis*, **55**(1), 1-10.

Popov, A., Kondratieva, E., Goupil, J.M., Mariey, L., Bazin, P., Gilson, J.-P., Travert, A., Maugé, F. 2010. Bio-oils hydrodeoxygenation: adsorption of phenolic molecules on oxidic catalyst supports. *The Journal of Physical Chemistry C*, **114**(37), 15661-15670.

Ranzi, E., Cuoci, A., Faravelli, T., Frassoldati, A., Migliavacca, G., Pierucci, S., Sommariva, S. 2008. Chemical kinetics of biomass pyrolysis. *Energy & Fuels*, **22**(6), 4292-4300.

Teella, A., Huber, G.W., Ford, D.M. 2011. Separation of acetic acid from the aqueous fraction of fast pyrolysis bio-oils using nanofiltration and reverse osmosis membranes. *Journal of Membrane Science*, **378**(1), 495-502.

Thomas, C., Vivier, L., Travert, A., Maugé, F., Kasztelan, S., Pérot, G. 1998. Deuterium tracer studies on hydrotreating catalysts. 2. Contribution of the hydrogen of the alumina support to HD exchange. *Journal of Catalysis*, **179**(2), 495-502.

Tischer, R.E., Narain, N.K., Stiegel, G.J., Cillo, D.L. 1987. Effect of phosphorus on the activity of nickel-molybdenum/alumina coal-liquid upgrading catalysts. *Industrial & Engineering Chemistry Research*, **26**(3), 422-426.

Tolman, C.A., Druliner, J.D., Krusic, P.J., Nappa, M.J., Seidel, W.C., Williams, I.D., Ittel, S.D. 1988. Catalytic conversion of cyclohexylhydroperoxide to cyclohexanone and cyclohexanol. *Journal of Molecular Catalysis*, **48**(1), 129-148.

Traynor, T., Brandvold, T.A. 2010. Methods for producing low oxygen biomass-derived pyrolysis oils, U.S. Patent Application 12/843,649.

Traynor, T., Brandvold, T.A., Abrahamian, J.F. 2011. Methods and catalysts for deoxygenating biomass-derived pyrolysis oil, U.S. Patent Application 13/150,844.

Venderbosch, R.H., Ardiyanti, A.R., Wildschut, J., Oasmaa, A., Heeres, H.J. 2010. Stabilization of biomass-derived pyrolysis oils. *Journal of Chemical Technology and Biotechnology*, **85**(5), 674-686.

Venderbosch, R.H., Prins, W. 2010. Fast pyrolysis technology development. *Biofuels, Bioproducts & Biorefining*, **4**(2), 178.

Wan, H., Vitter, A., Chaudhari, R.V., Subramaniam, B. 2014. Kinetic investigations of unusual solvent effects during Ru/C catalyzed hydrogenation of model oxygenates. *Journal of Catalysis*, **309**, 174-184.

Wildschut, J., Mahfud, F.H., Venderbosch, R.H., Heeres, H.J. 2009. Hydrotreatment of fast pyrolysis oil using heterogeneous noble-metal catalysts. *Industrial & Engineering Chemistry Research*, **48**(23), 10324-10334.

Wildschut, J., Melian-Cabrera, I., Heeres, H.J. 2010. Catalyst studies on the hydrotreatment of fast pyrolysis oil. *Applied Catalysis B: Environmental*, **99**(1), 298-306.

Wu, C., Wang, Z., Huang, J., Williams, P.T. 2013. Pyrolysis/gasification of cellulose, hemicellulose and lignin for hydrogen production in the presence of various nickel-based catalysts. *Fuel*, **106**, 697-706.

Xu, X., Zhang, C., Liu, Y., Zhai, Y., Zhang, R. 2013. Two-step catalytic hydrodeoxygenation of fast pyrolysis oil to hydrocarbon liquid fuels. *Chemosphere*, **93**(4), 652-660.

Yakovlev, V.A., Khromova, S.A., Sherstyuk, O.V., Dundich, V.O., Ermakov, D.Y., Novopashina, V.M., Lebedev, M.Y., Bulavchenko, O., Parmon, V.N. 2009. Development of new catalytic systems for upgraded bio-fuels production from bio-crude-oil and biodiesel. *Catalysis Today*, **144**(3), 362-366.

Yaman, S. 2004. Pyrolysis of biomass to produce fuels and chemical feedstocks. *Energy Conversion and Management*, **45**(5), 651-671.

Zacher, A.H., Olarte, M.V., Santosa, D.M., Elliott, D.C., Jones, S.B. 2014. A review and perspective of recent bio-oil hydrotreating research. *Green Chemistry*, **16**(2), 491-515.

Zhang, L., Liu, R., Yin, R., Mei, Y. 2013a. Upgrading of bio-oil from biomass fast pyrolysis in China: A review. *Renewable and Sustainable Energy Reviews*, **24**, 66-72.

Zhang, Q., Chang, J., Wang, T., Xu, Y. 2007. Review of biomass pyrolysis oil properties and upgrading research. *Energy Conversion and Management*, **48**(1), 87-92.

Zhang, S., Yan, Y., Li, T., Ren, Z. 2005. Upgrading of liquid fuel from the pyrolysis of biomass. *Bioresource Technology*, **96**(5), 545-550.

Zhang, X., Wang, T., Ma, L., Zhang, Q., Jiang, T. 2013b. Hydrotreatment of bio-oil over Ni-based catalyst. *Bioresource Technology*, **127**, 306-311.

Zhang, X.-S., Yang, G.-X., Jiang, H., Liu, W.-J., Ding, H.-S. 2013c. Mass production of chemicals from biomass-derived oil by directly atmospheric distillation coupled with co-pyrolysis. *Scientific Reports*, **3**.

Zhao, H.Y., Li, D., Bui, P., Oyama, S.T. 2011. Hydrodeoxygenation of guaiacol as model compound for pyrolysis oil on transition metal phosphide hydroprocessing catalysts. *Applied Catalysis A: General*, **391**(1), 305-310.

Chapter 3

3 Development of Inexpensive Transition Metal Catalysts for Hydrodeoxygenation of Pyrolysis Oil

3.1 Introduction

Biomass is recognized as a compelling source for renewable fuels and chemicals. Nowadays, fast pyrolysis is a feasible and effective conversion technology that can be used by industry for the production of liquid fuels from raw materials such as biomass (Zacher et al., 2014). The yield of the produced liquid phase can be as high as 75 wt.% of the original dry biomass, and this typically contains between 60 and 75 % of the initial biomass energy. Bio-oil has many advantages such as less toxic, carbon-neutral and better biodegradation, but also comes with a number of disadvantages, e.g., high contents of water and oxygen (30-50 wt.%), great molecular complexity, strong coking propensity, low pH value (high corrosiveness), high viscosity, chemical and thermal instability, low heating value, and poor ignition and combustion properties. There are many issues associated with the application of bio-oil (in its neat form or blended with other fuels) in combustion engine, these included but not limited to ignition and combustion difficulties, corrosion, coking, clogging, and engine seizure (Hossain & Davies, 2013). In addition, bio-oil is not suitable for direct use in the petroleum refinery as a replacement for conventional crude oils as the blend of bio-oil and petroleum would clog the processing equipment due to excessive coke deposition.

Thus, there are severe limitations for the direct integration of bio-oil into petroleum refinery processing and end use infrastructure (Bridgwater, 2012; de Miguel Mercader et al., 2010; Elliott, 2007; Fogassy et al., 2010), which is mainly due to the presence and high content of oxygen in bio-oil. Hydrodeoxygenation (HDO) of pyrolysis oil has emerged as a promising technology for bio-oil upgrading, by reducing the oxygen content, improving its heating value and stability, to allow further co-processing of the liquefied biomass with fossil crude feed in standard refinery infrastructures to produce advanced biofuels (de Miguel Mercader et al., 2010; Fogassy et al., 2010; French et al., 2010). During HDO, pyrolysis oil is treated at the temperatures between 150 and 450 °C

with high hydrogen pressures (5–25 MPa), in the presence of an active catalyst (de Miguel Mercader et al., 2011). Practically, the most prevailing route to remove oxygen is by expelling it in the form of water when it reacts with hydrogen. However, H_2 can be also consumed by cracking reactions for saturating double bonds. Thus, the efficiency of hydrogenation is one of the major concerns in hydro-processing (Elliott et al., 2009). The degree of bio-oil HDO depends on the severity of the process. Generally, higher temperatures (~400 °C) and higher H_2 pressures (~135 bar) result in a higher level of deoxygenation of bio-oil (Elliott et al., 2009). Elliott et al. reported a 99.3 % deoxygenation (250/410 °C, 135 bar, 6.67 h) (Elliott et al., 2012).

It is believed that the hydrogen-consuming heterogeneous reactions can take place at the exterior and interior surfaces of the catalyst. Both hydrogen and pyrolysis oil components need to enter the pores of the porous catalyst particles and react on the internal surface of the catalyst (de Miguel Mercader et al., 2011). The most commonly studied bio-oil HDO catalysts are petroleum hydrotreating catalysts: supported Ni-MoS_2 and Co-MoS_2 catalysts (Elliott, 2007; Furimsky, 2000). A sulfur-donating agent is added to ensure stability of active phase in conventional catalysts due to the absence of sulfur in most of biofeeds (Furimsky, 2013). For these catalysts, Ni or Co serve as promoters, donating electrons to the molybdenum atoms (Mortensen et al., 2011), which results in weakening the bond between molybdenum and sulfur and thereby generating a sulfur vacancy site. These sites are the active sites in both HDS and HDO reactions (Badawi et al., 2013; Mortensen et al., 2011; Romero et al., 2010; Ryymin et al., 2010). Wildschut et al. conducted a series of experiments with beech bio-oil using a batch reactor at a temperature of 350 °C and pressure of 200 bar over 4 h, using the above conventional hydrotreating catalysts in comparison to carbon-supported noble metal catalysts (Wildschut et al., 2009a; Wildschut et al., 2009b). They concluded that Ru/C and Pd/C appeared to be good catalysts for the process as they showed high oil yields and a high degree of deoxygenation efficiency comparable to Co-MoS_2/Al_2O_3, Pt/C and Ni-MoS_2/Al_2O_3. Sulfur is not a preferable additive due to its detrimental effects on the environment. Elliott et al conducted a series of two-stage experiments in a down flow reactor (250-410 °C and 135 bar, 6.67 h) with Pd/C and a proprietary metal sulfide catalyst (Elliott et al., 2009). They reported successful implementation of two-step

process configurations to achieve 98 to 99 percent deoxygenation of bio-oils from different types of biomass feedstock. Venderbosch et al. carried out a series of HDO experiments at temperatures of 250 and 350 °C and H_2 pressures of 100 and 200 bar. They found that the Ru/C catalyst exhibited superior catalytic activity when compared with the classical hydrotreating catalysts with respect to oil yield (up to 60 wt.%) and deoxygenation level (up to 90 wt. %) (Wildschut et al., 2009b). Therefore, the noble metal catalysts Pd, Rh, Ru, and Pt are promising catalysts for the HDO process, however, the high price of these metals severely limits their practical applications for bio-oil upgrading.

In view of this, a series of transition metal phosphide catalysts have been investigated because of their low cost (Hedrick, 2010). Li et al. tested the HDO of anisole over transition metal phosphide catalysts in a fixed-bed reactor and concluded that the HDO activity decreased in the following order: $Ni_2P/SiO_2 > NiMoP/SiO_2 > MoP/SiO_2$ (Li et al., 2011). Zhao et al. tested the HDO activity of some transition metal phosphide catalysts with guaiacol model compound in a fixed bed reactor at 300 °C under atmospheric pressure, and reported the activities of metal phosphides in the order of: $Ni_2P > Co_2P > Fe_2P \approx WP \approx MoP$ (Zhao et al., 2011).

Another key factor determining the HDO activity of catalysts is the type of support employed. γ-Al_2O_3 has been a widely used support for hydrotreating catalysts but it may result in severe coke formation due to its strong acidity (Zdražil, 2003). Carbon has proven to be an effective support for HDO catalysts with improved catalytic activity even in the presence of water and acidic components of bio-oil (Elliott, 2007). Recently, $MgAl_2O_4$ has received a growing interest as a catalyst support in the area of environmental emission control, petroleum processing and fine chemicals production as well as many catalytic reactions, owing to its high melting point, good chemical stability and high mechanical strength (Chiu & Ku, 2012; Xu et al., 2013). In addition, $Mg_6Al_2(CO_3)(OH)_{16}$ showed high stability under severe reaction conditions and excellent catalytic properties, as well as regeneration ability (Cavani et al., 1991; Parlett et al., 2013). Besides, it also has been successfully utilized as an inexpensive support for transition metal oxide catalysts (Vaccari, 1999).

The objective of this current study is to investigate inexpensive transition metal catalysts for HDO of pyrolysis oil, in which performance of Mo metal catalysts with/without P supported on Al_2O_3, activated carbon (AC), $MgAl_2O_4$ and $Mg_6Al_2(CO_3)(OH)_{16}$ were compared. The experiments were carried out in a 100 mL bench-scale reactor system using a wood-derived pyrolysis oil (from BTG Company) at a reaction temperature of 300 °C and initial hydrogen pressure of 50 bar for 3 h. Furthermore, the effects of Ni or Co promoter on the catalytic activities of MoP catalysts on the selected supports were investigated in comparison with a commercially available catalyst Ru/C, which is commonly recognized as an active catalyst for bio-oil hydrodeoxygenation (Matsumura et al., 2005; Wildschut et al., 2009b). The quality of the upgraded oils was characterized by Karl Fischer titration, gel permeation chromatography (GPC) and elemental analysis. Moreover, the fresh and spent selected catalysts were characterized with X-ray diffraction (XRD) and nitrogen isothermal adsorption for textural properties (specific surface area and pore size distribution).

3.2 Materials and methods

3.2.1 Materials

The commercial Ru/C catalyst (5 wt.% of active metal with a particle size of 14 μm and BET surface area of 810 m^2/g) was used as received. Ammonium molybdate tetrahydrate (81.0-83.0 % MoO_3 basis), synthetic hydrotalcite ($CH_{16}Al_2Mg_6O_{19}{\cdot}4H_2O$), magnesium nitrate hexahydrate (99 %), aluminum nitrate nonahydrate ($Al(NO_3)_3{\cdot}9H_2O$), Ammonium hydroxide solution (NH_4OH), nickel nitrate hexahydrate ($Ni(NO_3)_2{\cdot}6H_2O$), cobalt nitrate hexahydrate ($Co(NO_3)_2{\cdot}6H_2O$) are all ACS grade chemical reagents, purchased from Sigma-Aldrich and used as received. Al_2O_3 (with an average particle size of 100-500 μm and BET surface area of 156 m^2/g) was purchased from Sasol. Activated carbon, Norit ROW 0.8mm pellets, was supplied by Alfa Aesar. The hardwood sawdust fast pyrolysis oil (PO) was supplied by BTG (Enschede, The Netherlands) with water content of 24 wt.% (**Table 3-1**). The elemental composition and the HHV of the PO feed are presented in **Table 3-1** and are compared with another common bio-oil and crude oil from the literature. Phosphoric acid (Min. 85%) was purchased from Caledon. For the GPC analysis for the liquid products, HPLC grade solvent of tetrahydrofuran (THF) was used,

which containes 0.03 wt.% 2, 6-di-t-butyl-4-methyl-phenol as stabilizer. The solvent used in this study, i.e., acetone (99.5 vol.%) was obtained from Caledon supplier and ethanol (99.97%) from Commercial Alcohol Inc. Analytical grade (>99.9999%) hydrogen and nitrogen were obtained from Praxair company.

Table 3-1 Properties of the fast pyrolysis oil used in this study

	Fast pyrolysis oil[a]	Bio-oil[b]	Crude oil[c]
Water content (wt.%)	23.8	15-30	0.1
C (wt.%)	56	55-65	83-86
H (wt.%)	7	5-7	11-14
N (wt.%)	~0	~0	~0
O (wt.%)[d]	37	28-40	<1
HHV (MJ/kg)[e]	16	16-19	44

[a] Fast pyrolysis oil tested in our study, which was obtained from BTG company.

[b, c] From literature reference (de Miguel Mercader et al., 2011; Elliott et al., 2012; Elliott et al., 2009; French et al., 2010).

[d] Calculated by difference assuming negligible content of S in the woody biomass-derived bio-oil.

[e] Calculated by the Dulong formula, i.e., HHV (MJ/kg)=0.3383C+1.422 (H-O/8) where C, H and O were in terms of weight percentage on wet basis.

3.2.2 Catalysts preparation

Commercial available activated carbon (AC) and Al_2O_3 were directly used as catalyst support materials. $Mg_6Al_2(CO_3)(OH)_{16}$ was obtained by calcining $CH_{16}Al_2Mg_6O_{19}{\cdot}4H_2O$ at 500 °C for 6 h to expel all water. To prepare nanocrystalline $MgAl_2O_4$ (Magnesium aluminate), co-precipitation method was used, where $Al(NO_3)_3{\cdot}9H_2O$ and $Mg(NO_3)_2{\cdot}6H_2O$ were dissolved in distilled water with a molar ratio of 2:1 and stirred on hot plate at 50 °C. Then, ammonium hydroxide solution was added dropwise until the pH of the resulting mixture reached around 10 and then stirred for a further 1 h. The resultant slurry was kept at ambient temperature overnight with continuous stirring. Afterwards, the solid was separated by centrifugation and washed with excess amount of distilled

water to remove residual ammonia. Finally, the solid was dried at 120 °C for 12 h and calcined at 800 °C in air for 8 h.

Incipient wetness impregnation method was employed for the preparation of metal phosphide supported catalysts. First, the required quantity of ammonium molybdate tetrahydrate for obtaining final content of 14 wt.% MoO_3 was dissolved in a given amount of solvent (see **Table 3-2**). A calculated quantity of H_3PO_4 (2 wt.% P of support) was added dropwise to this solution. Then, 10 g of the support added to the resulting mixture. The solvent of the mixture was removed by rotary evaporation, and then dried at 100 °C overnight. The supported Mo metallic catalysts was calcinated in N_2 at 500 °C for 3 h, followed by reduction in H_2 (40 mL/min flow) at the heating rate of 5 °C/min for 3 h. The supported MoP catalysts were simultaneously calcinated and reduced in H_2 (40 mL/min flow) at the heating rate of 5 °C/min followed by constant temperature at 920 °C for 3 h. The detailed operating conditions for catalyst calcination/reduction are summarized in **Table 3-2**. All catalysts were ground with a mortar and pestle, and sieved to particles with a diameter between 180 and 420 μm (or 40-80 mesh). NiP/AC and CoP/AC catalysts were prepared by similar procedure as described above for MoP/AC, except that these catalysts were calcinated/reduced in H_2 at 600 °C for 3 h.

Table 3-2 Detailed conditions for preparation of Mo-based catalysts

Catalysts	Mo/AC	MoP/AC	Mo/ Al_2O_3	MoP/ Al_2O_3	Mo/ $Mg_6Al_2(CO_3)(OH)_{16}$	MoP/ $MgAl_2O_4$
Solvent	Water-ethanol[a]	Water-ethanol	Water	Water	Water	Water
Calcination Temp. (°C) and gas	500, N_2	920, H_2	500, N_2	920, H_2	500, N_2	920, H_2
Reduction Temp. (°C) and gas	600, H_2	–	600, H_2	–	600, H_2	–

[a] The ethanol-water mixture containing 20 vol.% ethanol.

3.2.3 Bio-oil HDO experimental procedure

Pyrolysis oil upgrading experiments were carried out in a stirred reactor (Parr 4590 Micro Bench top reactor) with a total volume of 100 mL. The schematic drawing of the reactor system is shown in **Fig. 3-1**. The operation temperature and pressure were set at 300 °C and 50 bar, respectively. In a typical run, 40 g pyrolysis oil and 2 g catalyst (5 wt.% of pyrolysis oil) were added into the reactor. The reactor was sealed and the residual air was removed by vacuum-purge with hydrogen at least three times. Before the experiment, the reactor was flushed with H_2 to a fixed pressure and then collected into a gasbag for quantification of the hydrogen consumption. If no leakage, the reactor was pressurized to 50 bar using hydrogen and then heated to 300 °C under agitation at 360 rpm for 3 h (including the heating time). The inside pressure of the reactor increased in the range of 110 to 170 bar during the reaction, and this depends on the type of catalyst is used. After the set reaction time elapsed, the reactor was quenched in an ice/water bath to ambient temperature. For each run the reaction pressure and temperature were recorded in intervals of 10 minutes during each run. Two or three duplicate runs were carried out for each condition to ensure the maximum relative error of the oil yield was within ±5%.

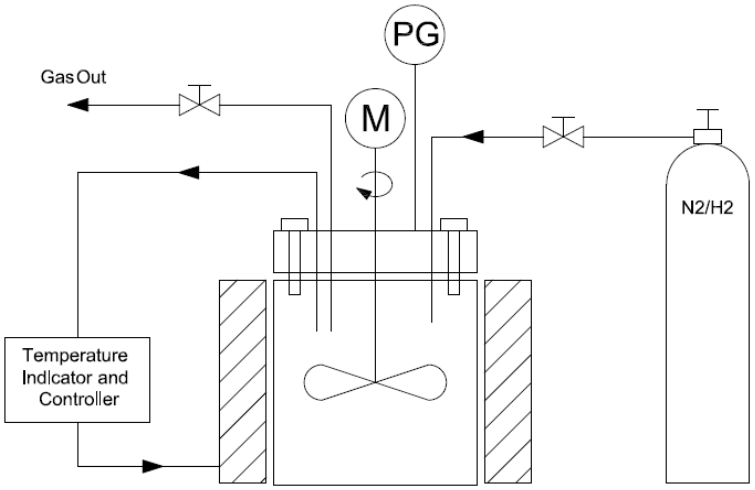

Figure 3-1 The diagram of the experimental apparatus

3.2.4 Products separation

The gas products were collected into a gasbag and analyzed using a Micro-GC equipped with a thermal conductivity detector (TCD). The quantification (in moles) of gas species (H_2, CO, CO_2, CH_4, C_2 and C_3 gases) was determined using N_2 internal standard for calculation of the yield of gas fraction (GF). For all experiments, the liquid phase consists of only two layers after reaction, a dark brown bottom layer and a top aqueous phase. Aqueous fraction (AF) was recovered directly by decanting, the organic fraction of the upgraded oil products was extracted with acetone, and the solid fraction was isolated from the liquid by filtration. The filtrated solids were washed repeatedly with acetone. The solid mass was dried and weighed. The weight of the solid (coke) was corrected for the catalyst intake. The oil fraction (OF) collected by evaporating the solvent under vacuum using rotary evaporator. Hydrogen consumption was calculated from the difference of initial amount of H_2 and the remaining H_2 in the reactor analyzed by GC-TCD. The weight of AF was obtained from the weight difference between total feed (PO and H_2) and other products (OF, GF and coke). The chemical composition of AF and coke were not analyzed in this study as OF and H_2 consumption were the main interests of this work. Yields of OF, AF, GF (H_2 was excluded) and coke were calculated by the weight percentage of the mass of each product to the mass of dry PO loaded and H_2 consumed during the reaction in each run. **Equation (3-1)** presented the calculation method for OF product. In addition, degree of deoxygenation (DOD), as defined in **Eq. (3-2)**, was used to evaluate the effectiveness of the HDO process.

$$\mathrm{Y}_{oil} = \left(\frac{m_{oil}}{m_{feed,dry}}\right) \cdot 100\% \qquad (3\text{-}1)$$

$$\mathrm{DOD} = \left(1 - \frac{O(wt\%)_{product\ oil}}{O(wt\%)_{feed,dry}}\right) \qquad (3\text{-}2)$$

The Y_{oil} is the total oil yield after HDO, m_{oil} is the total mass of product oil and $\mathrm{m}_{feed,dry}$ is the water free feedstock oil. For DOD equation, $O\ (wt.\%)_{product\ oil}$ and $O\ (wt.\%)_{feed\ oil}$ represent the weight percent of oxygen in the product oil and water free feed, respectively. The combination of these two parameters can achieve a relatively comprehensive summarization for HDO.

3.2.5 Oil fraction (OF) characterizations

The weight-average molecular weight (M_w), number-average molecular weight (M_n) and molecular weight polydispersity of the oil fraction (OF) phase were determined by GPC analysis on a Water Breeze gel permeation chromatography (GPC) instrument (1525 binary HPLC pump; UV detector at 270 nm; Water Styrange HR1 column at 40 °C) using THF as an eluent at a flow rate of 1 mL/min. Linear polystyrene standards were used as for molecular calibration. The elemental analysis was used to investigate the C, H, N content, and almost no S was detected in hardwood-derived oil. O content was calculated by the difference. Elemental analysis was conducted on a Thermo Fischer Flash EA 1112 series CHNS-O elemental analyzer. The results of elemental analysis were used to determine the degree of deoxygenation (DOD) and the ratios of H/C and O/C. The water content in the original pyrolysis oil was determined by Karl Fischer titration (Mettler Toledo V20), and the produced OF products are dry with negligible content of water. Higher Heating Value (HHV) of oil was also measured using an IKA Calorimeter System in addition to calculation with the Dulong formula for some oil samples.

3.2.6 Catalyst characterization

The XRD spectra for selected fresh and spent catalysts were collected on an X-ray diffractometer (Rigaku RINT 2500, Tokyo, Japan) with Cu K radiation (λ = 1.54059 Å) at 30 kV and 15 mA at a scan rate of 0.02 degrees per second over a 2θ range of 10° to 80°. The textural properties analysis was performed by N_2 isothermal adsorption (77 K) using Micrometrics ASAP 2010. Prior to N_2 adsorption test, the sample was degassed at 150 °C until a stable static vacuum of less than 5×10^{-3} Torr was achieved.

3.3 Results and discussion

3.3.1 Evaluation of the experimental error in product yields

At least duplicate experiments were conducted to obtain reliable product yields for each experimental condition. After each test, GF, OF, AF, and coke (or solid residue) products

were isolated from the oil to determine their yields. The elemental analysis were performed for the original PO, OF and coke to determine the C content. The C content of the gas phase can be calculated from the GC-TCD analysis. TOC-Vcpn (Shimadzu) was utilized to measure the amount of total organic carbon present in the AF product. To evaluate the experimental error, the experimental runs with MoP/Al_2O_3 and $MoP/MgAl_2O_4$ were selected for C balance calculation, as presented in **Table 3-3**. As can be seen from **Table 3-3**, the carbon balance for these two runs is good with a range of 89-93 wt.%. The loss of C might be partly related to the difficulties in the complete removal of coke from the reactor.

Table 3-3 Total carbon balance for two typical bio-oil HDO tests with MoP/Al_2O_3 and $MoP/MgAl_2O_4$

Catalysts	MoP/Al_2O_3	$MoP/MgAl_2O_4$
C (g) in OF	10.1	12.1
C (g) in AF	2.1	1.7
C (g) in GF	0.01	0.02
C (g) in coke	2.2	1.3
Total C balance (wt.%)	88.5	93.4

3.3.2 Performance of different Mo-based catalysts in HDO of fast pyrolysis oil

3.3.2.1 Product yields

Figure 3-2 shows effects of different in-house prepared catalysts on product yields and H_2 consumption compared with the commercial Ru/C catalyst from bio-oil HDO tests at 300 °C, 50 bar H_2 and 3 h. The oil fraction yield of the tests are presented in **Figure 3-3**. Poor hydrogenation catalysts caused the formation of coke by the re-polymerization/condensation reactions of the reaction intermediates or upgraded oil products during the bio-oil hydroprocessing process (Wildschut et al., 2010). It can be

seen from **Figs 3-2** and **3-3** that the bio-oil HDO with Ru/C and recycled Ru/C (Re-Ru/C, recovered after a HDO run) produced the highest OF yield and the lowest coke yield. The yield of coke or solid residue was found to be negligible for both catalysts, suggesting very high activity of Ru-based catalysts. The textural properties of the fresh and spent catalysts are showed in **Tables 3-6** and **3-7**, surface area of the spent Ru/C decreased largely from 810 to 172 m^2g^{-1}, total pore volume reduced from 0.68 to 0.38 cm^3/g but the average pore size increased from 3.4 to 8.7 nm, suggesting blocking of catalyst micropores by coke formation (although at a small scale). We may deduce that the activity of the Ru-based catalyst for bio-oil HDO depends less on catalyst surface area.

As shown in **Figures 3-2** and **3-3**, for the Mo based catalysts, the addition of only 2 wt.% P increased the OF yield appreciably. For example, the addition of P enhanced the bio-oil yield by around 9 % for both AC and Al_2O_3 supported Mo catalysts. However, addition of P also led to an increase in coke yield likely due to increases in the acidity of the catalyst. The results as shown in **Figs. 3-2** and **3-3** also clearly indicate that a higher oil yield was obtained when using an AC-supported catalyst rather than the Al_2O_3-supported one. This has been reported in many other studies, although Al_2O_3-supported catalysts generally have better activities compared to those supported on other supports, Al_2O_3 supported catalysts could be rapidly deactivated by coke deposition (as evidenced by the results shown in **Fig. 3-3**) due to the strong acidity of the alumina support (Centeno et al., 1995; Pines & Haag, 1960). $Mo/Mg_6Al_2(CO_3)(OH)_{16}$ catalyst produced the lowest OF yield, but in terms of the oil quality (M_w, H/C and O/C as illustrated in **Fig. 3-4**) the catalyst does show some promise; to be discussed in details in a later section. The oil yield in the blank tests (with absence of a catalyst) was higher than that in the tests with catalysts (such as Mo/Al_2O_3, MoP/Al_2O_3 and $Mo/MgAl_2O_4$), considering the poor quality of the oil product from the blank test in the absence of a catalyst (large M_w and low H/C) as shown in **Figs. 3-4** and **3-5** as well as **Table 3-4**.

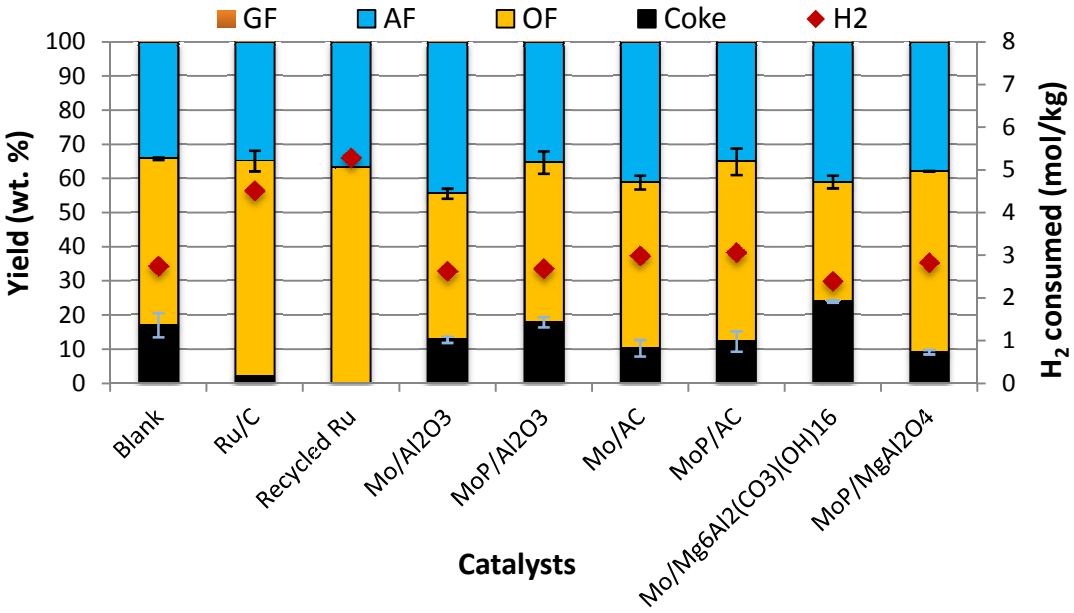

Figure 3-2 Effects of different in-house prepared catalysts on product yields and H_2 consumption compared with the commercial Ru/C catalyst (300 °C, 50 bar H_2, 3 h)

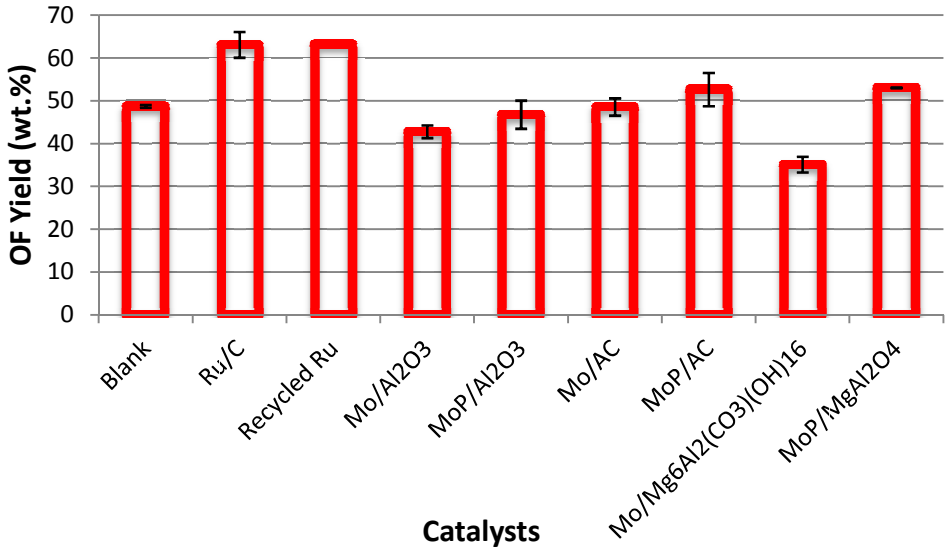

Figure 3-3 Yield of oil fraction from the HDO experiments with different in-house prepared catalysts compared with the commercial Ru/C catalyst (300 °C, 50 bar H_2, 3 h).

3.3.2.2 Gas analysis and H_2 consumption

In the bio-oil hydrodeoxygenation process, H_2 consumption has a direct relation with the catalyst's performance. **Fig. 3-2** shows the relationship between oil yield and H_2 consumption. The recycled and the fresh Ru/C catalysts exhibited the highest H_2 consumption among all other catalysts, which is in a good agreement with the highest oil yield for these catalysts (**Figure 3-3**). The high hydrogen consumption accompanied with a higher oil yield suggests increased HDO and hydro-cracking reactions of the pyrolysis oil. The H_2 consumption values for other catalysts show minor difference, even at a similar level to that of the blank test (ranging from 2.4 to 3.1 mol/kg feed).

3.3.2.3 Elemental analysis

The properties of the bio-oil products are of particular interest (Bridgwater & Boocock, 2006) in this work. The oxygen contents of the samples were determined by CHNS elemental analysis, and the higher heating value (HHV) of the oil sample can be calculated by the Dulong formula, i.e., HHV (MJ/kg)=0.3383C+1.422 (H-O/8) where C, H and O were in terms of weight percentage on dry basis. Two samples were taken for HHV measurement using an IKA Calorimeter System, in order to validate the HHV calculation method with the Dulong formula. It can be seen from **Table 3-4**, the calculated results are well in line with the measured results. As shown in **Table 3-4**, compared with the fresh bio-oil, all bio-oil samples exhibited increased carbon contents and reduced contents of oxygen, as expected, leading to significantly increase in the higher heating values. All of the bio-oils produced have HHV around 32-34 MJ/kg (except for that for Mo/Al_2O_3 with 28.8 MJ/kg) as compared to only 22.7 MJ/kg for the feed oil on dry basis (or 16 MJ/kg on wet basis given in **Table 3-1**). In view of degree of deoxygenation (DOD), catalysts of $MoP/MgAl_2O_4$, MoP/AC, Mo/AC and $Mo/Mg_6Al_2(CO_3)(OH)_{16}$ all performed better than the reference catalyst (Ru/C).

Table 3-4 Properties of the OF obtained from HDO of the pyrolysis oil with various catalysts (300 °C, 50 bar H_2, 3 h)

	PO feed[a]	Blank	Ru/C	Recycled Ru	Mo/Al_2O_3	MoP/Al_2O_3	Mo/AC	MoP/AC	$Mo/Mg_6Al_2(CO_3)(OH)_{16}$	$MoP/MgAl_2O_4$
C (wt.%)	56.0	77.3	71.0	73.4	66.5	68.4	72.4	75.5	71.2	74.9
H (wt.%)	7.24	7.61	8.55	8.43	7.68	8.43	8.10	8.36	8.54	7.28
O (wt.%)[b]	36.8	15.1	20.5	18.2	25.8	23.2	19.5	16.2	20.2	17.8
DOD	–	0.57	0.42	0.48	0.29	0.35	0.45	0.53	0.43	0.50
H/C (-)	1.54	1.17	1.43	1.37	1.38	1.47	1.33	1.32	1.43	1.16
O/C (-)	0.49	0.15	0.22	0.19	0.29	0.25	0.20	0.16	0.21	0.18
HHV (MJ/kg)[c]	22.7	34.3	32.5	33.6	28.8	31.0	32.5	34.5	32.7	32.5
HHV (MJ/kg)[d]	23.0	–	31.0	–	–	–	–	–	–	–

[a] Elemental composition of the pyrolysis oil feed on dry basis.

[b] Calculated by difference assuming negligible content of S in the woody biomass-derived bio-oil.

[c] Calculated by the Dulong formula, i.e., HHV (MJ/kg)=0.3383C+1.422 (H-O/8) where C, H and O were in terms of weight percentage.

[d] Measured using an IKA Calorimeter System.

The Van Krevelen plot is applied to evaluate the catalysts activities in terms of the O/C and H/C ratio of the upgraded oil products. The results are represented in **Fig. 3-4**. The elemental composition of the oil product obtained in the absence of a catalyst (blank) is also given as a measure of the thermal, non-catalytic pathway (Bridgwater & Boocock, 2006; Venderbosch et al., 2010). The product oil obtained from HDO process is usually targeted as a transportation fuel and the H/C ratio should be between 1.8 and 2.0 and O/C ratio preferably lower than 0.02 (Centi & van Santen, 2008). Obviously, the upgraded oil products obtained in this study (H/C = 1.1 – 1.5, and O/C = 0.1 – 0.3) are all yet to meet the standards for a transportation fuel under the operating condition (300 °C, 50 bar H_2, 3 h).

As can be seen from **Fig. 3-4**, the content of oxygen (as expressed by the O/C ratio) for all upgraded oil was substantially reduced as compared to the original pyrolysis oil. The H/C ratio is a measure of the hydrogenation activity, a higher H/C ratio corresponds to a higher catalyst activity for hydrogenation (Wildschut et al., 2010). In the tests with MoP/$MgAl_2O_4$ catalyst and in the absence of a catalyst, OF with a low O/C and H/C, was produced, suggesting that the upgrading proceeded mainly through thermal/hydro-cracking reactions rather than through hydrodeoxygenation. In this case, a highly viscous, paste like organic product was usually obtained (Elliott, 2007; Furimsky, 2013). The addition of P into the metallic catalysts supported on either AC or Al_2O_3 produced an OF with a lower O/C, constant or slightly higher H/C, compared with those without P, therefore we can conclude that P was beneficial from the deoxygenation aspect. There is no significant differences in O/C and H/C between the oils with fresh Ru/C and recycled Ru/C used, thus, deoxygenation activity seems unchanged with recycled Ru/C catalyst compared with the fresh catalyst.

Although Mo/$Mg_6Al_2(CO_3)(OH)_{16}$ obtained the lowest yield among all catalysts tested, the catalyst shows a similar degree of deoxygenation (O/C) and hydrogenation (H/C) compared with Ru/C. Also from **Table 3-5**, molecular weights of the oil products with Mo/$Mg_6Al_2(CO_3)(OH)_{16}$ and Ru/C are similar too.

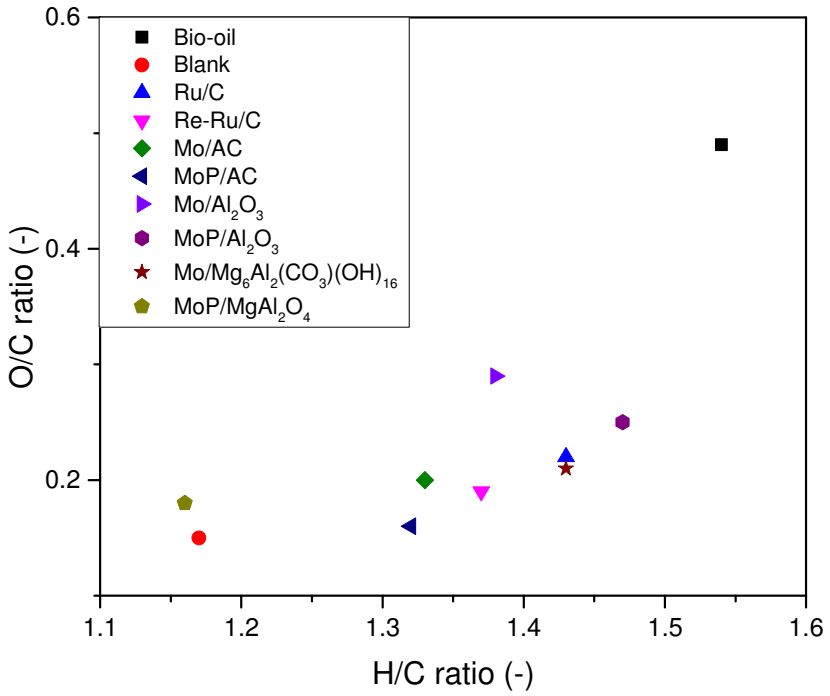

Figure 3-4 Van Krevelen plot for the original bio-oil and the upgraded oil obtained with different Mo-based catalysts, compared with the commercial Ru/C catalyst

3.3.2.4 Molecular weights

Due to the complex composition and intrinsic instability of bio-oils, chemical characterization of the oils is usually a great challenge. Gel permeation chromatography (GPC) was used to measure the relative molecular weights and distribution of the pyrolysis oil and its upgraded oil products. The separation mechanism of GPC is based on size exclusion: smaller molecules can access more pores, thus these molecules elute later than molecules with a larger size (Tung, 1966; Wu, 2003). Although GPC is not recommend to be used as an accurate method for molecular weight measurement for bio-oils (with non-linear and branched structure), it can give relative molecular weight and distribution. **Figure 3-5** shows molar mass distribution of the upgraded oil products obtained with different Mo-based catalysts, where W(logM), defined as the slope of the graph in which the cumulative mass, is plotted against the logarithm of the molecular weight (logM). This distribution can be obtained from the chromatogram and calibration curve that relates the elution time to the molecular mass (Bhattacharya et al., 2009; Hoekstra et al., 2011; Williams & Taylor, 1994). **Table 3-5** summarizes the GPC results of the bio-oil feed and the upgraded oil products obtained with different Mo-based catalysts, where number average molecular weight (M_n) and

weight average molecular weight (M_w) are calculated based on the GPC analysis and the polydispersity index (PD) was calculated by **Eq. (3-3)** (Li et al., 2014):

$$PD = \frac{M_w}{M_n} \qquad (3\text{-}3)$$

PD is a measure of the uniformity of the molecules in a mixture. A lower PD value indicates a higher uniformity of the molecular sizes. From the results shown in **Fig. 3-5** and **Table 3-5**, one can observe the molecular weight of all upgraded bio-oils obtained from catalytic HDO tests shifts to a lower M_w, while M_w of the oil product from HDO test without catalyst increased slightly. It can be also seen that HDO treatment with some catalysts such as Ru/C and $Mo/Mg_6Al_2(CO_3)(OH)_{16}$ in the HDO treatment resulted in not only reduced oxygen content, increased hydrogen content (by hydrogenation) and decreased molecular weight (M_n or M_w), and more uniform molecular weight distribution (smaller PD index).

From **Table 3-5**, the original fast pyrolysis oil has an M_w of 950 g/mol, M_n of 330 g/mol and PD of 2.87. OF obtained without catalyst exhibit increased M_w, which in good agreement with the reduced H/C displayed in the Van Krevelen plot (**Figure 3-4**), suggesting that in HDO test without a catalyst the reactions proceed mainly with polymerization/hydro-cracking rather than HDO. Commercial Ru/C showed the greatest effect on reducing the molecular weight of bio-oil and similar results were observed with Mo/AC and recycled Ru/C catalysts, which is consistent with the H_2 consumption results presented previously in **Fig. 3-2**. Larger H_2 consumption implies more intense hydrodeoxygenation reactions, producing less heavy oil components in the product oil. $Mo/Mg_6Al_2(CO_3)(OH)_{16}$ seems to be a more efficient catalyst for producing a low molecular weight oil product, with a M_w of only 680 g/mol, while the catalyst produced the lowest oil yield. Although the MoP/AC generated a relatively high bio-oil yield (around 53 wt.%) with a high DOD value of 0.53, the molecular weight of the oil product was higher than Mo/AC catalyst. Generally, the addition of P resulted in OF products with increased M_w likely due to the increased acidity for the metal phosphide species promoting re-polymerization reactions during the HDO process.

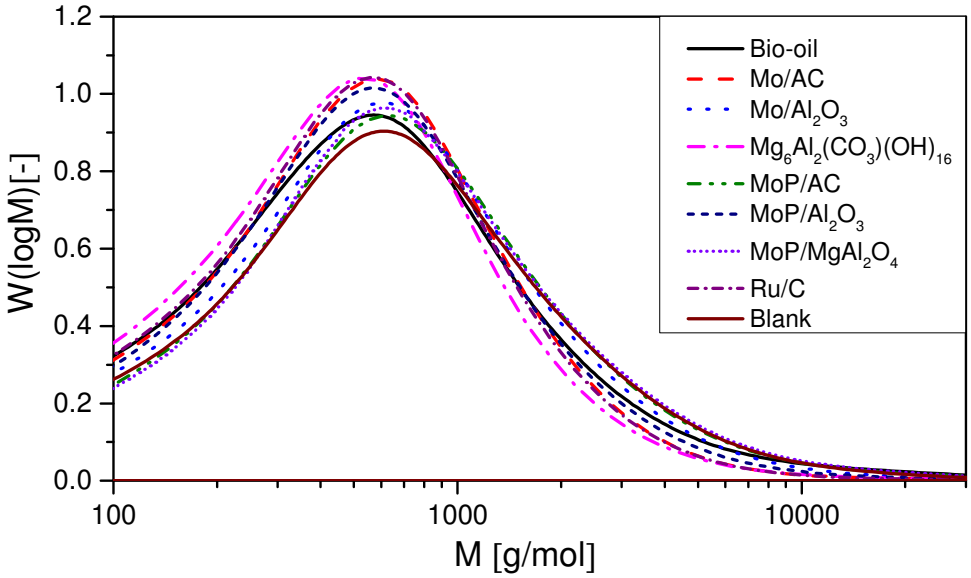

Figure 3-5 Molar mass distributions of the bio-oil feed and the upgraded oil products obtained with different Mo-based catalysts

Table 3-5 GPC results of the bio-oil feed and the upgraded oil products obtained with different Mo-based catalysts in comparison with Ru/C (300 °C, 50 bar H_2, 3 h)

	M_n[a]	M_w[b]	PD[c]		M_n	M_w	PD
Bio-oil feed	330	950	2.87	$Mo/Mg_6Al_2(CO_3)(OH)_{16}$	320	680	2.14
Blank	370	970	2.59	Recycled Ru	280	770	2.75
Ru/C	330	710	2.15	MoP/AC	390	940	2.45
Mo/AC	330	720	2.17	MoP/Al_2O_3	350	810	2.34
Mo/Al_2O_3	360	870	2.39	$MoP/MgAl_2O_4$	270	780	2.94

[a,b] The unit for M_n and M_w are g/mol (Dalton).

[c] PD: Polydispersity index (= M_w/M_n).

3.3.2.5 Performance of carbon-supported metal phosphide catalysts in HDO of fast pyrolysis oil

In the first stage of the experiments, Mo-based catalysts supported on different support materials with/without P were tested for HDO of the BTG pyrolysis oil, and the results were presented in the previous section. Among those, activated carbon supported catalysts exhibited superior activity than those supported on other supports (**Figs. 3-2** and **3-3**). The addition of P not only increased the oil yield, but also led to a higher degree of deoxygenation (**Table 3-4**). To investigate the effects of metal phosphide catalyst, in the second stage of the experiments, phosphides of three different transition metals (Mo, Ni and Co) are compared with Ru/C to assess the HDO performance with the BTG pyrolysis oil under the same conditions (300 °C, 50 bar H_2, 3 h).

3.3.2.6 Product yields

Fig 3-6 shows the total oil yield and H_2 consumption over three different metal phosphide catalysts compared with the commercial Ru/C catalyst. Although Ru/C still showed the best catalyst activity, producing the highest oil yield (63 wt.%), the greatest hydrogen consumption (4.5 mol/kg feed), and the lowest coke formation (2 wt.%), the performance of NiP/AC shall also be noted (with 58 wt.% oil yield and 4 wt.% coke yield), much better than MoP/AC and CoP/AC catalysts.

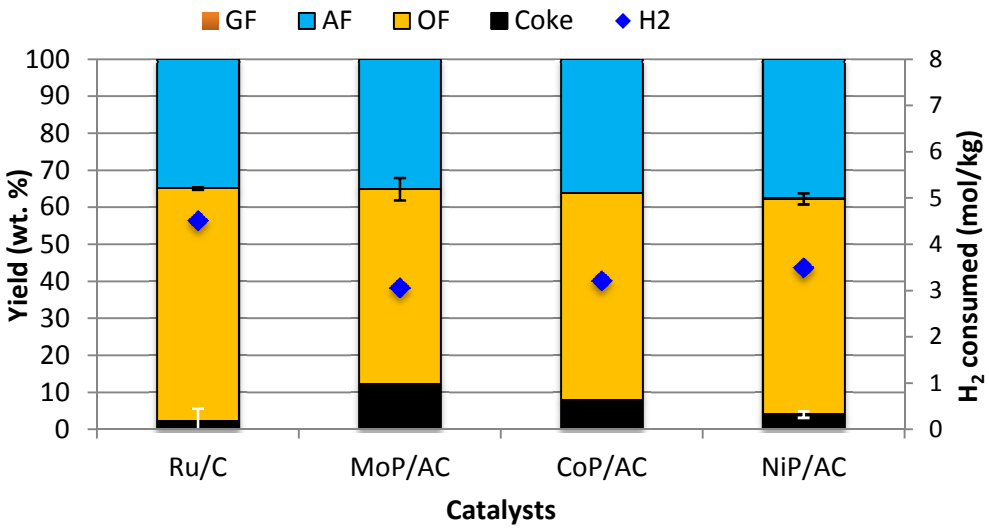

Figure 3-6 Product yields and H_2 consumption in the HDO tests with carbon-supported metal phosphide catalysts in comparison with Ru/C (300 °C, 50 bar H_2, 3 h)

3.3.2.7 Elemental analysis

The elemental composition of the upgraded oil products were analyzed, and it was found that the oxygen content of all oils fell within a narrow range of 17.7 to 20.5 wt.%. As shown in **Table 3-6**, compared with the fresh bio-oil, upgrade bio-oil samples with three phosphide metal catalysts exhibited increased carbon contents and reduced contents of oxygen, which leads to significantly increased heating values. Bio-oils produced have HHV around 32-34 MJ/kg (similar with Ru/C upgraded bio-oil) as compared to only 22.7 MJ/kg for the feed oil on dry basis (or 16 MJ/kg on wet basis given in **Table 3-1**). As also illustrated in the Van Krevelen plot (**Fig 3-7**), all oils obtained with the metal phosphide catalysts have similar ratios of O/C and H/C, falling in a very narrow range: 0.16-0.22 and 1.31 – 1.36, respectively. The commercial Ru/C produced upgraded oil with the highest H/C ratio 1.43. With respect to the yields and composition of the upgraded oil products and prices of the catalysts, NiP/AC seems to be the most promising catalyst, deserving more research on its performance in bio-oil HDO.

Table 3-6 Properties of the OF obtained from HDO of the pyrolysis oil with various phosphide catalysts (300 °C, 50 bar H_2, 3 h)

	PO feed[a]	Ru/C	MoP/AC	NiP/AC	CoP/AC
C (wt.%)	56.0	71.0	75.5	72.5	73.4
H (wt.%)	7.24	8.55	8.36	8.30	8.17
O (wt.%)[b]	36.8	20.5	16.2	19.2	18.4
DOD	-	0.42	0.53	0.46	0.48
H/C (-)	1.54	1.43	1.32	1.36	1.33
O/C (-)	0.49	0.22	0.16	0.20	0.19
HHV (MJ/kg)[c]	22.7	32.5	34.5	32.9	33.2

[a] Elemental composition of the pyrolysis oil feed on dry basis.

[b] Calculated by difference assuming negligible content of S in the woody biomass-derived bio-oil.

[c] Calculated by the Dulong formula, i.e., HHV (MJ/kg)=0.3383C+1.422 (H-O/8) where C, H and O were in terms of weight percentage.

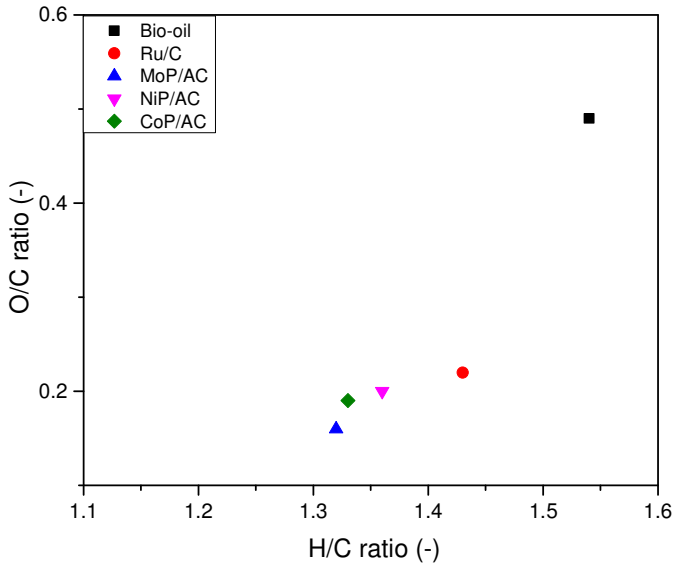

Figure 3-7 Van Krevelen plot for the original bio-oil and the upgraded oil products obtained from HDO tests with carbon-supported metal phosphide catalysts in comparison with Ru/C (300 °C, 50 bar H_2, 3 h)

3.3.2.8 Molecular weights and distribution

Fig. 3-8 shows molecular weight distribution for the upgraded oils from HDO with various metal phosphide catalysts in comparison with the oil product with Ru/C and the bio-oil feed. **Table 3-6** presents the number average molecular weight and weight average molecular weight as well as PD index for the upgraded oils. The upgraded oil with the commercial Ru/C exhibits smaller molecule weight than the oil products with the other three metal phosphide catalysts. These results clearly demonstrated that the commercial Ru/C still has the best effect on decreasing the molecular weight of bio oil, but again NiP/AC seems to be the most promising catalyst among the three metal phosphide catalysts tested in this study in regards of hydrogenation property, oil yield, coke yield and molecular weight.

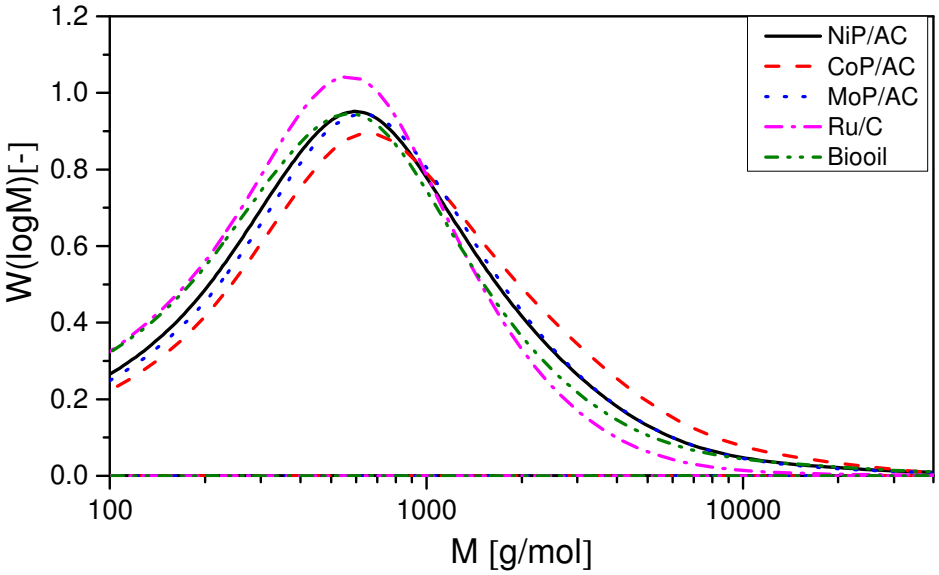

Figure 3-8 Molar mass distribution of the bio-oil feed and the upgraded oil products from HDO tests with carbon-supported metal phosphide catalysts in comparison with Ru/C (300 °C, 50 bar H_2, 3 h)

Table 3-7 GPC results of the bio-oil feed and the upgraded oil products from HDO tests with carbon-supported metal phosphide catalysts in comparison with Ru/C (300 °C, 50 bar H_2, 3 h)

	M_n[a]	M_w[b]	PD[c]		M_n	M_w	PD
Bio-oil feed[b]	330	950	2.87	Ru/C	330	710	2.15
MoP/AC	390	940	2.45	NiP/AC	300	810	2.69
CoP/AC	290	870	2.98				

[a,b] The unit for M_n and M_w are Dalton.

[c] PD: Polydispersity index (= M_w/M_n).

3.3.3 Characterization of the fresh/spent catalysts

3.3.3.1 Textural properties

Table 3-8 Textural properties of the supports and fresh catalysts

Sample	S_{BET} (m^2g^{-1})	V_{total} (cm^3g^{-1})	D (nm)
AC	1342	0.64	1.9
Ru/C	810	0.68	3.4
Mo/AC	1305	0.64	2.0
MoP/AC	1312	0.64	1.9
Al_2O_3	156	0.43	11
Mo/ Al_2O_3	137	0.34	10
MoP/ Al_2O_3	110	0.33	12
$Mo/Mg_6Al_2(CO_3)(OH)_{16}$	140	0.20	5.7
$MoP/MgAl_2O_4$	104	0.24	9.4
NiP/AC	1324	0.64	2.0
CoP/AC	1318	0.66	2.0

Table 3-9 Textural properties of spent catalysts

Sample	S_{BET} (m^2g^{-1})	V_{total} (cm^3g^{-1})	D(*nm*)
Ru/C	172	0.38	8.7
MoP/AC	7	0.01	3.5
NiP/AC	8	0.01	5.8
CoP/AC	6	0.01	5.4

Table 3-8 illustrates the textural properties of all support materials and fresh catalysts employed in this study. The surface area of activated carbon is almost 12 times larger than that of Al_2O_3. As shown in the Table, metal loading did not reduce the BET specific surface area of the support to a large extent. **Table 3-9** presents textural properties of spent carbon-supported metal phosphide catalysts after the HDO operation. The BET specific surface area and total pore volume of all MoP, NiP and CoP catalysts drastically decreased in the HDO process, while the surface area and total pore volume of the spent commercial Ru/C also decreased substantially However, compared with the spent AC-MoP, CoP and NiP catalysts (S_{BET} 6-8 m^2g^{-1}, V_{total} 0.01 cm^3g^{-1}) (**Table 3-9**), the spent Ru/C has much greater BET surface area and pore volume (172 m^2g^{-1} and 0.38 cm^3g^{-1}, respectively), thus the spent Ru/C catalyst can be recycled and reused for bio-oil HDO (**Figures 3-2** and **3-3**). The pore diameter for all spent catalysts increased to some extent, implying that some micropores of the fresh catalysts were plugged by coke deposition.

X-ray diffraction (XRD) measurements of the fresh catalysts were conducted to investigate the crystalline structure of the metallic or metal phosphide species on different supports. **Figure 3-9** illustrates XRD patterns for the Mo-based catalysts supported on various support materials including $MgAl_2O_4$, AC, $Mg_6Al_2(CO_3)(OH_{16})$ and Al_2O_3. The XRD pattern of $MgAl_2O_4$ support is almost identical to the standard pattern of this compound (PDF33-853), indicating the target support materials were successfully synthesized. MoP supported on $MgAl_2O_4$ shows three major peaks at 32.3°, 43.5° and 58.0° (in line well with the XRD of pure MoP compounds PDF 24-771). However, the MoP peaks in the supported catalyst are much broader implying that smaller crystals of MoP formed. For the MoP/AC catalyst, two major MoP peaks were observed and in Mo/AC catalyst characteristic peaks of MoO_3 crystalline phase at $2\theta = 18.6°, 28.8°, 31.7°$ and 34.3° were detected. The detection of MoO_3 instead of Mo metallic species suggesting the failure of formatting Mo metal due to the low reduction temperature. In $Mo/Mg_6Al_2(CO_3)(OH_{16})$ catalyst, no Mo-related species were detected, suggesting that the Mo species are highly dispersed on the $Mg_6Al_2(CO_3)(OH_{16})$ support. In $MoP/MgAl_2O_4$ catalyst, the characteristic XRD lines of Mg-Al-O (periclase) type structure (JCPDS87-653) were observed at 2θ=43° and 2θ=63° (Yadav & Kadam, 2013). For Al_2O_3 supported Mo and MoP catalysts, there is no MoO_3 peak detectable in Mo/Al_2O_3 catalyst, and only small peaks detected in the MoP/Al_2O_3 catalyst that can be ascribed to the diffraction of MoP (PDF 324-771), suggesting good dispersion of Mo or MoP species in the Al_2O_3-supported catalysts.

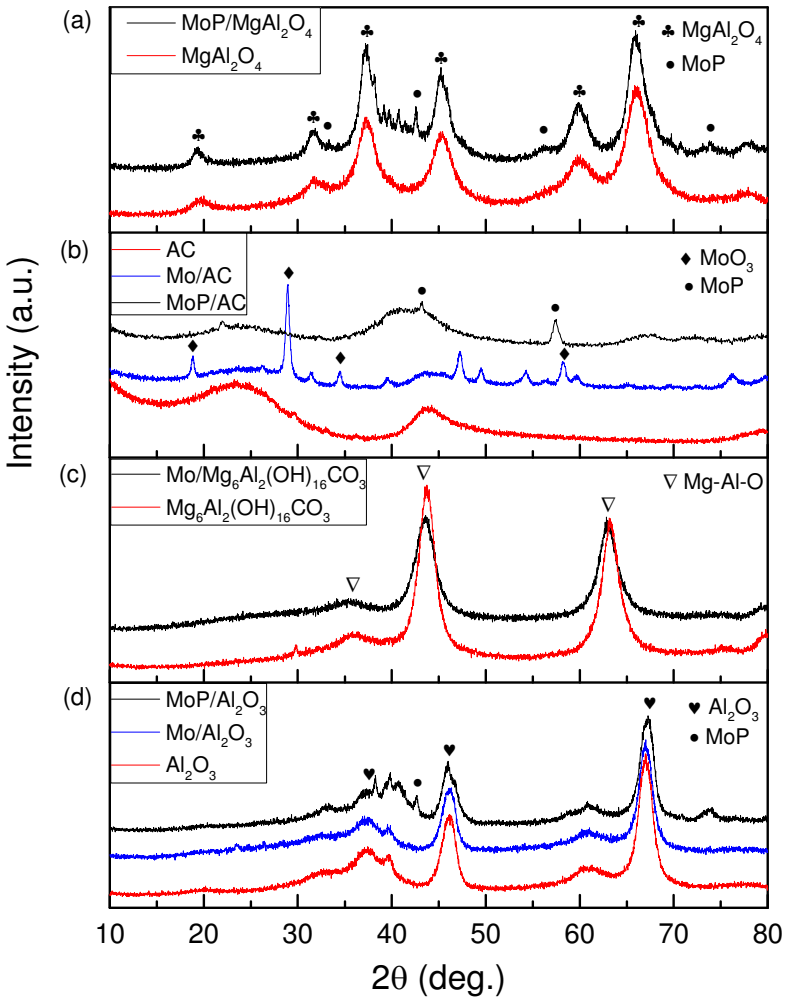

Figure 3-9 X-Ray diffraction patterns for Mo-based catalysts supported on $MgAl_2O_4$ (a); Activated carbon (b), $Mg_6Al_2(CO_3)(OH_{16})$ (c), and Al_2O_3 (d)

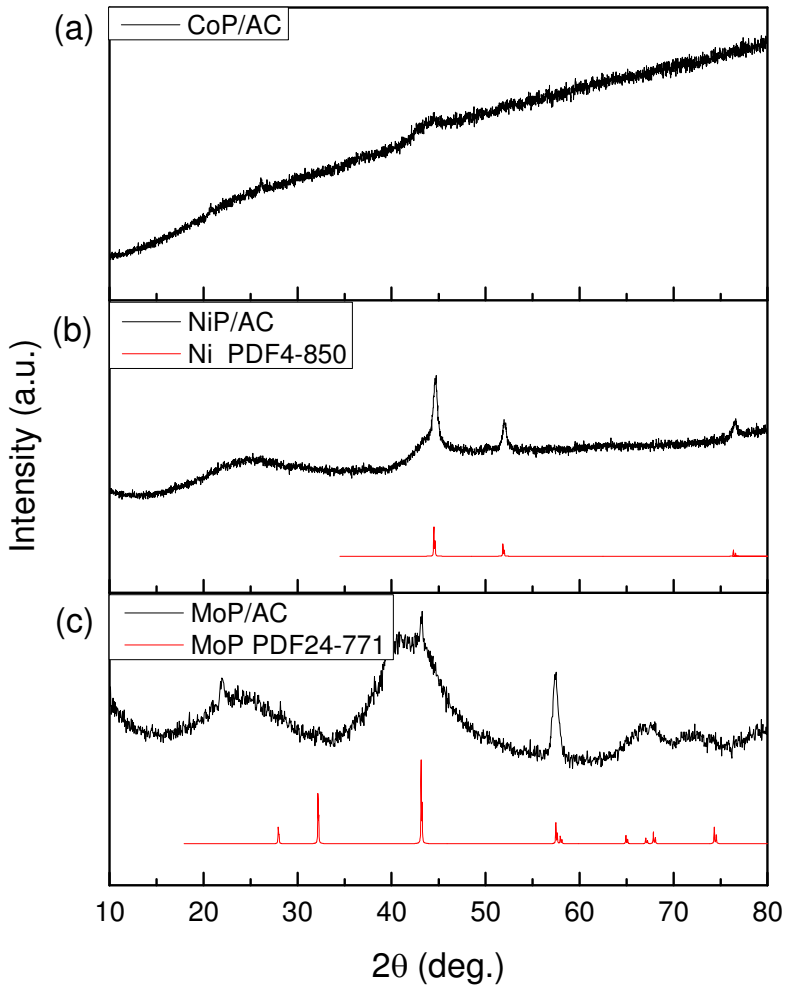

Figure 3-10 X-Ray diffraction patterns of activated carbon (AC) supported transition metal phosphide catalysts. (a) CoP/AC (b) NiP/AC (c) MoP/AC

Fig 3-10 Shows comparison of the XRD pattern of AC-supported transition metal phosphide catalysts. The diffraction pattern for MoP/AC shows three major peaks at 2θ = 32.3°, 43.5° and 58.0°, ascribed to the XRD pattern of MoP. Although, NiP/AC catalyst was prepared in the same manner as MoP/AC catalyst (except for a lower calcination temperature), the XRD pattern only exhibits metallic Ni peaks (PDF4-850) while no XRD lines of NiP were observable, suggesting excellent dispersion state of the NiP particles, which is in good agreement with its superb HDO activity in relation to MoP/AC and CoP/AC catalysts as discussed previously. The diffraction

patterns for CoP/AC showed strong background signals because of fluorescence (Wang et al., 2002). However, no Co related phase was detectable, suggesting good dispersion of the CoP species on AC too (Wang et al., 2002).

3.4 Conclusions

In this study, hydrodeoxygenation (HDO) of a wood derived fast pyrolysis oil was investigated at 300 °C with initial 50 bar H_2 pressure in a 100 mL batch reactor system for 3 h using Mo-based catalysts (with/without P) supported on four different supports (Al_2O_3, activated carbon, $Mg_6Al_2(CO_3)(OH)_{16}$, and $MgAl_2O_4$). In addition, the catalytic activities of AC-supported transition metal phosphides (MoP, NiP and CoP) were compared with the commercial Ru/C catalyst for bio-oil HDO. Some key conclusions are summarized as follows:

(1) Ru/C and recycled Ru/C catalyst produced the highest OF and the lowest coke yield and displayed the best hydrogenation activities, resulting in the higher H/C ratio for the upgraded oils with very low molecular weight.

(2) Addition of small amount of P to the Mo catalysts supported on both AC and Al_2O_3 led to increased degree of deoxygenation (DOD) and nearly 9 % increased oil yield compared with those without P.

(3) HDO operation without catalyst or with MoP/$MgAl_2O_4$ catalyst produced OF with decreased molar ratios of both O/C and H/C, suggesting that the upgrading proceeded mainly through thermal/hydro-cracking reactions rather than through HDO/hydrogenation reactions.

(4) AC was chosen as the best support materials for metal phosphides in terms of the HDO activities. With respect to the yields and composition of the upgraded oil products and prices of the catalysts, NiP/AC was chosen as the most promising catalyst among all transition metal phosphide catalysts (CoP/AC, NiP/AC and MoP/AC) as well as the commercial noble metal catalyst (Ru/C).

References

Badawi, M., Paul, J.F., Payen, E., Romero, Y., Richard, F., Brunet, S., Popov, A., Kondratieva, E., Gilson, J.P., Mariey, L. 2013. Hydrodeoxygenation of phenolic compounds by sulfided (Co)Mo/Al_2O_3 catalysts, a combined experimental and theoretical study. *Oil & Gas Science and Technology–Revue d'IFP Energies nouvelles*, **68**(5), 829-840.

Bhattacharya, P., Steele, P.H., Hassan, E.B.M., Mitchell, B., Ingram, L., Pittman Jr, C.U. 2009. Wood/plastic copyrolysis in an auger reactor: Chemical and physical analysis of the products. *Fuel*, **88**(7), 1251-1260.

Bridgwater, A.V. 2012. Review of fast pyrolysis of biomass and product upgrading. *Biomass and Bioenergy*, **38**, 68-94.

Bridgwater, A.V., Boocock, D.G.B. 2006. Science in thermal and chemical biomass conversion. CPL Press.

Cavani, F., Trifirò, F., Vaccari, A. 1991. Hydrotalcite-type anionic clays: Preparation, properties and applications. *Catalysis Today*, **11**(2), 173-301.

Centeno, A., Laurent, E., Delmon, B. 1995. Influence of the support of CoMo sulfide catalysts and of the addition of potassium and platinum on the catalytic performances for the hydrodeoxygenation of carbonyl, carboxyl, and guaiacol-type molecules. *Journal of Catalysis*, **154**(2), 288-298.

Centi, G., van Santen, R.A. 2008. Catalysis for renewables: from feedstock to energy production. John Wiley & Sons.

Chiu, P.-C., Ku, Y. 2012. Chemical looping process-A novel technology for inherent CO_2 capture. *Aerosol Air Quality Research*, **12**, 1421-1432.

de Miguel Mercader, F., Groeneveld, M.J., Kersten, S.R.A., Way, N.W.J., Schaverien, C.J., Hogendoorn, J.A. 2010. Production of advanced biofuels: Co-processing of upgraded pyrolysis oil in standard refinery units. *Applied Catalysis B: Environmental*, **96**(1), 57-66.

de Miguel Mercader, F., Koehorst, P.J.J., Heeres, H.J., Kersten, S.R.A., Hogendoorn, J.A. 2011. Competition between hydrotreating and polymerization reactions during pyrolysis oil hydrodeoxygenation. *AIChE Journal*, **57**(11), 3160-3170.

Elliott, D.C. 2007. Historical developments in hydroprocessing bio-oils. *Energy & Fuels*, **21**(3), 1792-1815.

Elliott, D.C., Hart, T.R., Neuenschwander, G.G., Rotness, L.J., Olarte, M.V., Zacher, A.H., Solantausta, Y. 2012. Catalytic hydroprocessing of fast pyrolysis bio-oil from pine sawdust. *Energy & Fuels*, **26**(6), 3891-3896.

Elliott, D.C., Hart, T.R., Neuenschwander, G.G., Rotness, L.J., Zacher, A.H. 2009. Catalytic hydroprocessing of biomass fast pyrolysis bio‐oil to produce hydrocarbon products. *Environmental Progress & Sustainable Energy*, **28**(3), 441-449.

Fogassy, G., Thegarid, N., Toussaint, G., van Veen, A.C., Schuurman, Y., Mirodatos, C. 2010. Biomass derived feedstock co-processing with vacuum gas oil for second-generation fuel production in FCC units. *Applied Catalysis B: Environmental*, **96**(3), 476-485.

French, R.J., Hrdlicka, J., Baldwin, R. 2010. Mild hydrotreating of biomass pyrolysis oils to produce a suitable refinery feedstock. *Environmental Progress & Sustainable Energy*, **29**(2), 142-150.

Furimsky, E. 2000. Catalytic hydrodeoxygenation. *Applied Catalysis A: General*, **199**(2), 147-190.

Furimsky, E. 2013. Hydroprocessing challenges in biofuels production. *Catalysis Today*, **217**, 13-56.

Hedrick, J.B. 2010. Mineral Commodity Summaries, Rare Earths.

Hoekstra, E., Kersten, S.R.A., Tudos, A., Meier, D., Hogendoorn, K.J.A. 2011. Possibilities and pitfalls in analyzing (upgraded) pyrolysis oil by size exclusion chromatography (SEC). *Journal of Analytical and Applied Pyrolysis*, **91**(1), 76-88.

Hossain, A.K., Davies, P.A. 2013. Pyrolysis liquids and gases as alternative fuels in internal combustion engines–A review. *Renewable and Sustainable Energy Reviews*, **21**, 165-189.

Li, D., Berruti, F., Briens, C. 2014. Autothermal fast pyrolysis of birch bark with partial oxidation in a fluidized bed reactor. *Fuel*, **121**, 27-38.

Li, K., Wang, R., Chen, J. 2011. Hydrodeoxygenation of anisole over silica-supported Ni2P, MoP, and NiMoP catalysts. *Energy & Fuels*, **25**(3), 854-863.

Matsumura, Y., Minowa, T., Potic, B., Kersten, S.R.A., Prins, W., van Swaaij, W.P.M., van de Beld, B., Elliott, D.C., Neuenschwander, G.G., Kruse, A. 2005. Biomass gasification in near-and super-critical water: status and prospects. *Biomass and Bioenergy*, **29**(4), 269-292.

Mortensen, P.M., Grunwaldt, J.D., Jensen, P.A., Knudsen, K.G., Jensen, A.D. 2011. A review of catalytic upgrading of bio-oil to engine fuels. *Applied Catalysis A: General*, **407**(1), 1-19.

Parlett, C.M.A., Wilson, K., Lee, A.F. 2013. Hierarchical porous materials: catalytic applications. *Chemical Society Reviews*, **42**(9), 3876-3893.

Pines, H., Haag, W.O. 1960. Alumina: Catalyst and Support. I. Alumina, its Intrinsic Acidity and Catalytic Activity1. *Journal of the American Chemical Society*, **82**(10), 2471-2483.

Romero, Y., Richard, F., Brunet, S. 2010. Hydrodeoxygenation of 2-ethylphenol as a model compound of bio-crude over sulfided Mo-based catalysts: Promoting effect and reaction mechanism. *Applied Catalysis B: Environmental*, **98**(3), 213-223.

Ryymin, E.-M., Honkela, M.L., Viljava, T.-R., Krause, A.O.I. 2010. Competitive reactions and mechanisms in the simultaneous HDO of phenol and methyl heptanoate over sulphided NiMo/γ-Al_2O_3. *Applied Catalysis A: General*, **389**(1), 114-121.

Tung, L.H. 1966. Method of calculating molecular weight distribution function from gel permeation chromatograms. *Journal of Applied Polymer Science*, **10**(3), 375-385.

Vaccari, A. 1999. Clays and catalysis: a promising future. *Applied Clay Science*, **14**(4), 161-198.

Venderbosch, R.H., Ardiyanti, A.R., Wildschut, J., Oasmaa, A., Heeres, H.J. 2010. Stabilization of biomass‐derived pyrolysis oils. *Journal of chemical technology and biotechnology*, **85**(5), 674-686.

Wang, X., Clark, P., Oyama, S.T. 2002. Synthesis, characterization, and hydrotreating activity of several iron group transition metal phosphides. *Journal of Catalysis*, **208**(2), 321-331.

Wildschut, J., Arentz, J., Rasrendra, C.B., Venderbosch, R.H., Heeres, H.J. 2009a. Catalytic hydrotreatment of fast pyrolysis oil: model studies on reaction pathways for the carbohydrate fraction. *Environmental Progress & Sustainable Energy*, **28**(3), 450-460.

Wildschut, J., Mahfud, F.H., Venderbosch, R.H., Heeres, H.J. 2009b. Hydrotreatment of fast pyrolysis oil using heterogeneous noble-metal catalysts. *Industrial & Engineering Chemistry Research*, **48**(23), 10324-10334.

Wildschut, J., Melian-Cabrera, I., Heeres, H.J. 2010. Catalyst studies on the hydrotreatment of fast pyrolysis oil. *Applied Catalysis B: Environmental*, **99**(1), 298-306.

Williams, P.T., Taylor, D.T. 1994. The molecular weight range of pyrolytic oils derived from tyre waste. *Journal of Analytical and Applied Pyrolysis*, **29**(2), 111-128.

Wu, C.-S. 2003. Handbook of size exclusion chromatography and related techniques: Revised and expanded. CRC Press.

Xu, C.C., Sang, L., Bao, D., Siddiqui, H., Abbott, K., Balasundharam, V., Chad, J., Freeman, Z., Vanegas, J.C., Maddox, E. 2013. Innovation in green process engineering undergraduate laboratory course-integrated laboratories for particulate operations, heat transfer and mass transfer courses. *Proceedings of the Canadian Engineering Education Association*.

Yadav, G.D., Kadam, A.A. 2013. Selective engineering using Mg–Al calcined hydrotalcite and microwave irradiation in mono-transesterification of diethyl malonate with cyclohexanol. *Chemical Engineering Journal*, **230**, 547-557.

Zacher, A.H., Olarte, M.V., Santosa, D.M., Elliott, D.C., Jones, S.B. 2014. A review and perspective of recent bio-oil hydrotreating research. *Green Chemistry*, **16**(2), 491-515.

Zdražil, M. 2003. MgO-supported Mo, CoMo and NiMo sulfide hydrotreating catalysts. *Catalysis Today*, **86**(1), 151-171.

Zhao, H.Y., Li, D., Bui, P., Oyama, S.T. 2011. Hydrodeoxygenation of guaiacol as model compound for pyrolysis oil on transition metal phosphide hydroprocessing catalysts. *Applied Catalysis A: General*, **391**(1), 305-310.

Chapter 4

4 Hydrodeoxygenation of fast pyrolysis oil with novel activated carbon-supported NiP and CoP catalysts

4.1 Introduction

Nowadays the majority of world's energy consumption is derived from fossil fuels. However, due to rapid dwindling of petroleum deposits (also finite nature of fossil fuels) and the increased environmental concern associated with their use, leading to increased urgency to find alternative sustainable carbon resources for the production of fuels and chemicals (Huber et al., 2006; Román-Leshkov et al., 2007). Over the recent decades, particular attention has been towards the utilization of biomass for the production of renewable fuels and chemicals. Unlike fossil deposits, the use of biomass as a carbon feedstock has an environmental advantage, because the CO_2 emitted during the biomass transformation can be recycled for plant re-growth by CO_2 fixation through the photosynthesis process.

Several routes have been developed for conversion of biomass into liquids and chemicals, including fast pyrolysis (Czernik & Bridgwater, 2004), gasification (Czernik & Bridgwater, 2004; Tijmensen et al., 2002), liquefaction, etc., among which, fast pyrolysis is by far the only industrially realized route. Pyrolysis oil (so called bio-oil) is produced by rapid heating of biomass to 450-600 °C in the absence of oxygen followed by rapid quenching of the vapor products. In this process, the oil yield can reach as high as 75 wt.% of the original dry biomass (Bridgwater, 2003), and a pyrolysis oil typically contained 60-70 % of the initial energy of the biomass (Huber et al., 2006; Mohan et al., 2006). Pyrolysis oil is a complex mixture of hundreds of compounds and mainly consists of hydroxyl aldehydes, hydroxyketones, sugars, carboxylic acids, esters, furans, guaiacols and phenols (Mohan et al., 2006). However, due to the high oxygen content (normally about 40-50 %), the heating value of the pyrolysis oil is only in the vicinity of 16-18 MJ/kg, which is unfavorable for use by internal combustion engines. Other demerits associated with pyrolysis oil include: insolubility with petroleum fuels, thermal and chemical instability, coke formation during processing and high acidity. All these shortcomings would hamper the direct use of pyrolysis oil as transportation fuel (Breaking the et al., 2008; Zhao et al., 2011). In order to remove oxygen, further upgrading of bio-oil is required. Two

general methods have been developed for upgrading pyrolysis oils: hydrodeoxygenation (HDO) and catalytic cracking over zeolite-based catalysts (Mortensen et al., 2011). However, catalytic cracking has two main disadvantages associated with it: (i) severe catalyst deactivation due to extensive carbon deposition on catalyst surface, and (ii) a low oil yield (normally around 25 %) and poor quality of the upgraded oil products (Mortensen et al., 2011). In contrast, an HDO process could effectively reduce the oxygen content of a bio-oil with high pressure H_2 in the presence of a HDO catalyst, while maintaining a high oil yield.

Different heterogeneous catalysts have been explored for HDO of bio-oil, including the traditional hydrotreating catalysts such as alumina supported sulfided CoMo or NiMo catalysts. Alumina-supported metal oxides with or without pre-reduction have also been studied for HDO of bio-oil model compounds or real bio-oils (Elliott, 2007; Furimsky, 2000). Even though these catalysts demonstrated to be active for oxygen removal, a short lifetime of the catalysts caused by sulfide phase decomposition and/or coke deposition over a short period of time makes these catalysts less useful for bio-oil upgrading. Alternatively, noble metal catalysts such as Ru, Rh, Pd and Pt have demonstrated promising for HDO of pyrolysis oil, as they produce upgraded oil with a much higher oil yield and improved quality. However, the high prices of these noble metal catalysts makes them unattractive for industrialization. Thus, development of inexpensive and highly active catalysts for bio-oil HDO is of great significance.

In recent years, inexpensive transition metal phosphides have received increasing attention for Hydrodesulfurization (HDS) and Hydrodenitrogenation (HDN) of petroleum derived oils. Recently, Zhao et al. (Zhao et al., 2011) investigated the HDO activity of different transition metal phosphides catalysts in a fixed bed reactor using guaiacol as a model compound for pyrolysis oil, and Ni_2P showed superior activity to other phosphide catalysts. The following effects of phosphrous in metal phosphide catalysts have been discussed in several reports: (a) forming stabilizing solutions that allow high metal concentration in the catalyst preparation (Bridgwater, 1999); (b) improving the catalyst dispersion (Meinshausen et al., 2009); (c) optimizing acidity (Meinshausen et al., 2009); (d) improving the catalyst's resistance to coke deposition (Czernik & Bridgwater, 2004); (e) increasing strength and stability of the support (Venderbosch & Prins, 2010); (f) forming new active species for HDO reactions (Elliott et al., 1990).

In our previous studies, we prepared Ni, Co and Mo phosphide catalysts supported on activated carbon (AC) and tested their HDO activities for pyrolysis oil upgrading. Both Ni and Co phosphides showed similar catalytic activities in terms of overall oil yield and the degree of deoxygenation when compared with those of a commercial HDO catalyst (Ru/C), as discussed in Chapter 3 of this thesis. It was observed that catalyst support would significantly affects the activities of HDO catalysts (Bui et al., 2011). Our research as reported in Chapter 3 also demonstrated that catalyst support played an important role in the performance of the catalyst in bio-oil HDO. For example, HDO operation with MoP/$MgAl_2O_4$ catalyst produced OF with decreased molar ratios of both O/C and H/C, suggesting that the upgrading proceeded mainly through thermal/hydro-cracking reactions rather than through HDO/hydrogenation reactions. AC was chosen as the best support materials for metal phosphides in terms of the HDO activities. With respect to the yields and composition of the upgraded oil products and prices of the catalysts, NiP/AC was chosen as the most promising catalyst among all transition metal phosphide catalysts (CoP/AC, NiP/AC and MoP/AC, all containing 2 wt.% P in relation to the AC support) as well as the commercial noble metal catalyst (Ru/C).

In the present study, the amounts of phosphorous addition to the AC-supported Ni and Co phosphide catalysts were optimized by varying the metal/P ratio (mol/mol). Moreover, the effects of Ru as a co-catalyst in these AC-supported metals or metal phosphides catalysts were also investigated. The effects of the AC-supported Ni and Co phosphide catalysts with different phosphorus contents or with/without Ru addition on their HDO performance were studied systematically, in comparison with the performance of the commercial Ru/C, widely used in literature (de Miguel Mercader et al., 2010; Wildschut et al., 2009). The properties of upgraded oils were measured by GC/MS, GPC and elemental analysis. In addition, fresh and spent samples of some selected catalyst were characterized by XRD, TEM, XPS and BET measurements.

4.2 Materials and methods

4.2.1 Materials

The commercial Ru/C catalyst supplied by Sigma Aldrich was used as received. It contains 5 wt.% of Ru metal, with a mean particle size of 14 um and BET specific surface area of 810 m^2/g.

ACS reagent grade chemicals, including nickel nitrate hexahydrate ($Ni(NO_3)_2 \cdot 6H_2O$), cobalt nitrate hexahydrate ($Co(NO_3)_2 \cdot 6H_2O$), and ruthenium nitrosyl nitrate in dilute nitric acid ($HN_4O_{10}Ru$), were also purchased from Sigma-Aldrich. The support used in this study was activated carbon (Norit ROW 0.8mm pellets from Alfa Aesar). Phosphoric acid (Min. 85 %), acetone (95.5 %), HPLC grade tetrahydrofuran (THF) with 0.03 wt.% 2, 6-di-t-butyl-4-methyl-phenol as a stabilizer were purchased from Caledon. Pure ethanol (99.97 %) was supplied by Commercial Alcohol Inc. Hardwood sawdust fast pyrolysis oil (PO) was supplied by BTG Company (Enschede, The Netherlands) with water content of 24 wt.%. Analytical grade (>99.9999%) hydrogen and nitrogen were purchased from Praxair.

4.2.2 Catalysts preparation

A series of AC-supported HDO (Ni and Co) catalysts were prepared by incipient wetness impregnation method, keeping the metal content constant while varying the phosphorus content. For Ni-based catalysts, the prepared catalyst samples had an initial Ni/P molar ratio of 5/2, 3/2, 1/1, 1/2, 1/3 and Ni without P. In preparation of the AC-supported nickel phosphide catalysts by incipient wetness impregnation method, firstly, 4.62 g $Ni(NO_3)_2 \cdot 6H_2O$ was dissolved in 12 g water-ethanol solution (4/1 w/w) in a flask to form a clear solution, then the corresponding amount of H_3PO_4 (as shown in **Table 4-1**) was added dropwise followed by addition 10 g of activated carbon support. After impregnation, the powder sample was dried at 100 °C overnight. The samples were then simultaneously calcined/reduced by heating it at 5 °C/min in a tubular reactor under flowing hydrogen (40 mL/min) to convert the metal phosphate into metal phosphide, at 600 °C for 3 h. Before the calcination operation, all samples were flushed with hydrogen several times to eliminate oxygen in the tubular reactor. The sample was then cooled in N_2 to room temperature and was passivated in this N_2 flow for 1 h, after which the catalyst samples were grounded with a mortar and pestle, and sieved to particle size between 180 and 420 μm for use (i.e., a mesh size of 20/80). Similar procedure was employed for the preparation Co based catalysts by varying the Co/P ratio with and without phosphorous.

Table 4-1 The amounts of H_3PO_4 added in different AC-supported metal phosphide catalysts

Catalyst name	M[a]	M/P=5/2	M/P=3/2	M/P=1/1	M/P=1/2	M/P=1/3
H_3PO_4 (g)	0	0.37	1.22	1.83	3.67	5.50

[a] M refers to Ni or Co metal.

Being slightly different from the aforementioned method for mono-metal phosphide catalysts, in the preparation of bimetallic phosphide catalysts (CoRuP or NiRuP), 3.33 g $HN_4O_{10}Ru$ (0.5 wt.% of AC) was added drop wise before adding H_3PO_4, followed by the similar procedure as described previously. The M/P molar ratio of bimetallic catalysts was fixed at 3/2. The amount of chemicals added in preparation of different AC-supported bimetallic phosphide catalysts are listed in **Table 4-2.**

Table 4-2 The amount of chemicals added in preparation of different AC-supported bimetallic phosphide catalysts

Series name	NiRu	NiRuP	CoRu	CoRuP
$M(NO_3)_2{\cdot}6H_2O$(g)[a]	4.62	4.62	4.61	4.61
$HN_4O_{10}Ru$ (g)	3.33	3.33	3.33	3.33
H_3PO_4 (g)	0	1.22	0	1.22

[a] M refers to Ni or Co.

4.2.3 General reaction procedure

Pyrolysis oil HDO experiments were carried out using a stirred reactor (Parr 4590 Micro Bench top reactor) with a total volume of 100 mL. The schematic drawing of the reactor system is shown in **Fig. 4-1**. The operation temperature and pressure were fixed at 300 °C and 50 bar, respectively. In a typical run, 40 g pyrolysis oil and 2 g catalyst (5 wt.% of pyrolysis oil) were added into the reactor. The reactor was sealed and the residual air was removed by vacuum-purge with hydrogen at least three times. Before the experiment, the reactor was flushed and charged with H_2 to 50 bar and then collected into a gasbag for hydrogen quantification prior to

the HDO experiment. If no leakage, the reactor was pressurized to 50 bar using hydrogen and then heated to 300 °C under agitation at 360 rpm for 3 h (including the heating time). The inside pressure of the reactor increased to 110 to 170 bar during the reaction, depends on the type of catalyst used. After the set reaction time elapsed, the reactor was quenched in an ice/water bath to ambient temperature. The reaction pressure and temperature were recorded at every 10 minutes intervals during each run. Two or three duplicate runs were carried out for each condition to ensure the maximum relative error of the oil yield was within ±5 %.

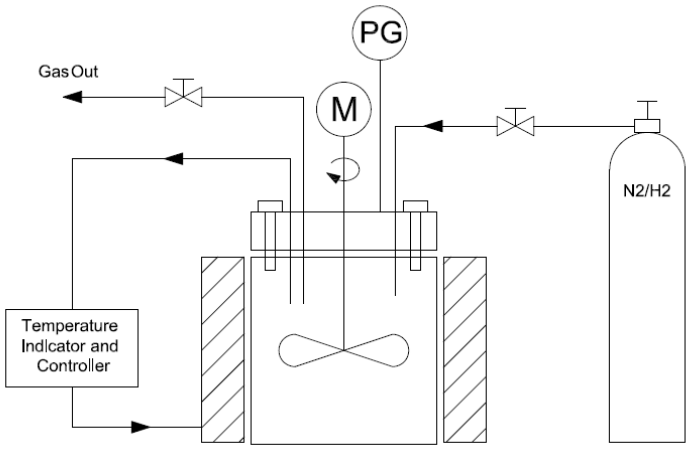

Figure 4-1 Schematic diagram of the reactor system for bio-oil HDO experiments

4.2.4 Products separation

The gas products were collected into a gasbag and analyzed using a Micro-GC equipped with thermal conductivity detector (TCD). The quantification (in moles) of gas species (H_2, CO, CO_2, CH_4, C_2 and C_3 gases) were determined using an N_2 internal standard for calculation of the gas fraction (GF) yield. For all experiments, once complete, the liquid phase consists of only two layers, a dark brown bottom layer and a top aqueous phase. Aqueous fraction (AF) was recovered directly by decanting, the organic fraction of the upgraded oil products was extracted with acetone, and the solid fraction was isolated from the liquid by filtration. The filtrated solids were washed repeatedly with acetone. The solid mass was dried and weighed. The weight of the solid (coke) was corrected for the catalyst intake. The oil fraction (OF) collected by evaporating the solvent under vacuum by using rotary evaporator. Hydrogen consumption was calculated

from the difference of initial amount of H_2 and the remaining H_2 in the reactor analyzed by GC-TCD. The weight of AF was obtained from the weight difference between total feed (PO and H_2) and other products (OF, GF and coke). The chemical composition of AF and coke were not analyzed in this study as OF and H_2 consumption were the main interests of this work. Yields of OF, AF, GF (H_2 was excluded) and coke were calculated by the weight percentage of the mass of each product to the mass of dry PO loaded and H_2 consumed during the reaction in each run. Yields of OF, AF, GF (H_2 was excluded) and coke were calculated using the weight percentage of the mass of each product to the mass of dry PO loaded and H_2 consumed during the reaction in each run. **Equation (4-1)** presented the calculation method for OF product. In addition, degree of deoxygenation (DOD), as defined in **Eq. (4-2)**, was used to evaluate the effectiveness of the HDO process.

$$\mathrm{Y}_{oil} = \left(\frac{m_{oil}}{m_{feed,dry}}\right) \cdot 100\% \qquad (4\text{-}1)$$

$$\mathrm{DOD} = \left(1 - \frac{O(wt\%)_{product\ oil}}{O(wt\%)_{feed,dry}}\right) \qquad (4\text{-}2)$$

The Y_{oil} is the total oil yield after HDO, m_{oil} is the total mass of product oil and $\mathrm{m}_{feed,dry}$ is the water free feedstock oil. For DOD equation, $O\ (wt.\%)_{product\ oil}$ and $O\ (wt.\%)_{feed\ oil}$ represent the weight percent of oxygen in the product oil and water free feed, respectively. The combination of these two parameters can achieve a relatively comprehensive summarization for HDO.

4.2.5 Oil fraction (OF) characterization

Volatile compositions of the obtained fresh OF products were analyzed using a GC-MS (Shimazu QP2010S) with an SHRXI MS column (30 m × 0.25 mm × 0.25 um) and the temperature program of the column was heating from 50 to 280 °C (10 °C/min, hold for 30 min). The molecular weights and their distributions of the OF were analyzed on a Water Breeze gel permeation chromatography (GPC) instrument (1525 binary HPLC pump; UV detector at 270 nm; Water Styrange HR1 column at 40 °C) using THF as an eluent at a flow rate of 1 mL/min

and polystyrene was used as an internal standard. Thermo Fischer Flash EA 1112 series CHNS-O elemental analyzer was used to investigate the C, H, N contents. As negligible S was detected in the hardwood-derived oil used in this study, O content (wt.%) could be calculated by difference (100 wt.% – C– H – N). The results of elemental analysis were used to determine the degree of deoxygenation (DOD) and the molar ratios of H/C and O/C. Higher Heating Value (HHV) of oil was also measured using an IKA Calorimeter System in addition to calculation with the Dulong formula for some oil samples.

4.2.6 Catalyst characterization

The XRD spectra were collected on an X-ray diffractometer (Rigaku RINT 2500, Tokyo, Japan) with Cu K radiation (λ = 1.54059 Å) at 30 kV and 15 mA with a scan rate of 0.02° per second over a 2θ range from 10° to 80°. The BET analysis was performed using Micrometrics ASAP 2010. Prior to BET measurement, the sample was degassed at 150 °C under a stable static vacuum of less than 5×10^{-3} Torr. The XPS analyses were carried out on a Kratos Axis Ultra spectrometer using a monochromatic Al K(alpha) source (15mA, 14kV). XPS can detect all elements except hydrogen and helium, probes the surface of the sample to a depth of 5-7 nm, and has detection limits ranging from 0.1 to 0.5 atomic percent depending on the element. The instrument was calibrated to give a binding energy (BE) of 83.96 eV for the Au $4f_{7/2}$ line for metallic gold and the spectrometer dispersion was adjusted to give a BE of 932.62 eV for the Cu $2p_{3/2}$ line of metallic copper. The Kratos charge neutralizer system was used on all specimens. Survey scan analyses were carried out with an analysis area of 300 x 700 microns and a pass energy of 160 eV. Spectra were analyzed using CasaXPS software. TEM images were acquired using a JEOL JEM-2100F field emission transmission electron microscope equipped with an ultra-high resolution pole-piece operating at 200 kV. The elemental compositions were obtained using an X-ray energy dispersive spectrometer (EDS) from Oxford Instruments. The ground catalyst powder was first dispersed in 99% EtOH, followed by sonication for 5 minutes to disperse the catalyst particles. The TEM specimen was then prepared by adding a microdrop of the dispersion onto a copper grid coated with carbon film (300 mesh, EMS).

4.3 Results and Discussion

4.3.1 HDO oil composition and yield

Initially, we tested HDO of pyrolysis oil over Ni and Co-based catalysts with various M/P ratios and later compared their catalytic activities by adding Ru (with $HN_4O_{10}Ru$ solution) as a co-catalyst to the metal phosphides or metallic catalysts. In order to know the effect of phosphorus on HDO of pyrolysis oil we also compared Ni or Co catalysts without phosphorus. The upgraded oil yields from HDO of pyrolysis oil over different catalysts are shown in **Figure 4-2**. Due to the loss of water and the transfer of highly oxygenated components to the aqueous products, the resulted overall oil yield was in the range of 30 - 65 wt.%. As clearly shown in **Figure 4-2**, the oil yields with either Ni or Co-based catalysts varied drastically from 29 wt.% (M/P = 1/3) to 66 wt.% (M/P = 3/2) by varying M/P ratio. For both Ni and Co-based catalysts the oil yield reached the maximum at about M/P = 3/2. The oil yield was decreased significantly with further increasing P amount or decreasing the M/P ratio. The difference in catalytic activity while varying the M/P ratio might be due to the formation of new active species on catalyst surface and changes in acidity of the catalysts.

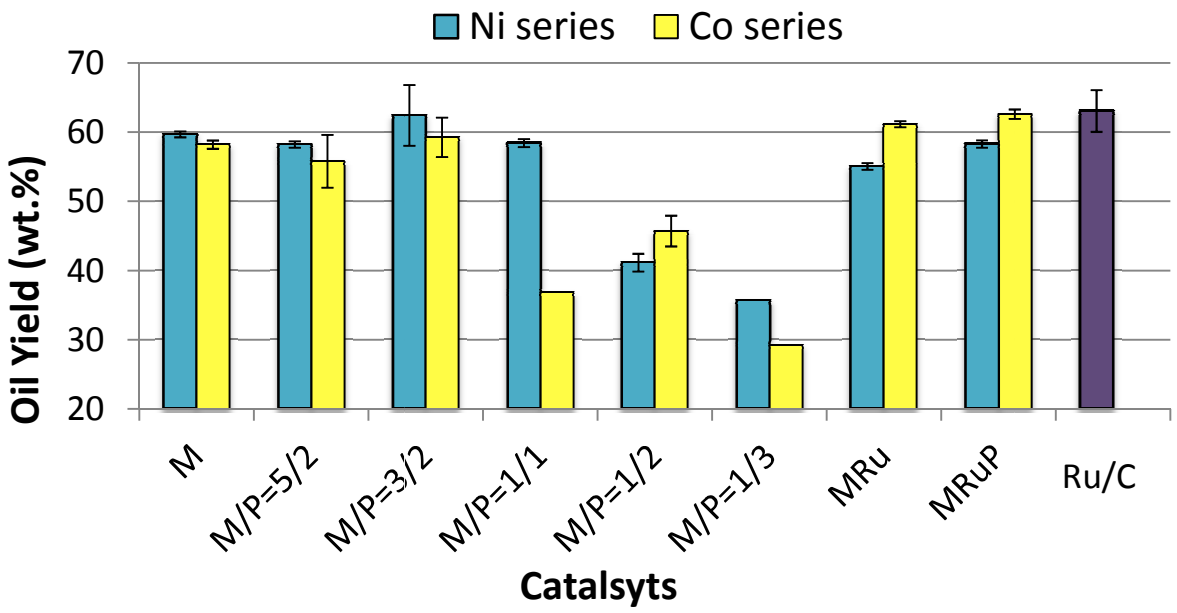

Figure 4-2 Yield of upgraded oil from HDO of pyrolysis oil over Ni and/or Co catalysts with different M/P ratios compared with Ru/C (300 °C, 50 bar H_2, 3 h)

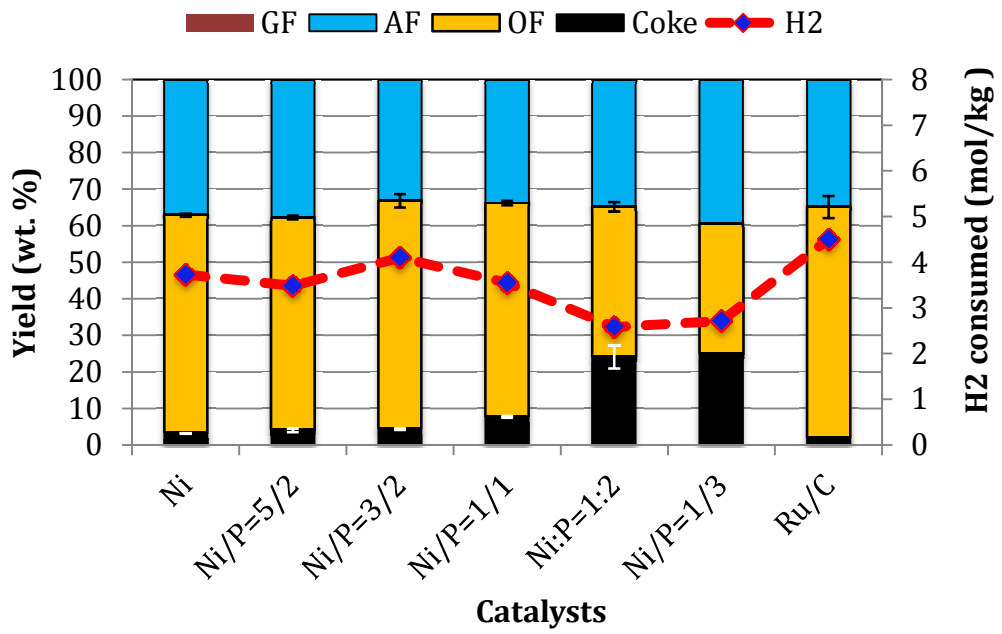

Figure 4-3 Effects of phosphorus content in Ni-based catalysts on product yields and H_2 consumption compared with Ru/C (300 °, 50 bar H_2, 3 h)

The decrease in oil yield with increasing phosphorus content was further investigated. In all tests, the amount of gas products was very small, so detailed discussion on gas formation was not performed in this study. However, hydrogen consumption is believed to associate with hydrogenation and deoxygenation reactions. **Figure 4-3** illustrates effects of phosphorus content in Ni-based catalysts on product yields and H_2 consumption compared with Ru/C at 300 °C, 50 bar H_2 and 3 h. Generally, the oil yield has a positive correlation with H_2 consumption and the degree of deoxygenation (DOD) showing in **Table 4-4** and **4-5**. **Figure 4-3** shows that coke yield increased almost monotonically with increase of phosphorus content, when M/P < 3/2 accompanied with a decrease in oil yield. The decrease of oil yield at M/P < 3/2 was likely caused by catalyst deactivation due to coke deposition over the active sites. The results in **Figures 4-2** and **4-3** also clearly demonstrate that the Ru/C catalyst is still more effective than the nickel phosphide catalysts with respect to the oil yield, H_2 consumption and coke formation.

Figure 4-4 shows effects of phosphorus content in Co-based catalysts on product yields and H_2 consumption compared with Ru/C. Compared to that illustrated in **Figure 4-3**, the coke formation with the Co-based catalysts is much higher than that of Ni-based catalysts, and surprisingly, both Ni and Co phosphide catalysts with M/P ratio 3/2 gave the highest oil yield, while the cobalt-based catalysts generally have low HDO activities over the Ni-based catalysts. Deposition of large amounts of coke with decreases of M/P ratio (or increase of P addition amount) might be due to the increased acidity of the catalysts.

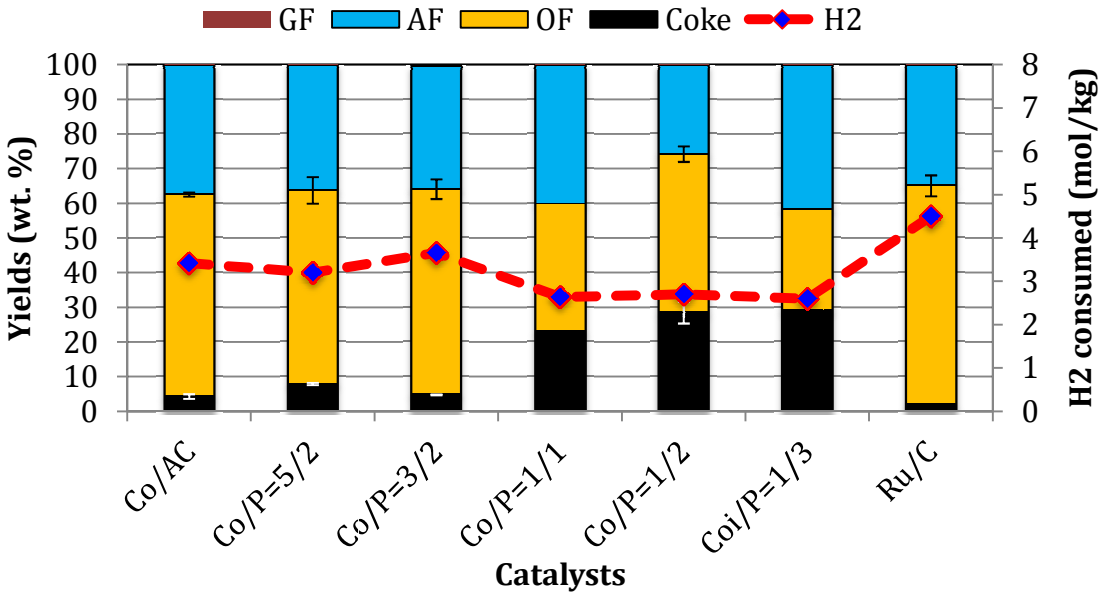

Figure 4-4 Effects of phosphorus content in Co-based catalysts on product yields and H_2 consumption compared with Ru/C (300 °C, 50 bar H_2, 3 h)

Moreover, performance of the bimetallic catalysts (NiRu, NiRuP, CoRu or CoRuP) in HDO of pyrolysis oil with respect to product yields and H_2 consumption compared with Ru/C was examined and compared in **Figure 4-5**. It can be deduced from that there was no obvious difference in either H_2 consumption or products (oil and coke) yields among all bimetallic catalysts used in this study.

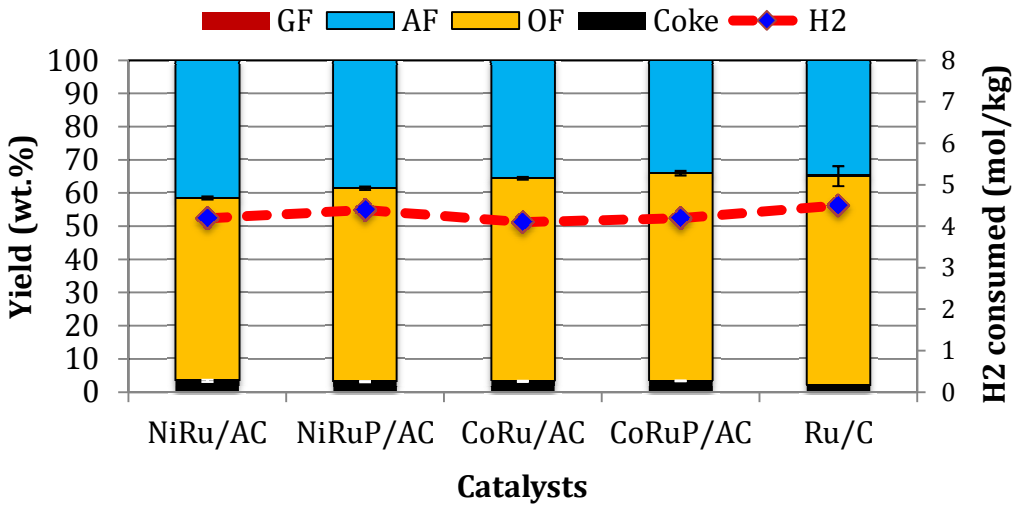

Figure 4-5 Performance of the bimetallic catalysts in HDO of pyrolysis oil with respect to product yields and H_2 consumption compared with Ru/C (300 °C, 50 bar H_2, 3 h)

4.3.2 Properties of HDO products

4.3.2.1 Molecular weight distribution

Gel permeation chromatography (GPC) was used to determine the molecular weight distribution of the bio-oil feed and upgraded bio-oil produced using different HDO catalysts, as shown in **Figure 4-6** and **Figure 4-7**. In molecular weight distribution curves, *W(logM)* (in y-axis) is defined as the slope of the graph in which the cumulative mass is plotted against the logarithm of the molecular weight (*logM* in x-axis) (Hoekstra et al., 2011). The GPC curves in both figures show a broad peak, suggesting relatively wide distribution of molecular weight for all bio-oil

samples. The average molecular weights (M_w and M_n) and polydispersity (PD = M_w/M_n) of the upgraded bio-oils are given in **Table 4-3**. The bio-oil feed has an M_w of 940 Da, M_n of 330 Da and PD of 2.87. The molecular weight and distribution of upgraded bio-oils varied largely by different Ni/Co catalysts: The M_n, M_w and PD of the upgraded oils with Ni catalysts are in the range of 320-400 Da, 700-1060 Da and 1.83-3.05, respectively. And the corresponding values for Co catalysts are 290-460 Da, 620-1260 Da and 1.82-2.98, respectively. Generally, the Ni-based catalysts are more effective for decreasing the molecular weight of bio-oil than the Co-based catalysts. It shall be noted that with the CoP/AC catalyst at Co/P=3/2, the yield of the upgraded oil was the highest, but the oil's molecular weight significantly increased, suggesting self-polymerization or condensation reactions of the reaction intermediates or products. For both Ni and Co catalysts, the molecular weight of upgraded oil largely shifted to a smaller M_w with MoP/AC catalyst at M/P = 1/3, though the oil yield was the lowest with this catalyst.

Moreover, the results of GPC analysis revealed that the addition of Ru to either NiP or CoP catalyst significantly reduced the molecular weight at a given P content. In contrast, for NiRu or CoRu catalysts, the addition of P had little effect on varying the molecular weight distribution of the upgraded oil, but the oil yield did increase slightly by P addition, suggesting positive effect of P-addition on bio-oil HDO. It is also clearly shown in **Table 4-3**, both NiRu/AC and NiRuP/AC (with only 0.5 wt.% Ru in AC support) are promising inexpensive catalysts that produced a high yield of upgraded oil products with lower molecular weight distribution, comparable with those of the commercial Ru/C (containing 5 wt.% Ru in AC support).

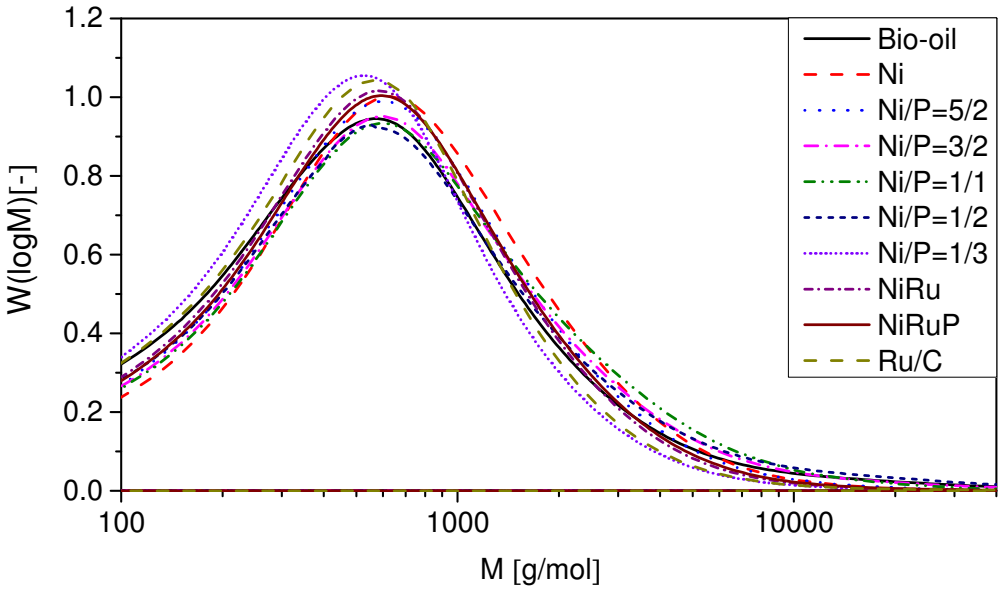

Figure 4-6 Molar mass distribution of the bio-oil feed and the upgraded oil products obtained with different Ni-based catalysts in comparison with Ru/C

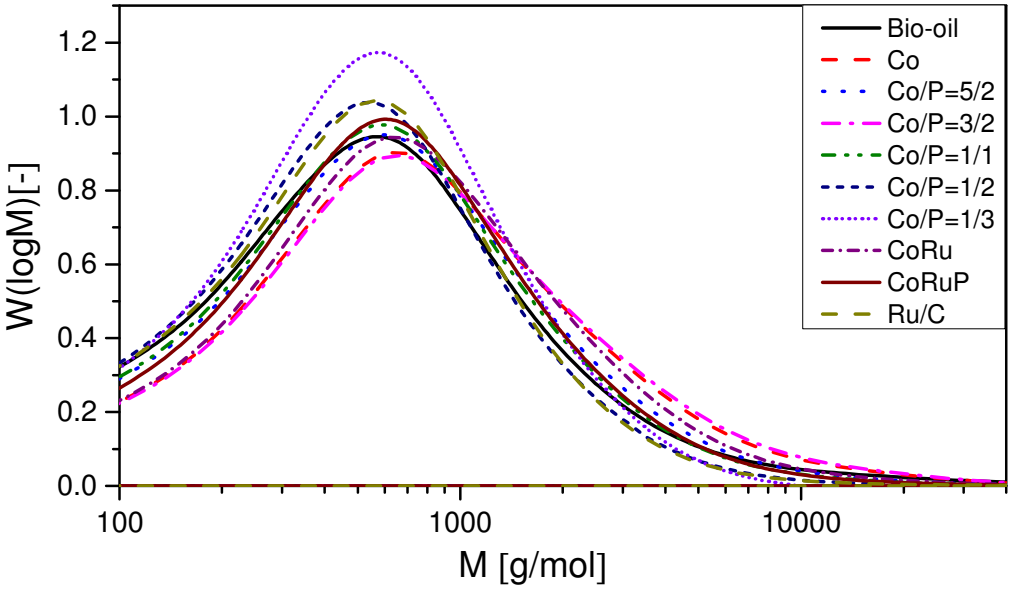

Figure 4-7 Molar mass distribution of the bio-oil feed and the upgraded oil products obtained with different Co-based catalysts in comparison with Ru/C

Table 4-3 GPC results of bio-oil feed and the upgraded oil products obtained with different catalysts in comparison with Ru/C (300 °C, 50 bar H_2, 3 h)

Catalyst	M_n[a]	M_w[b]	PD[c]	Catalyst	M_n	M_w	PD
Bio-oil[d]	330	950	2.87	Ru/C	330	710	2.15
Ni	360	850	2.38	Co	440	1180	2.67
Ni/P=5/2	300	810	2.69	Co/P=5/2	290	870	2.98
Ni/P=3/2	380	870	2.28	Co/P=3/2	460	1260	2.67
Ni/P=1/1	400	1060	2.64	Co/P=1/1	400	840	2.08
Ni/P=1/2	300	890	2.95	Co/P=1/2	340	740	2.16
Ni/P=1/3	220	660	3.05	Co/P=1/3	340	620	1.82
NiRu	380	690	1.83	CoRu	360	870	2.42
NiRuP	330	700	2.14	CoRuP	390	900	2.29

[a,b] The unit for M_n and M_w are Dalton.

[c] PD: Polydispersity (=M_w/M_n).

[d] Bio-oil feed.

4.3.2.2 Elemental analysis

The properties of the bio-oil products are of particular interest in this work. The oxygen contents of the samples were analyzed by CHNS elemental analysis, and the higher heating value (HHV) of the oil sample was calculated using the Dulong formula, i.e., HHV (MJ/kg)=0.3383C+1.422 (H-O/8) where C, H and O were elemental composition of the oil in weight percentage on dry basis. Two samples were taken for HHV measurement with an IKA Calorimeter System, in order to validate the HHV calculation method using the Dulong formula. For feed bio-oil and the OF obtained with Ru/C, the measured HHV is 23.0 MJ/kg and 31.0 MJ/kg, respectively, compared with 22.7 MJ/kg and 32.5 MJ/kg by calculation, as shown in **Tables 4-4** and **4-5**. These results suggest a good agreement of the calculated HHV and the measured values. As given in **Table 4-4** for Ni-based catalysts and **Table 4-5** for Co-based catalysts, all bio-oil samples exhibited

higher carbon contents and lower concentration of oxygen, leading to significantly increase of higher heating values. The upgraded bio-oils exhibited HHV around 32-36 MJ/kg (except Co/P=1/3 with 29.3 MJ/kg), in relation to the HHV of only 22.7 MJ/kg on dry basis (or 16 MJ/kg on wet basis) for the bio-oil feed. The oil products obtained with catalysts of Ni/P=3/2, Ni/P=1/1 and Co/P=3/2 have an HHV of 37.2 MJ/kg, 37.0 MJ/kg and 36.2 MJ/kg, respectively, higher than that obtained with other catalysts tested. Simply in accordance to the Dulong formula, higher oxygen content in a bio-oil corresponds to a lower HHV of the oil. Thus, for Ni-based phosphide catalysts, the degree of deoxygenation (DOD) showed a similar trend, i.e., the DOD increased with P content, reached the highest value of 0.65 at Ni/P=3/2 and 1/1, but decreased gradually when further increasing the P content in the NiP catalyst. Similar results were obtained with the Co-based catalysts, and the highest DOD (= 0.65) was achieved with CoP/AC catalysts at Co/P = 3/2. The addition of Ru into either Ni/AC or NiP/AC or Co/AC or CoP/AC had insignificant effects on the DOD or the oil properties (e.g., O/C ratio), although it did increase H_2 consumption in HDO of the bio-oil.

The Van Krevelen plot is presented to evaluate the catalysts' activities based on the O/C and H/C ratios of the upgraded oil products, as shown in **Figure 4-8** and **Figure 4-9** for the Ni-based catalysts and Co-based catalysts, respectively. The ultimate goal of bio-oil HDO was to obtain a liquid bio-fuel with an oxygen content close to zero and a H/C ratio close to 2 (Venderbosch et al., 2010). Obviously, the upgraded oil products obtained in this study under the operating condition (300 °C, 50 bar H_2, 3 h) (H/C = 1.3 – 1.5, and O/C = 0.1 – 0.2) are yet to meet the above ultimate goal of bio-oil HDO. Nevertheless, compared with the bio-oil feed with an H/C and O/C ratio of 1.49 and 1.54, respectively, the upgraded oil with the commercial Ru/C catalyst has a H/C and O/C of 1.43 and 0.22, respectively, suggesting excellent HDO activity of the catalyst (Wildschut et al., 2009; Wildschut et al., 2010). From the **Tables 4-4** and **4-5** and **Figures 4-8** and **4-9**, all upgraded oils have a markedly reduced O/C ratio and slightly lower H/C ratio when compared with the bio-oil feed. For either Ni or Co-based catalysts, the O/C and H/C ratios decreased with increasing the addition of P up to Ni/P or Co/P = 3/2, where the O/C = 0.11-0.12 and H/C = 1.26-1.29, suggesting improved HDO activity but deteriorated hydrogenation activity. With further increase of P addition, reverse trends were observed, i.e., both O/C and H/C ratios increase with increasing P addition, suggesting deteriorated HDO

activity but improved hydrogenation activity. On the other hand, adding a small amount (0.5 wt.%) of Ru to the metal or metal phosphide catalysts significantly increased the catalysts' hydrogenation activities (leading to a higher H/C ratio for the resulted oil products), while it showed a marginally effect on the catalysts' HDO activities. Noticeably, in-house prepared NiRu/AC catalyst exhibited better performance than commercial Ru/C with regards to H/C and O/C.

Comparing the overall performance of the metal or metal phosphide catalysts, the Ni-based catalysts showed generally better hydrogenation and HDO activities than Co-based catalysts.

Table 4-4 Properties of the OF obtained from HDO of the pyrolysis oil with various Ni-based catalysts (300 °C, 50 bar H_2, 3 h)

	PO feed[a]	Ru/C	Ni	Ni/P=5/2	Ni/P=3/2	Ni/P=1/1	Ni/P=1/2	Ni/P=1/3	NiRu	NiRuP
C (wt.%)	56.0	71.0	72.8	72.5	79.8	80.0	73.9	72.0	73.4	73.1
H (wt.%)	7.24	8.55	8.37	8.30	8.64	8.42	7.93	8.06	9.07	8.55
O (wt.%)[b]	36.8	20.5	18.8	19.2	11.6	11.6	18.1	20.0	17.6	18.3
DOD	–	0.42	0.47	0.46	0.65	0.65	0.49	0.44	0.49	0.48
H/C (-)	1.54	1.43	1.37	1.36	1.29	1.26	1.28	1.33	1.47	1.39
O/C (-)	0.49	0.22	0.19	0.20	0.11	0.11	0.18	0.21	0.18	0.19
HHV (MJ/kg)[c]	22.7	32.5	33.2	32.9	37.2	37.0	33.1	32.3	34.6	33.6
HHV (MJ/kg)[d]	23.0	31.0	–	–	–	–	–	–	–	–

[a] Elemental composition of the pyrolysis oil feed on dry basis.

[b] Calculated by difference assuming negligible content of S in the woody biomass-derived bio-oil.

[c] Calculated by the Dulong formula, i.e., HHV (MJ/kg)=0.3383C+1.422 (H-O/8) where C, H and O were in terms of weight percentage.

[d] Measured on an IKA Calorimeter System.

Table 4-5 Properties of the OF obtained from HDO of the pyrolysis oil with various Ni-based catalysts (300 °C, 50 bar H_2, 3 h)

	PO feed[a]	Ru/C	Co	Co/P=5/2	Co/P=3/2	Co/P=1/1	Co/P=1/2	Co/P=1/3	CoRu	CoRuP
C (wt.%)	56.0	71.0	72.6	73.4	78.8	73.0	71.9	66.0	71.8	73.2
H (wt.%)	7.24	8.55	8.23	8.17	8.32	7.76	8.10	8.14	8.49	8.44
O (wt.%)[b]	36.8	20.5	19.2	18.4	12.9	19.2	20.0	25.8	19.7	18.4
DOD	–	0.42	0.46	0.48	0.62	0.46	0.43	0.28	0.44	0.48
H/C (-)	1.54	1.43	1.35	1.33	1.26	1.27	1.34	1.47	1.41	1.37
O/C (-)	0.49	0.22	0.20	0.19	0.12	0.20	0.21	0.29	0.21	0.19
HHV (MJ/kg)[c]	22.7	32.5	32.9	33.2	36.2	32.3	32.3	29.3	32.9	33.5
HHV (MJ/kg)[d]	23.0	31.0	–	–	–	–	–	–	–	–

[a] Elemental composition of the pyrolysis oil feed on dry basis.

[b] Calculated by difference assuming negligible content of S in the woody biomass-derived bio-oil.

[c] Calculated by the Dulong formula, i.e., HHV (MJ/kg)=0.3383C+1.422 (H-O/8) where C, H and O were in terms of weight percentage.

[d] Measured with an IKA Calorimeter System.

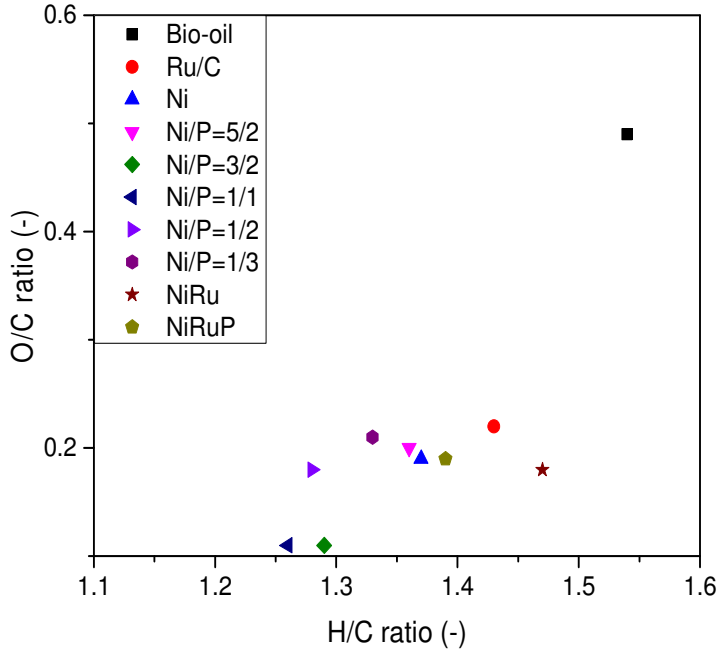

Figure 4-8 Van Krevelen plot for feed bio-oil and the upgraded oil obtained with different Ni-based catalysts, compared with Ru/C

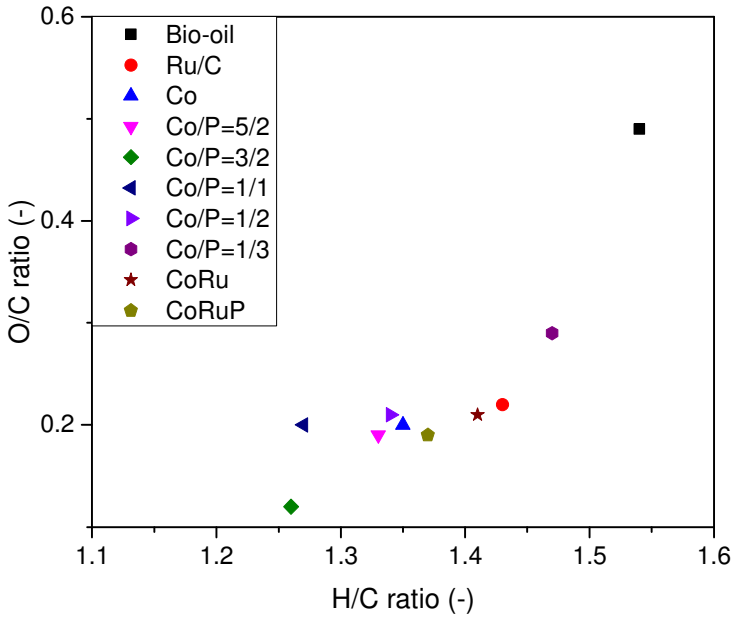

Figure 4-9 Van Krevelen plot for feed bio-oil and the upgraded oil obtained with different Co-based catalysts compared with Ru/C

4.3.2.3 GC-MS analysis

HDO upgrading of fast pyrolysis oil involves complex reactions, such as cracking, decarbonylation, hydrocracking, polymerization, hydrogenation and hydrodeoxygenation, producing oil products with a very complex composition (Lu et al., 2009; Zacher et al., 2014). GC-MS was used to analyze the volatile components of the upgraded oil products obtained at 300 °C, 50 bar H_2 and 3 h. The GC-MS spectra of a typical oil product (obtained with NiRu/AC catalyst) and the original PO are displayed in **Figure 4-10 (a)** and (**b**), respectively. The relative area % for each compound was defined by the percentage of the chromatographic area of the specific compound out of total area. More than 20 different compounds with a relative peak area > 1% were detected by GC-MS, and these compounds are listed in **Table 4-6**. It should be noted that only volatile fraction of oil could pass through the GC column and be detected by the MS (Cheng et al., 2012).

The organic components detected in the oils are in good agreement with those reported in literature (Peng et al., 2008; Xu et al., 2010). The detectable peaks in the upgraded oil are much less when compared with those of the original pyrolysis oil. For example, D-Allose - a derivative of glucose obtained by dehydration (Fullana et al., 2005) was detected in the original pyrolysis oil, but it disappeared after HDO over NiRu/Ac catalyst. Acetic acid is a carboxylic acid present in in crude bio-oil at high concentration (relative content about 13 %), but it was detected in the upgraded oil products after HDO processing. The second largest component in crude bio-oil is 1-hydroxy-2-propanone (accounted for 9 % in total) belongs to ketone functional group. This component could be transformed into propanol, propane or other ketones during HDO treatment (Gayubo et al., 2010; Wang et al., 2009). As shown in **Table 4-6**, 4 kinds of aldehydes are detected (Succindialdehyde, furfural, vanillin and apocynin) in the original bio-oil. Surprisingly, no aldehyde was detected after the hydroprocessing. Phenolic compounds are mainly derived from the depolymerized products of lignin (Nan et al., 2014), and they account for up to 92 % in total of the compounds detectable in the upgraded bio-oil.

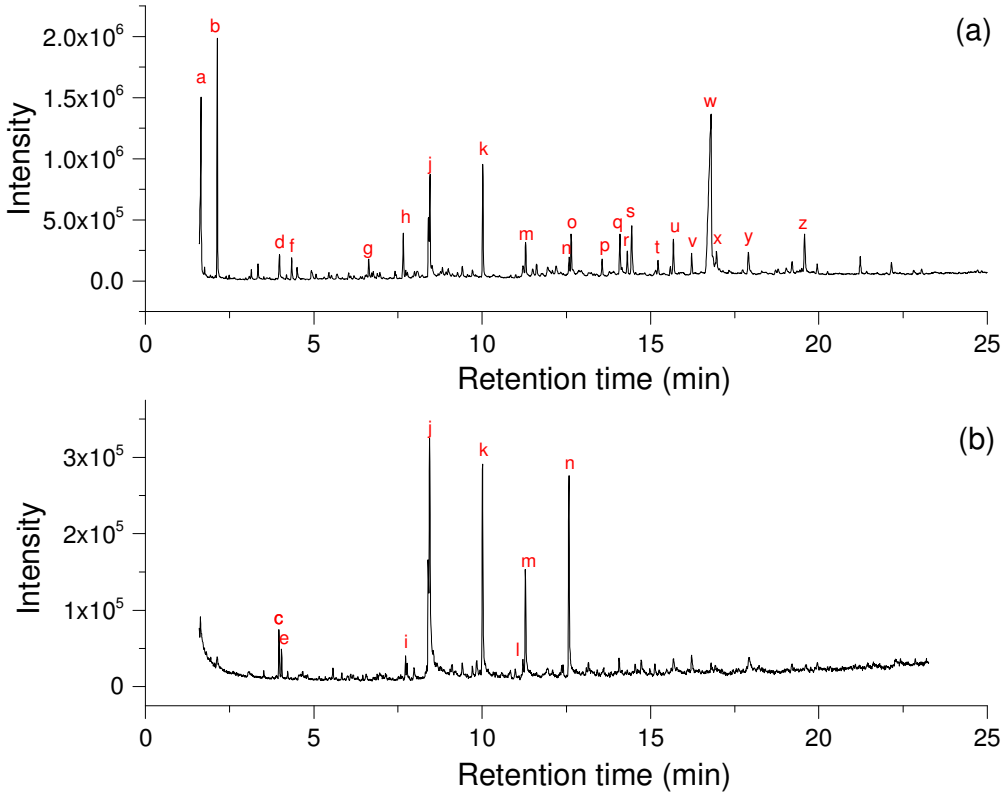

Figure 4-10 GC-MS spectra of the original pyrolysis oil (a) and the upgraded oil obtained with NiRu/AC catalyst (b)

Table 4-6 Chemical composition of the bio-oil feed and the upgraded bio-oil obtained by HDO over NiRu/AC catalyst at 300 °C, 50 bar H_2, 3 h

NO.	Ret. Time (min)	Relative composition by area (%)		Compound name	Group
		PO	NiRu/AC		
a	1.650	12.976	-	Acetic acid	Acids
b	2.134	9.171	-	2-Propanone, 1-hydroxy-	Ketones
c	3.967	-	4.483	2-Pentanone, 4-hydroxy-4-methyl-	Ketones
d	3.985	1.568	-	Succindialdehyde	Aldehydes

e	4.043	-	2.278	Cyclopentanone, 2-methyl-	Ketones
f	4.342	1.344	-	Furfural	Aldehydes
g	6.632	1.126	-	2(5H)-Furanone	Ketones
h	7.662	2.733	-	1,2-Cyclopentanedione, 3-methyl-	others
i	7.727	-	1.482	2-Cyclopenten-1-one, 2,3-dimethyl-	Ketones
j	8.451	4.872	26.983	Phenol, 2-methoxy-	Phenolics
k	10.023	6.892	23.925	Creosol	Phenolics
l	11.213	-	2.979	1,4-Benzenediol, 2,3,5-trimethyl-	Phenolics
m	11.295	2.465	15.104	Phenol, 4-ethyl-2-methoxy-	Phenolics
n	12.587	1.268	22.765	Phenol, 2-methoxy-4-propyl-	Phenolics
o	12.644	3.074	-	Eugenol	Phenolics
p	13.566	1.340	-	trans-Isoeugenol	Phenolics
q	14.095	2.190	-	trans-1-Methoxy-1-butene	others
r	14.311	1.395	-	trans-Isoeugenol	Phenolics
s	14.444	3.848	-	Vanillin	Aldehydes
t	15.221	1.038	-	Phenol, 2-methoxy-4-propyl-	Phenolics
u	15.679	2.545	-	Apocynin	Aldehydes
v	16.226	1.373	-	Ethyl homovanillate	others
w	16.798	31.394	-	D-Allose	others
x	16.964	1.918	-	2,5-Dihydroxy-4-isopropyl-2,4,6-cycloheptatrien-1-one	others
y	17.905	2.315	-	Homovanillic acid	Acids
z	19.579	3.153	-	2-Propenal, 3-(4-hydroxy-3-methoxyphenyl)-	others
Total area (%)		100.000	-		

4.3.3 Characterization of catalysts

4.3.3.1 X-ray diffraction (XRD)

In order to examine the variations in crystalline structures of the NiP/AC and CoP/AC catalysts with different P addition amounts (or varying M/P ratios), these catalysts were characterized by XRD. The XRD patterns of NiP/AC and CoP/AC catalysts are shown in **Figure 4-11** and **Figure 4-12**, respectively. For the Ni-based catalysts (**Fig. 4-11**), with the increase of Ni/P ratio form 5/2 to 3/2, the XRD pattern of metallic Ni was found to transform into Ni_2P species. With further increasing Ni/P ratios from 1/1 to 1/2 or 1/3, a new species $Ni_{12}P_5$ (PDF4-7-1-33 was formed besides Ni_2P. We may conclude from the XRD pattern that both these species Ni_2P and $Ni_{12}P_5$ species would be responsible for the high catalytic activity for the NiP/AC in HDO processing of bio-oil, as proven by Chen et al. (2014a) in a previous research using Ni phosphide catalysts for HDO of bio-oil model compounds. Moreover, increasing the phosphorus content led to broadening of the Ni_2P peaks, suggesting the formation of finer crystallites of Ni_2P at a high P content, and greater dispersion of Ni phosphate on the surface during the calcination/reduction stage. For the Co-based catalysts, the XRD pattern did not exhibit any characteristic peaks related to CoP or Co_2P. It might suggest that cobalt phosphide be well dispersed on the AC support and probably the particle size is below the detection limit of XRD. Addition of a small amount of phosphorus would bring about some positive effects on oil yield for both Ni and Co series catalysts, in good agreement with our previous results discussed in Chapter 3. Nevertheless, for metal phosphide catalyst with a low M/P ratio, the oil yield decreased significantly on both types of catalysts. We also performed XRD measurements for the MRu/AC and MRuP/AC (not illustrated here). Unsurprisingly, no peak for Ru was observed due to the amount of Ru added (0.5 wt.%) below the detection limit for XRD.

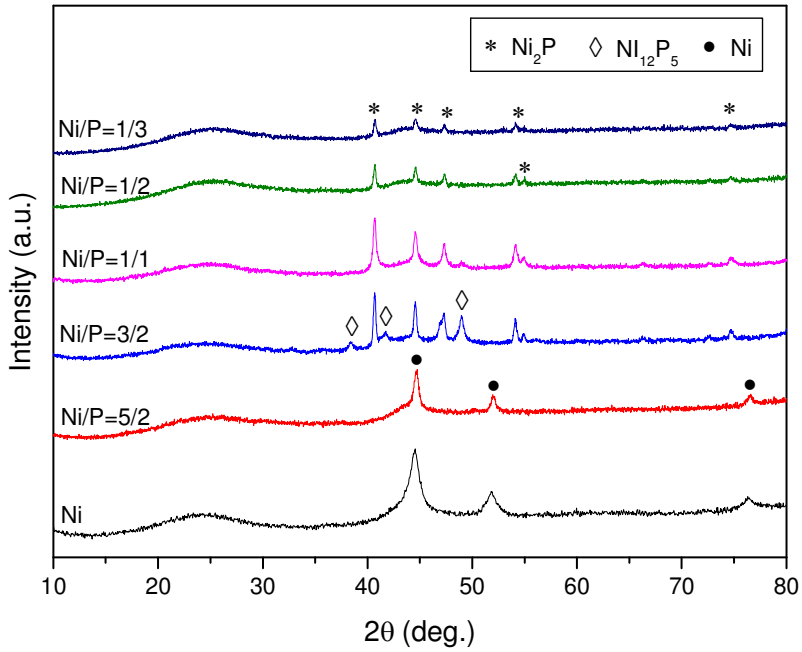

Figure 4-11 X-Ray diffraction patterns for catalysts with different ratios of Ni/P supported on AC. (Ni PDF4-850, $Ni_{12}P_5$ PDF4-7-1-33, Ni_2P PDF3-953)

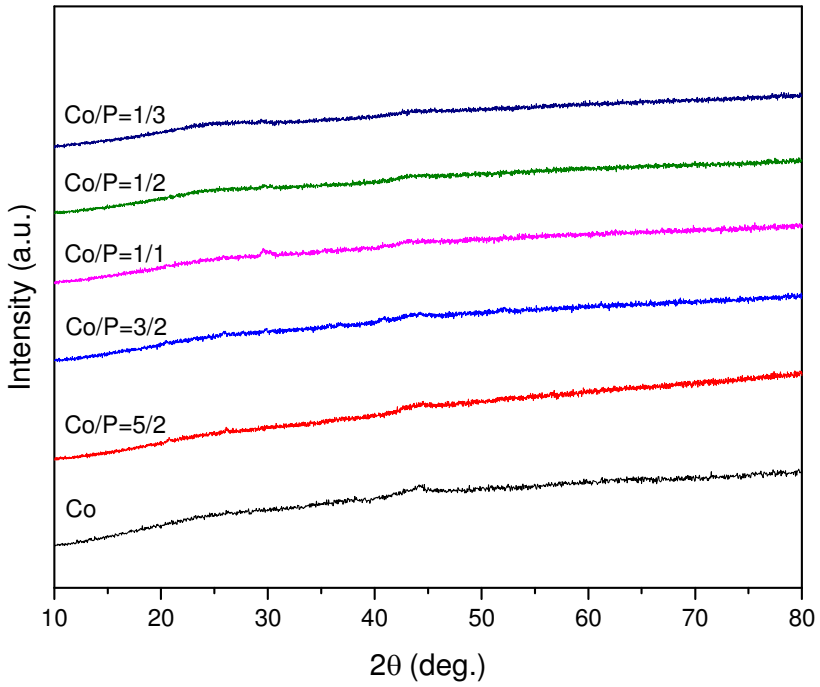

Figure 4-12 X-Ray diffraction patterns for catalysts with different ratios of Co/P supported on AC

4.3.3.2 X-ray photoelectron spectroscopy (XPS)

Table 4-7 Spectral parameters obtained by XPS analysis

Sample	Binding energy (eV)							
	Nickle catalysts				Cobalt catalysts			
	Ni $2p_{3/2}$		P $2p_{3/2}$		Co $2p_{3/2}$		P $2p_{3/2}$	
	Ni^{2+}	Ni_2P (or $Ni_{12}P_5$ or Ni)	Ni_2P or $Ni_{12}P_5$ or Ni)	PO_4^{3-}	Co^{2+}		HPO_3H^-	PO_4^{3-}
M/P=1/3	857.5	853.1	129.7	134.7	782.2	777.9	133.3	134.8
M/P=3/2	857.6	853.0	130.0	134.6	782.0	777.8	133.2	135.0

X-ray photoelectron spectroscopy was used to determine the electronic states of individual elements presented in the catalyst sample. **Table 4-7** compiles the Ni $2p_{3/2}$, Co $2p_{3/2}$, and P $2p_{3/2}$ binding energy values. **Figure 4-13** and **Figure 4-14** illustrates XPS core level spectra of Metal *2p* and P *2p* for NiP and CoP catalysts with 2 different levels of P addition. For the NiP catalysts with a Ni/P molar ratio of 3/2 and 1/3, the deconvoluted XPS spectra of Ni *2p* showed various binding energy values at 857.5 eV and 853.1 eV, indicating that Ni exists in different oxidation states of Ni^{2+} and Ni_2P, where the binding energy values were assigned according to some literatures (Cecilia et al., 2009c). The XRD results of Ni/P=3/2 catalyst as discussed previously in **Figure 4-11** reveal the formation of two phases of nickel phosphide species (Ni_2P and $Ni_{12}P_5$) on AC, however, limited by XPS peak resolution, the XPS spectra peak at the binding energy of 853.1 eV cannot be further deconvoluted into two peaks, due to the fact that Ni_2P and $Ni_{12}P_5$ have very close binding energy values. Moreover, the binding energy of Ni $2p_{3/2}$ for Ni_2P and $Ni_{12}P_5$ in nickel phosphide was very close to that of metallic Ni (852.5 - 853), thus the existence of metallic Ni cannot be ruled out. Furthermore, Ni $2p_{3/2}$ spectra also exhibit higher binding energy values: one at 857.0 eV and another at 862.0 eV. These peaks can be assigned to oxidized Ni^{2+} species and the Ni^{2+} species possibly interacting with unreduced PO_4^{3-} anions as a result of superficial passivation and broad shake-up satellite (Cecilia et al., 2009a). The additional three peaks were observed at 872.0, 877.0 and 881.0 eV, corresponding to Ni $2p_{1/2}$ energy levels (Cecilia et al., 2009b). On the other hand, P $2p_{3/2}$ shows two photoelectron peaks: one at lower binding energy (129.6 eV) and another at higher value (134.5 eV), which may be assigned to the

reduced $P^{\delta-}$ in Ni_2P and the unreduced PO_4^{3-} species (Cecilia et al., 2009b). When the reduced samples were exposed to air, superficial oxidation could happen and thus transferring phosphide to phosphate (PO_4^{3-} species).

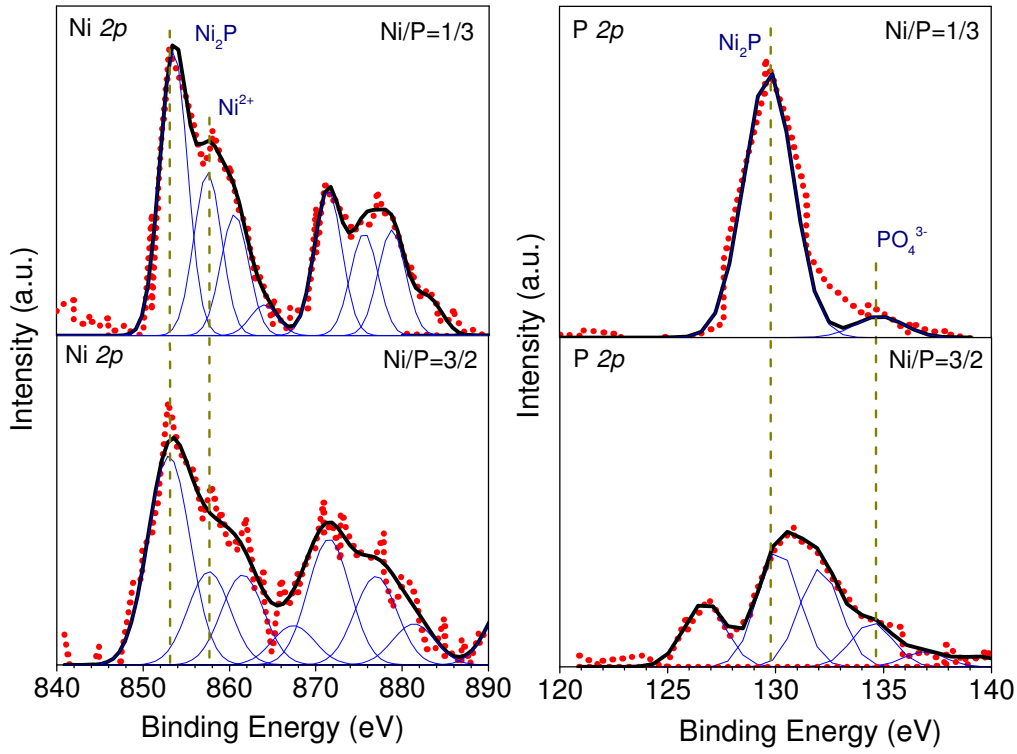

Figure 4-13 XPS spectra for NiP/AC catalysts with Ni/P=1/3 and Ni/P=3/2

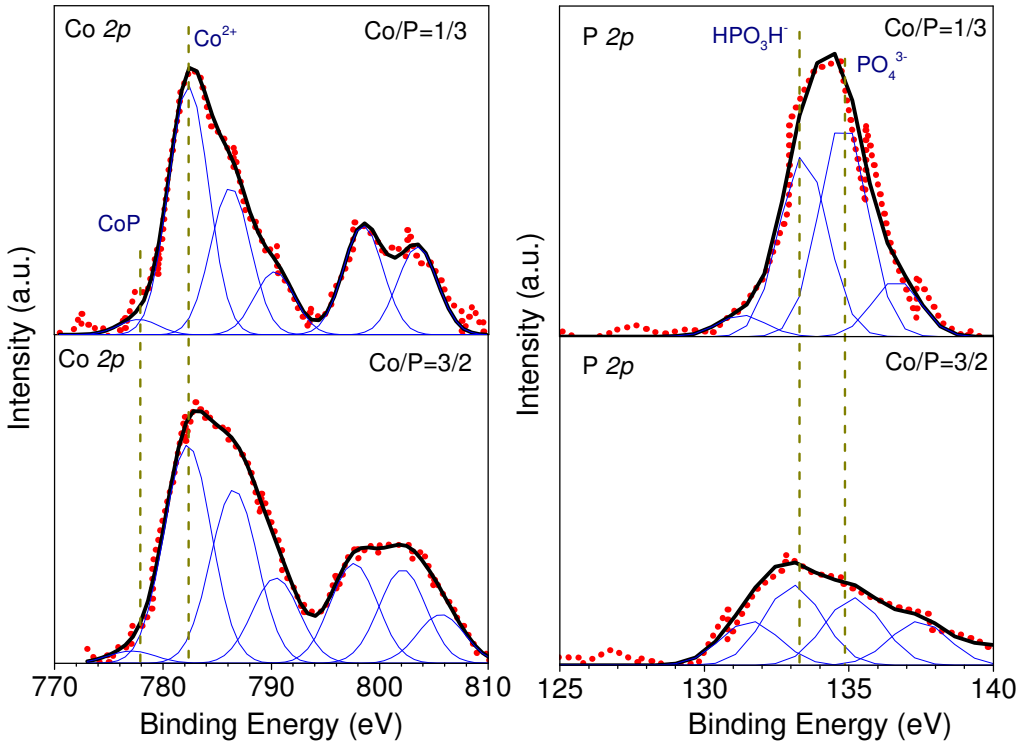

Figure 4-14 XPS spectra for CoP/AC catalysts with Co/P=1/3 and Co/P=3/2

From **Figure 4-14**, two major component peaks were observed by deconvoluting the Co $2p_{3/2}$ broad peak into two peaks. The first component peak is centered at around *c.a.* 777.8 eV that can be assigned to $Co^{\delta+}$ from cobalt phosphides such as Co_2P or CoP phase (Cecilia et al., 2013; Blanchard et al., 2008). The second component peak centered at about 782.0 eV which can be assigned to Co^{2+} from such as a divalent species forming $Co(HPO_3H)_2$ (Cecilia et al., 2009a). Between the spectra of two CoP catalysts with varying P content levels, no obvious differences are observed among the Co 2*p* signals, except for a slight increase in the peak intensity for the catalyst with a higher P content. On the other hand, the P $2p_{3/2}$ core-level spectra for the CoP catalysts can be deconvoluted into two component peaks: HPO_3H^- species at around 133.2 eV (Cecilia et al., 2009c) and PO_4^{3-} species at 135.0 eV (Cecilia et al., 2009a). The presence of HPO_3H^- species may be due to a partial reduction of the precursor (Cecilia et al., 2009c; Cecilia et al., 2013). Similarly, when the reduced samples were exposed to air, superficial oxidation could happen and thus transferring phosphide to phosphate (PO_4^{3-} species), as evidenced by the XPS analysis (**Table 4-7**).

4.3.3.3 Transmission electron microscopy (TEM) measurements

The morphologies of the AC-supported metal phophide were characterized by TEM. The TEM images of the NiP/AC with Ni/P = 3/2 and CoP/AC with Co/P = 3/2 along with their particle size distribution and Energy Dispersive Spectrum (EDS) spectra are illustrated in **Figure 4-15**. The dark globular particles in the gray carbon matraix are metal phosphide species confirmed by EDX analysis. For the NiP/AC catalyst, the particle size distribution curves clearly show that the NiP nanoparticles are approximately about 1-3 nm in size, while for the CoP/AC catalyst the particle size is in the range of 1-4 nm. Both Ni and Co phosphide nanoparticles are in a spherical shape with good distribtion and no aggregation, suggesting good dispersion of the metal phosphide nanoparticles on the carbon support. The EDX analysis of both these catalysts shows the presence of Ni, Co and P elements and their atomic ratios are closed to theoritical values.

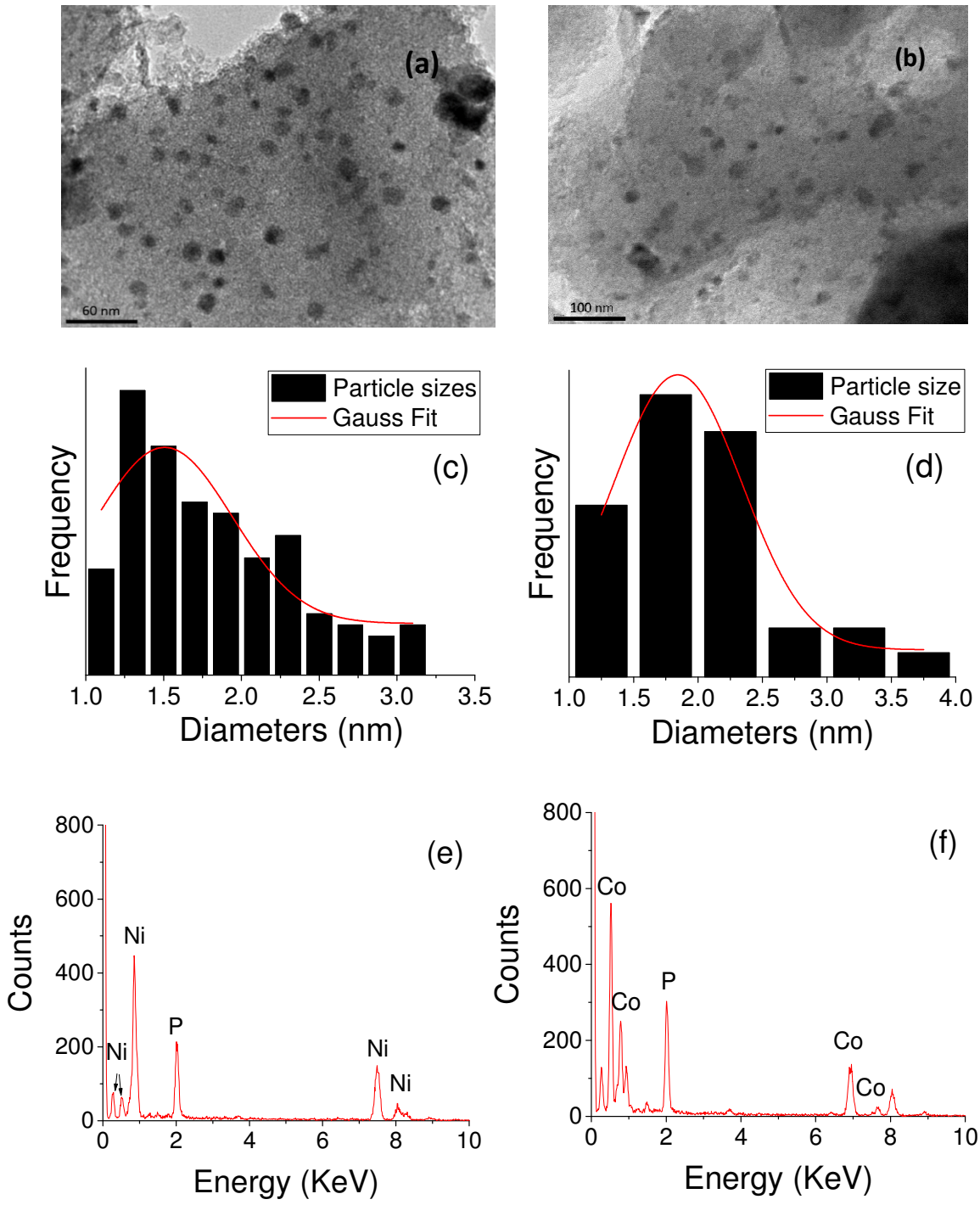

Figure 4-15 TEM micrographs of NiP/AC with Ni/P=3/2 (a) and CoP/AC with Co/P=3/2 (b); Histograms of particle size distribution for Ni/P=3/2 (c) and Co/P=3/2 (d); and Energy Dispersive Spectrum (EDS) for Ni/P=3/2 (e) and Co/P=3/2 (f).

4.3.3.4 Textural properties

Table 4-8 Textural properties of the fresh and spend catalysts

	Fresh catalysts			Spend catalysts		
Sample	S_{BET} (m^2g^{-1})	V_{total} (cm^3g^{-1})	D(*nm*)	S_{BET} (m^2g^{-1})	V_{total} (cm^3g^{-1})	D(*nm*)
AC	1342	0.64	1.9	-	-	-
Ru/C	810	0.68	3.4	172	0.38	8.7
Ni/P=5/2	1324	0.64	2.0	8	0.01	5.8
Ni/P=3/2	1172	0.57	2.0	10	0.02	6.4
Ni/P=1/3	1248	0.63	2.0	-	-	-
NiRuP	1212	0.61	2.0	9	0.01	6.0
Co/P=5/2	1318	0.66	2.0	6	0.01	5.4
Co/P=3/2	1154	0.57	2.0	9	0.01	5.9
Co/P=1/3	1322	0.67	2.0	-	-	-
CoRuP	1024	0.52	2.0	-	-	-

Table 4-8 summarizes the textural properties of fresh and spent catalysts. The fresh AC-supported catalysts have a BET surface area between 1024~1324 m^2g^{-1} and a total pore volume V_{total} ~0.6 cm^3g^{-1} with an average pore diameter (D) of ~2 nm (between micropore and mesopore sizes), while the commercial Ru/C catalyst shows a smaller BET surface area (810 m^2g^{-1}) and a larger average pore diameter (3.4 nm - mesopores). The textural properties of several typical spent catalysts were also measured. Obviously, all spent catalysts (including the commercial Ru/C) show significantly decreased BET surface area and total pore volume, while the average pore tripled in diameter. The decrease of surface area and pore volume in the spent catalysts can be explained by the deposition of coke and large molecular weight substances during the HDO process, confirmed by the formation of substantial yield of coke and solid residues (**Figures 4-3 ~ 4-5**). The increase of catalysts average pore diameter for the spent catalysts is likely due to the

plugging of the miropores by coke deposition or the collapsing of the pores of the support materials under the harsh reaction conditions. It can be noted that the commercial Ru/C catalyst exhibits more stable properties after the HDO process than other in-house prepared AC-supported Ni or Co-based catalysts.

4.4 Conclusions

In this work, a series of inexpensive AC-supported nickel or cobalt phosphide catalysts were synthesized for bio-oil HDO. The additional amounts of phosphorous in the AC-supported Ni and Co phosphide catalysts were optimized by varying the metal/P ratio (i.e., 5/2, 3/2, 1/1, 1/2, 1/3 mol/mol). Moreover, the effects of Ru as a co-catalyst (with very small addition 0.5 wt.%) in these AC-supported metals or metal phosphides catalysts were also investigated. All HDO tests were carried out in a 100 mL bench-scale reactor system using a wood-derived pyrolysis oil at 300 °C with an initial hydrogen pressure of 50 bar for 3 h. Some key conclusions are summarized as follows:

(1) For both Ni and Co catalysts, when adding a small amount of phosphorous to a certain level (up to M/P = 3/2), the H_2 consumption, oil yield and the degree of deoxygenation (DOD) can be significantly improved. Further increasing the level of P addition led to detrimental effects on the performance of the catalysts.

(2) For either Ni or Co-based catalysts, the O/C and H/C ratios of the upgraded oil products decreased with increasing the addition of P up to Ni/P or Co/P = 3/2, where the O/C = 0.11-0.12 and H/C = 1.26 -1.29, suggesting improved HDO activity but deteriorated hydrogenation activity. With further increase of P addition, reverse trends were observed, i.e., both O/C and H/C ratios increase with increasing P addition, suggesting deteriorated HDO activity but improved hydrogenation activity.

(3) Ni-based catalysts produced upgraded oil products with a lower molecular weight than those of Co-based catalysts in HDO of pyrolysis oil.

(4) Addition of a small amount of Ru to both Ni and Co catalysts did not improve the oil yield substantially but could significantly reduce the molecular weight of the upgraded oil. Moreover, adding a small amount (0.5 wt.%) of Ru to the metal or metal phosphide catalysts increased the

catalysts' hydrogenation activities (leading to a higher H/C ratio for the resulted oil products), while it showed a marginally effect on the catalysts' HDO activities.

(5) The XRD and XPS results suggest that Ni_2P and $Ni_{12}P_5$ might be active species of the NiP/AC.

References

Blanchard, P.E.R., Grosvenor, A.P., Cavell, R.G., Mar, A. 2008. X-ray Photoelectron and Absorption Spectroscopy of Metal-Rich Phosphides M_2P and M_3P (M= Cr – Ni). *Chemistry of Materials*, **20**(22), 7081-7088.

Huber, G. W. 2008. Breaking the chemical and engineering barriers to lignocellulosic biofuels: next generation hydrocarbon biorefineries. Washington, DC: National Science Foundation, Chemical, Biogengineering, Environmental and Transport Systems Division.

Bridgwater, A.V. 1999. Principles and practice of biomass fast pyrolysis processes for liquids. *Journal of Analytical and Applied Pyrolysis*, **51**(1), 3-22.

Bridgwater, A.V. 2003. Renewable fuels and chemicals by thermal processing of biomass. *Chemical Engineering Journal*, **91**(2), 87-102.

Bui, V.N., Laurenti, D., Delichère, P., Geantet, C. 2011. Hydrodeoxygenation of guaiacol: Part II: Support effect for CoMoS catalysts on HDO activity and selectivity. *Applied Catalysis B: Environmental*, **101**(3), 246-255.

Cecilia, J.A., Infantes-Molina, A., Rodríguez-Castellón, E., Jiménez-López, A. 2009a. Dibenzothiophene hydrodesulfurization over cobalt phosphide catalysts prepared through a new synthetic approach: Effect of the support. *Applied Catalysis B: Environmental*, **92**(1), 100-113.

Cecilia, J.A., Infantes-Molina, A., Rodríguez-Castellón, E., Jiménez-López, A. 2013. Gas phase catalytic hydrodechlorination of chlorobenzene over cobalt phosphide catalysts with different P contents. *Journal of Hazardous Materials*, **260**, 167-175.

Cecilia, J.A., Infantes-Molina, A., Rodríguez-Castellón, E., Jiménez-López, A. 2009b. The influence of the support on the formation of Ni2P based catalysts by a new synthetic approach. Study of the catalytic activity in the hydrodesulfurization of dibenzothiophene. *The Journal of Physical Chemistry C*, **113**(39), 17032-17044.

Cecilia, J.A., Infantes-Molina, A., Rodríguez-Castellón, E., Jiménez-López, A. 2009c. A novel method for preparing an active nickel phosphide catalyst for HDS of dibenzothiophene. *Journal of Catalysis*, **263**(1), 4-15.

Chen, J., Shi, H., Li, L., Li, K. 2014a. Deoxygenation of methyl laurate as a model compound to hydrocarbons on transition metal phosphide catalysts. *Applied Catalysis B: Environmental*, **144**, 870-884.

Cheng, S., Wilks, C., Yuan, Z., Leitch, M., Xu, C.C. 2012. Hydrothermal degradation of alkali lignin to bio-phenolic compounds in sub/supercritical ethanol and water–ethanol co-solvent. *Polymer Degradation and Stability*, **97**(6), 839-848.

Czernik, S., Bridgwater, A.V. 2004. Overview of applications of biomass fast pyrolysis oil. *Energy & Fuels*, **18**(2), 590-598.

de Miguel Mercader, F., Groeneveld, M.J., Kersten, S.R.A., Way, N.W.J., Schaverien, C.J., Hogendoorn, J.A. 2010. Production of advanced biofuels: Co-processing of upgraded pyrolysis oil in standard refinery units. *Applied Catalysis B: Environmental*, **96**(1), 57-66.

de Miguel Mercader, F., Koehorst, P.J.J., Heeres, H.J., Kersten, S.R.A., Hogendoorn, J.A. 2011. Competition between hydrotreating and polymerization reactions during pyrolysis oil hydrodeoxygenation. *AIChE Journal*, **57**(11), 3160-3170.

Elliott, D.C. 2007. Historical developments in hydroprocessing bio-oils. *Energy & Fuels*, **21**(3), 1792-1815.

Elliott, D.C., Baker, E.G., Beckman, D., Solantausta, Y., Tolenhiemo, V., Gevert, S.B., Hörnell, C., Östman, A., Kjellström, B. 1990. Technoeconomic assessment of direct biomass liquefaction to transportation fuels. *Biomass*, **22**(1), 251-269.

Fullana, A., Contreras, J.A., Striebich, R.C., Sidhu, S.S. 2005. Multidimensional GC/MS analysis of pyrolytic oils. *Journal of Analytical and Applied Pyrolysis*, **74**(1), 315-326.

Furimsky, E. 2000. Catalytic hydrodeoxygenation. *Applied Catalysis A: General*, **199**(2), 147-190.

Gayubo, A.G., Valle, B., Aguayo, A.T., Olazar, M., Bilbao, J. 2010. Pyrolytic lignin removal for the valorization of biomass pyrolysis crude bio‐oil by catalytic transformation. *Journal of Chemical Technology and Biotechnology*, **85**(1), 132-144.

Hoekstra, E., Kersten, S.R.A., Tudos, A., Meier, D., Hogendoorn, K.J.A. 2011. Possibilities and pitfalls in analyzing (upgraded) pyrolysis oil by size exclusion chromatography (SEC). *Journal of Analytical and Applied Pyrolysis*, **91**(1), 76-88.

Huber, G.W., Iborra, S., Corma, A. 2006. Synthesis of transportation fuels from biomass: chemistry, catalysts, and engineering. *Chemical Reviews*, **106**(9), 4044-4098.

Lu, Q., Li, W.-Z., Zhu, X.-F. 2009. Overview of fuel properties of biomass fast pyrolysis oils. *Energy Conversion and Management*, **50**(5), 1376-1383.

Meinshausen, M., Meinshausen, N., Hare, W., Raper, S.C.B., Frieler, K., Knutti, R., Frame, D.J., Allen, M.R. 2009. Greenhouse-gas emission targets for limiting global warming to 2 ℃. *Nature*, **458**(7242), 1158-1162.

Mohan, D., Pittman, C.U., Steele, P.H. 2006. Pyrolysis of wood/biomass for bio-oil: a critical review. *Energy & Fuels*, **20**(3), 848-889.

Mortensen, P.M., Grunwaldt, J.D., Jensen, P.A., Knudsen, K.G., Jensen, A.D. 2011. A review of catalytic upgrading of bio-oil to engine fuels. *Applied Catalysis A: General*, **407**(1), 1-19.

Nan, W., Krishna, C.R., Kim, T.J., Wang, L.J., Mahajan, D. 2014. Catalytic upgrading of switchgrass-derived pyrolysis oil using supported ruthenium and rhodium catalysts. *Energy & Fuels*, **28**(7), 4588-4595.

Peng, J., Chen, P., Lou, H., Zheng, X. 2008. Upgrading of bio-oil over aluminum silicate in supercritical ethanol. *Energy & Fuels*, **22**(5), 3489-3492.

Román-Leshkov, Y., Barrett, C.J., Liu, Z.Y., Dumesic, J.A. 2007. Production of dimethylfuran for liquid fuels from biomass-derived carbohydrates. *Nature*, **447**(7147), 982-985.

Tijmensen, M.J.A., Faaij, A.P.C., Hamelinck, C.N., van Hardeveld, M.R.M. 2002. Exploration of the possibilities for production of Fischer Tropsch liquids and power via biomass gasification. *Biomass and Bioenergy*, **23**(2), 129-152.

Venderbosch, R.H., Ardiyanti, A.R., Wildschut, J., Oasmaa, A., Heeres, H.J. 2010. Stabilization of biomass‐derived pyrolysis oils. *Journal of Chemical Technology and Biotechnology*, **85**(5), 674-686.

Venderbosch, R.H., Prins, W. 2010. Fast pyrolysis technology development. *Biofuels, Bioproducts and Biorefining*, **4**(2), 178-208.

Wang, S., Gu, Y., Liu, Q., Yao, Y., Guo, Z., Luo, Z., Cen, K. 2009. Separation of bio-oil by molecular distillation. *Fuel Processing Technology*, **90**(5), 738-745.

Wildschut, J., Mahfud, F.H., Venderbosch, R.H., Heeres, H.J. 2009. Hydrotreatment of fast pyrolysis oil using heterogeneous noble-metal catalysts. *Industrial & Engineering Chemistry Research*, **48**(23), 10324-10334.

Wildschut, J., Melian-Cabrera, I., Heeres, H.J. 2010. Catalyst studies on the hydrotreatment of fast pyrolysis oil. *Applied Catalysis B: Environmental*, **99**(1), 298-306.

Xu, Y., Wang, T., Ma, L., Zhang, Q., Liang, W. 2010. Upgrading of the liquid fuel from fast pyrolysis of biomass over MoNi/γ-Al_2O_3 catalysts. *Applied Energy*, **87**(9), 2886-2891.

Zacher, A.H., Olarte, M.V., Santosa, D.M., Elliott, D.C., Jones, S.B. 2014. A review and perspective of recent bio-oil hydrotreating research. *Green Chemistry*, **16**(2), 491-515.

Zhao, H.Y., Li, D., Bui, P., Oyama, S.T. 2011. Hydrodeoxygenation of guaiacol as model compound for pyrolysis oil on transition metal phosphide hydroprocessing catalysts. *Applied Catalysis A: General*, **391**(1), 305-310.

Chapter 5

5 Conclusions and recommendations for future work

5.1 Conclusions

In this study, hydrodeoxygenation (HDO) of a wood derived fast pyrolysis oil was investigated at 300 °C with an initial 50 bar H_2 pressure in a 100 mL batch reactor system for 3 h using Mo-based catalysts (with/without P) supported on four different supports (Al_2O_3, activated carbon, $Mg_6Al_2(CO_3)(OH)_{16}$, and $MgAl_2O_4$). In addition, the catalytic activities of AC-supported transition metal phosphides (MoP, NiP and CoP) were compared with the commercial Ru/C catalyst for bio-oil HDO. The additional amounts of phosphorous in the AC-supported Ni and Co phosphide catalysts were optimized by varying the metal/P ratio (i.e., 5/2, 3/2, 1/1, 1/2, 1/3 mol/mol). Moreover, the effects of Ru as a co-catalyst (with very small addition 0.5 wt.%) in these AC-supported metals or metal phosphides catalysts were also investigated. Some key conclusions are summarized as follows:

(1) Ru/C and recycled Ru/C catalyst produced the highest OF and the lowest coke yield and displayed the best hydrogenation activities, resulting in the higher H/C ratio for the upgraded oils with very low molecular weight.

(2) Addition of small amount of P to the Mo catalysts supported on both AC and Al_2O_3 led to increased degree of deoxygenation (DOD) and nearly 9 % increased oil yield compared with those without P.

(3) HDO operation without catalyst or with $MoP/MgAl_2O_4$ catalyst produced OF with decreased molar ratios of both O/C and H/C, suggesting that the upgrading proceeded mainly through thermal/hydro-cracking reactions rather than through HDO/hydrogenation reactions.

(4) AC was chosen as the best support materials for metal phosphides in terms of the HDO activities. Considering the yields and composition of the upgraded oil products and prices of the catalysts, NiP/AC was chosen as the most promising catalyst among all transition metal phosphide catalysts (CoP/AC, NiP/AC and MoP/AC) as well as the commercial noble metal catalyst (Ru/C).

(5) For both Ni and Co catalysts, when adding a small amount of phosphorous to a certain level (up to M/P = 3/2), the H_2 consumption, oil yield and the degree of deoxygenation (DOD) can be significantly improved. Further increasing the level of P addition led to detrimental effects on the performance of the catalysts.

(6) For either Ni or Co-based catalysts, the O/C and H/C ratios of the upgraded oil products decreased with increasing the addition of P up to Ni/P or Co/P = 3/2, where the O/C = 0.11 - 0.12 and H/C = 1.26 - 1.29, suggesting improved HDO activity but deteriorated hydrogenation activity. With further increase of P addition, reverse trends were observed, i.e., both O/C and H/C ratios increase with increasing P addition, suggesting deteriorated HDO activity but improved hydrogenation activity.

(7) Ni-based catalysts produced upgraded oil products with a lower molecular weight than those of Co-based catalysts in HDO of pyrolysis oil.

(8) Addition of a small amount of Ru to both Ni and Co catalysts did not improve the oil yield substantially but could significantly reduce the molecular weight of the upgraded oil. Moreover, adding a small amount (0.5 wt.%) of Ru to the metal or metal phosphide catalysts increased the catalysts' hydrogenation activities (leading to a higher H/C ratio for the resulted oil products), while it showed a marginally effect on the catalysts' HDO activities

(9) The XRD and XPS results suggest that Ni_2P and $Ni_{12}P_5$ might be active species of the NiP/AC

5.2 Recommendations for future work

The research in this thesis demonstrates that activated carbon could be a superior support for inexpensive metal phosphide (NiP or CoP) catalysts for HDO of pyrolysis oil. However, the author believes that further research is an essential step toward developing nobel carbon-supported metal phosphides catalysts. Possible further research areas are as follows:

(1) The activated carbon used in this work mainly contains micropores. Thus, it is interesting to examine the performance of NiP or CoP catalysts-supported on mesoporous carbon

support in HDO of pyrolysis oil in terms of oil yield, DOD, and properties of the upgraded oil products (molecular weight and distribution, O/C and H/C ratios, and HHV).

(2) Carbon-supported catalysts are difficult for regeneration and reuse after being deactivated. Thus, the lifetime of the carbon-supported metal phosphide catalysts shall be examined using a flow reactor, and strategies need to be developed to extend the lifetime of the carbon-supported catalysts for HDO of bio-oils.

Curriculum Vitae

Name: Cheng Guo

Post-secondary Education and Degrees:
The University of Western Ontario
Windsor, Ontario, Canada
2013-2015 M.E.Sc

South China University of Technology
Guangzhou, Guangdong, China
2009-2013 B.Sc

Honours and Awards:
Western Engineering Scholarship
2013-2015

Merit Scholarship
2011-2012

Related Work Experience
Research Assistant
The University of Western Ontario
2013-2015

Mitacs Inspiring Innovation Internship
2014 (4 months)

Publications:

Lü, Huan, and Cheng GUO. "Interaction between latex microspheres and antibody proteins revealed by fluorescence spectroscopy." *Spectroscopy and Spectral Analysis* 32.8 (2012): 2166-2170.

C. Guo, Z. Yuan, C. Xu, S. Rohani, Q He, Develop of inexpensive catalysts for bio-oil upgrading by hydrodeoxygenation. Advanced Biofuels Symposium Program, Ottawa, Canada (2014).

C. Guo, Z. Yuan, C. Xu, S. Rohani, Q He, Studies of the synthesis of Ni and Co phosphides and their activity in hydrodeoxygenation of fast pyrolysis oil. Advanced Biofuels Symposium Program, Montreal, Canada (2015).